LBNL-45881

Steric and Electronic Effects of 1,3-Disubstituted Cyclopentadienyl Ligands on Metallocene Derivatives of Cerium, Titanium, Manganese, and Iron

Chadwick Dean Sofield
Ph.D. Thesis

Department of Chemistry
University of California, Berkeley

and

Chemical Sciences Division
Ernest Orlando Lawrence Berkeley National Laboratory
University of California
Berkeley, CA 94720

May 2000

This work was supported by the Director, Office of Science, Office of Basic Energy Sciences, Chemical Sciences Division, of the U.S. Department of Energy under Contract No. DE-AC03-76SF00098.

DISCLAIMER

DISCLAIMER

Portions of this document may be illegible in electronic image products. Images are produced from the best available original document.

Steric and Electronic Effects of 1,3-Disubstituted Cyclopentadienyl Ligands on Metallocene Derivatives of Cerium, Titanium, Manganese, and Iron

by

Chadwick Dean Sofield

B.S. (Yale University) 1990

A dissertation submitted in partial satisfaction of the

requirements for the degree of

Doctor of Philosophy
in

Chemistry

in the

GRADUATE DIVISION

of the

UNIVERSITY OF CALIFORNIA, BERKELEY

Committee in charge:

Professor Richard A. Andersen, Chair
Professor John Arnold
Professor Clayton J. Radke

Spring 2000

Abstract

Steric and Electronic Effects of 1,3-Disubstituted Cyclopentadienyl Ligands on Metallocene Derivatives of Cerium, Titanium, Manganese, and Iron

by

Chadwick Dean Sofield

Doctor of Philosophy in Chemistry

University of California, Berkeley

Professor Richard A. Andersen, Chair

Sterically demanding 1,3-disubstituted cyclopentadienyl ligands were used to modify the physical properties of the corresponding metallocenes. Sterically demanding ligands provided kinetic stabilization for trivalent cerium compounds. Tris(di-*t*-butylcyclopentadienyl)cerium was prepared and anion competition between halides and cyclopentadienyl groups which had complicated synthesis of the tris(cyclopentadienyl)compound was qualitatively examined. Bis(di-*t*-butylcyclopentadienyl)cerium methyl was prepared and its rate of decomposition, by ligand redistribution, to tris(di-*t*-butylcyclopentadienyl)cerium was shown to be slower than the corresponding rate for less sterically demanding ligands.

Asymmetrically substituted ligands provided a symmetry label for examination of chemical exchange processes. Tris[trimethylsilyl(*t*-butyl)cyclopentadienyl]cerium was prepared and the rate of interconversion between the C_1 and C_3 isomers was examined. The enthalpy difference between the two distereomers is 7.0 kJ/mol.

The sterically demanding cyclopentadienyl ligands *ansa*-di-*t*-butylcyclopentadiene ($Me_2Si[(Me_3C)_2C_5H_3]_2$), *ansa*-bis(trimethylsilyl)cyclopentadiene ($Me_2Si[(Me_3Si)_2C_5H_3]_2$), and tetra-*t*-butylfulvalene and metallocene derivatives of the ligands were prepared and their structures were examined by single crystal X-ray crystallography.

The effect that substitutents on the cyclopentadienyl ring have on the π- electron system of the ligand was examined through interaction between ligand and metal orbitals. A series of 1,3-disubstituted manganocenes was prepared and their electronic states were determined by solid-state magnetic susceptibility, electron paramagnetic resonance, X-ray crystallography, and variable temperature UV-vis spectroscopy. Spin-equilibria in $[(Me_3C)_2C_5H_3]_2Mn$ and $[(Me_3C)(Me_3Si)C_5H_3]_2Mn$ were examined and indicate an enthalpy difference of 15 kJ/mol between the high-spin and low-spin forms.

Cyclopentadienyl groups resistant to intramolecular oxidative addition allowed isolation of compounds susceptible to intramolecular decomposition. A kinetically stable, base-free titanocene was prepared using di-*t*-butylcyclopentadienyl ligands and the reactivity of the compound toward small molecules was investigated. The titanocene reacts reversibly with hydrogen to form the titanocene dihydride and the equilibrium in solution between titanocene dihydride, and titanocene and hydrogen, was examined.

Acknowledgements

The author thanks everyone who has contributed to his continuing education in chemistry. In particular, Alan Vaughan and Lisa Crocker were generous with their time, expertise, and part of their research projects and provided an ideal introduction to organometallic synthesis. Mike Heinekey and Greg Hillhouse made room in their laboratories and imparted a fascination with molecules that is undiminished, even after ten years in graduate school. Wayne Lukens and Laura Blosch are always eager to talk about chemistry and their thoughtful contributions and criticisms are invaluable. Discussions with Fred Hollander, Norman Edelstein, Jerry Bucher, Tom Lawhead, and Mike Press made results clearer and experiments easier.

Dick Andersen shared an interest in molecules that have something to teach to chemists about chemistry, even when the molecules have no obvious practical application. Dick's perspective on experiments and unparalleled knowledge of the literature were instrumental in preparing new compounds without unnecessary effort. As many have discovered, he is a valuable resource for the entire department.

to my parents

Table of Contents

Chapter 1

Cyclopentadienyl Ligands in Organometallic Chemistry

In the first half of this century, cyclopentadiene was primarily a building block in organic chemistry. Most notably used as by Diels and Alder in reactions of the type that bear their names, cyclopentadiene also contains an active methylene group, which has been exploited to functionalize the diene[1].

The cyclopentadienyl fragment is an obvious starting material for preparation of fulvalene (Figure 1).

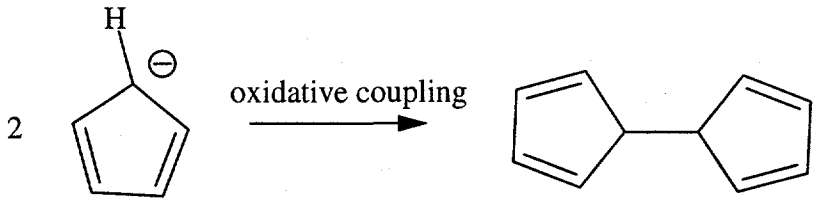

Figure 1: Scheme for preparation of fulvalene

Noting that biphenyl had been prepared from phenyl-Grignard and anhydrous iron(III) chloride, Kealy and Pauson attempted to prepare fulvalene from cyclopentadienylmagnesium bromide and ferric chloride[2].

$$6RMgBr + 2FeCl_3 \xrightarrow{Et_2O} 3R_2 + 2Fe + 3MgBr_2 + 3MgCl_2$$

The remarkably stable, orange product was correctly analyzed as $C_{10}H_{10}Fe$ and the authors suggested that resonance stabilization based on the aromatic cyclopentadienyl moiety accounted for the unusual stability of the organo-iron species (Figure 2). The

aromaticity of the cyclopentadienyl anion plays an important role in the stability of bis(cyclopentadienyl)iron but the proposed coordination of the ligands was incorrect.

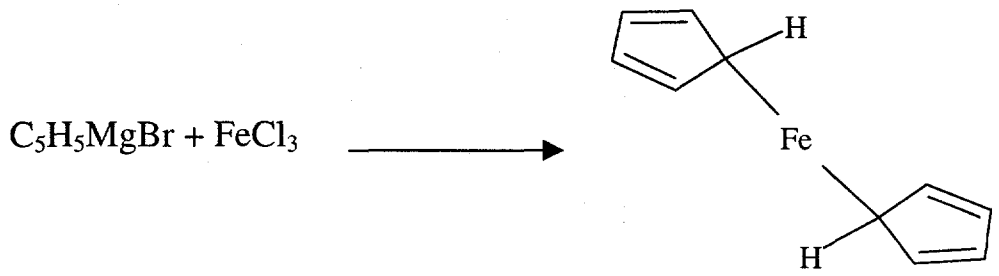

Figure 2: Organo-iron complex proposed by Kealy and Pauson[2,3]

Wilkinson, Fischer, and coworkers correctly identified the "sandwich" compound, ferrocene (Figure 4)[4,5], and developed the chemistry of the cyclopentadienyl ligand and related π-complexes in work that would earn the Nobel Prize in chemistry in 1973.

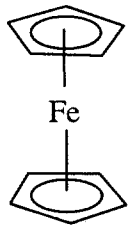

Figure 3: Bis(cyclopentadienyl)iron as proposed by Wilkinson and Fischer

Wilkinson described his formulation of the η^5-cyclopentadienyl ligand as the resonance equivalent of a σ-bond and two π-bonds between the metal and each ligand (Figure 4)[6].

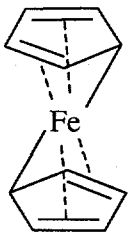

Figure 4: Wilkinson's localized ferrocene bonding scheme

Cyclopentadienyl ligands, in this model, are three-coordinate ligands, which contribute six electrons to the valence shell. The stability of ferrocene is consistent with an 18-electron compound, isoelectronic with krypton. Orbital treatments of cyclopentadienyl ligands reach similar conclusions. The six π-electrons occupy the a_1 and e_1 orbitals of the cyclopentadienyl fragment (Figure 5) and the three, filled cyclopentadienyl orbitals typically interact with three, metal-based orbitals

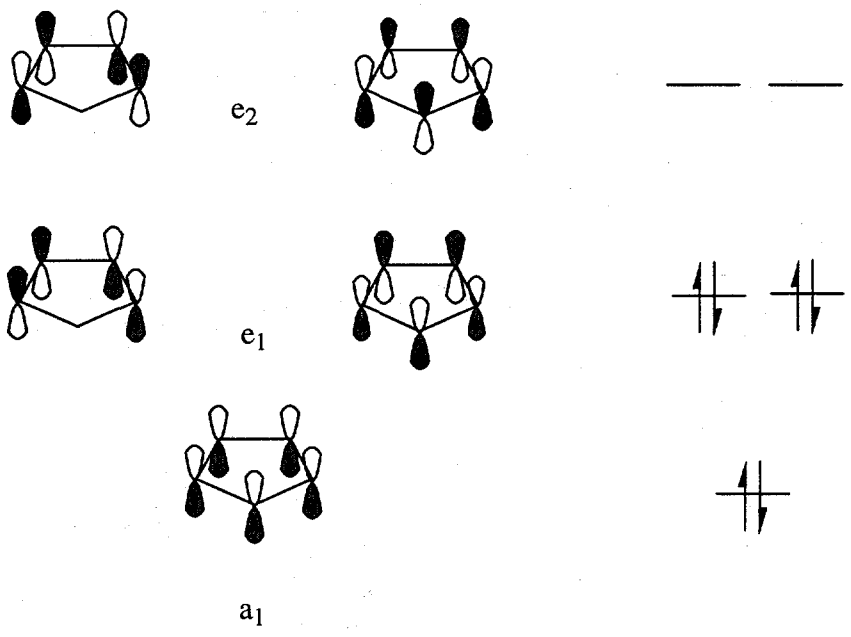

Figure 5: Orbital diagram of a cyclopentadienyl ligand

Synthesis of cyclopentadienyl compounds is generally achieved using alkali- or alkaline earth metal cyclopentadienides and metal halides but numerous other strategies have been employed[7].

Since the cyclopentadienyl ring can be derivatized with substituents, the electronic and steric contributions of the ligand are adjustable and the symmetry and reactivity of cyclopentadienyl compounds can be modified. For these reasons, cyclopentadienyl ligands have become ubiquitous in organometallic chemistry.

Kinetic Stabilization

The coordination sites occupied by cyclopentadienyl ligands are, in most instances, unavailable for use in reaction pathways and the ligands often make the reactivity of a compound more selective. For synthetic and mechanistic chemists, the kinetic stability imparted by cyclopentadienyl groups is an invaluable property that simplifies preparations and analysis of reactions[8]. Sterically demanding cyclopentadienyl ligands can be used to occupy not only the orbitals of a metal center, but also a greater portion of the coordination sphere in which metal-centered reactions take place. Activation barriers for decomposition reactions can be increased by making the reactive site too "crowded" to accommodate the coordination environment required for some decompositions.

Sterically demanding cyclopentadienyl ligands have also been used to prepare compounds of previously unknown stoichiometry. For example, the unsubstituted cyclopentadienyl compound, $(C_5H_5)_2UCl_2$, is unstable with respect to disproportionation to $(C_5H_5)_3UCl$ and $(C_5H_5)UCl_3$[9]. The increased steric bulk of the pentamethylcyclopentadienyl ligand allows $(Me_5C_5)_2UCl_2$ to be isolated, presumably due to the steric impediment to formation of $(Me_5C_5)_3UCl$[10].

In Chapter 2 of this dissertation, sterically demanding cyclopentadienyl ligands are used in an attempt to prevent decomposition of bis(cyclopentadienyl)cerium alkyls, both by kinetically stabilizing the Cp'_2CeR moiety and by inhibiting redistribution to Cp'_3Ce species (Cp' = substituted cyclopentadienyl ligand).

Asymmetrically Substituted Cyclopentadienyl Ligands

Symmetry considerations play a fundamental role in spectroscopy and substituted cyclopentadienyl ligands were first employed by Wilkinson and Reynolds to assess the change in CO stretching frequencies in $(\pi\text{-}C_5H_5)M(CO)_3$ and $(\pi\text{-}MeC_5H_4)M(CO)_3$ (M = Fe, Co, Mn) resulting from the decrease in symmetry[11]. No change was observed in the infrared spectrum that could be attributed to the reduction in symmetry of the molecule but this result was anticipated since little evidence of interaction between the cyclopentadienyl fragment and the carbonyl groups was detected in prior studies[12]. Presumably, the potential energy difference between different ring orientations is small so that "all" ring orientations exist in the sample and the effect on the carbonyl region of the infrared spectrum is not resolvable.

Even in molecules that have pronounced deviation from idealized symmetry, fluxional processes have been shown to add time-averaged symmetry elements to cyclopentadienyl compounds[13-15]. A cyclopentadienyl ligand that is not susceptible to time averaging will provide more information about a compound than one subject to real or time averaged symmetry elements. Some of the implications of asymmetrically substituted cyclopentadienyl rings are investigated in Chapter 3.

Electronic Influence of the Cyclopentadienyl π-Electrons

The bis(methylcyclopentadienyl) compounds reported by Wilkinson and Reynolds displayed different physical properties, which were attributed, in part, to the

electron-donating methyl groups[11]. Numerous alkylated and arylated cyclopentadienyl ligands have been prepared in order to adjust the electronic contribution of the substituent to the π-electron system of the cyclopentadienyl ring[16,17].

Most notably, substituents on cyclopentadienyl ligands have been used to perturb the electronic structure of manganocenes. Electron donating groups tend to increase the ligand field interaction and favor a low-spin compound, whereas manganocenes with lesser ligand field interactions are likely to be high-spin compounds. In the continuum between strong field and weak field ligands, there are cyclopentadienyl complexes that exhibit both high-spin and low-spin electronic configurations simultaneously and some new examples of such compounds are described in Chapter 4.

Resistance of Substituted Cyclopentadienyl Ligands to Intramolecular Oxidative Addition

Cyclopentadienyl groups are spectator ligands in the vast majority of compounds that contain the ligands, but reactions involving the cyclopentadienyl ligands are common. Organic chemists have been interested in the aromatic chemistry of ferrocene since its discovery and functionalized ferrocenes and ferrocenyl ligands are countless[6,18].

Intramolecular oxidative addition of cyclopentadienyl ligand, C-H bonds has been observed for several early metallocenes[19-22]. This reaction is undesirable since the reactivity of the resulting metal hydride species is difficult to distinguish from reactivity

of the metallocenes. The uncertainty in the nature of the material complicates synthetic and mechanistic studies.

The early transition and early lanthanide metals, which exhibit intramolecular oxidative addition, have relatively large ionic radii and are coordinatively unsaturated. The proximity of the cyclopentadienyl C-H bond to the open reaction site facilitates addition of the C-H bond.

Permethylated cyclopentadienyl ligands were first used in an attempt to prevent intramolecular C-H activation in titanocene and substituted cyclopentadienyl ligands have recently been used to successfully prevent the reaction[23]. In Chapter 5, a titanocene species is described, which does not exhibit intramolecular oxidative addition, but does exhibit intermolecular chemistry similar to that observed for decamethyltitanocene. The role of equilibria in titanocene chemistry is explored through the reversible oxidative addition of hydrogen.

References

1)Wilson, P. J., Jr.; Wells, J. H. *Chem. Rev.*, **1944**, *34*, 1-50.

2)Kealy, T. J.; Pauson, P. L. *Nature*, **1951**, *168*, 1039-1040.

3)Miller, S. A.; Tebboth, J. A.; Tremaine, J. F. *J. Chem. Soc.*, **1952**, 623-635.

4)Wilkinson, G.; Rosenblum, M.; Whiting, M. C.; Woodward, R. B. *J. Am. Chem. Soc.*, **1952**, *74*, 2125-2126.

5)Fischer, E. O.; Pfab, W. *Z. Naturforsch., B*, **1952**, *7*, 377.

6)Wilkinson, G. *J. Organomet. Chem.*, **1975**, *100*, 273-278.

7)Elschenbroich, C.; Salzer, A. *Organometallics*; VCH Publishers: New York, 1989.

8)Collman, J. P.; Hegedus, L. S.; Norton, J. R.; Finke, R. G. *Principles and Applications of Organotransition Metal Chemistry*; University Science Books: Mill Valley, CA, 1987.

9)Ernst, R. D.; Kennely, W. J.; Day, C. S.; Day, V. W.; Marks, T. J. *J. Am. Chem. Soc.*, **1979**, *101*, 2656-2664.

10)Manriquez, J. M.; Fagan, P. J.; Marks, T. J. *J. Am. Chem. Soc.*, **1978**, *100*, 3939-3941.

11)Reynolds, L. T.; Wilkinson, G. *J. Inorg. Nucl. Chem*, **1959**, *9*, 86-92.

12)Cotton, F. A.; Liehr, A. D.; Wilkinson, G. *J. Inorg. Nucl. Chem.*, **1955**, *1*, 175-186.

13)McKinney, M. A.; Haworth, D. T. *J. Chem. Educ.*, **1980**, *57*, 110-112.

14)Cotton, F. A. *J. Organomet. Chem.*, **1975**, *100*, 29-41.

15)Mann, B. E. *Comprehensive Organometallic Chemistry*; Pergammon Press: New York, 1982; Vol. 3, pp 89-171.

16)Robbins, J. L.; Edelstein, N. M.; Cooper, S. R.; Smart, J. C. *J. Am. Chem. Soc.*, **1979**, *101*, 3853-3857.

17)Robbins, J. L.; Edelstein, N. M.; Spencer, B.; Smart, J. C. *J. Am. Chem. Soc.*, **1982**, *104*, 1882-1893.

18)Togni, A.; Hayashi, T. *Ferrocenes : Homogeneous Catalysis, Organic Synthesis, Materials Science*; VCH Publishers: New York, 1995.

19)Tebbe, F. N.; Parshall, G. W. *J. Am. Chem. Soc.*, **1971**, *93*, 3793-3795.

20)Guggenberger, L. J.; Tebbe, F. N. *J. Am. Chem. Soc.*, **1971**, *93*, 5924-5925.

21)Cooper, N. J.; Green, M. L. H.; Couldwell, C.; Prout, K. *J. Chem. Soc., Chem. Comm.*, **1977**, 145-146.

22)Brintzinger, H. H.; Bercaw, J. E. *J. Am. Chem. Soc.*, **1970**, *92*, 6182-6185.

23)Bercaw, J. E.; Brintzinger, H. H. *J. Am. Chem. Soc.*, **1971**, *93*, 2045-2046.

Chapter 2

Sterically Demanding Cyclopentadienyl Ligands

The chemistry of lanthanide-carbon bonds is underdeveloped compared with analogous chemistry in the transition series. Although the lack of orbital participation in bonding and the few stable oxidation states prohibit some common organometallic phenomena[1], the lanthanide elements exhibit chemistry unobserved in the transition series.

Lanthanide elements tend to form compounds with high coordination numbers attributed to the large ionic radii and to the lack of orbital restrictions on bonding. The ionic radii of the lanthanide elements in the +3 oxidation state lie between 1.15 and 1.00 Å. Typical radii for transition metal +3 cations are 0.63 to 0.86 Å[2].

In addition to a larger coordination sphere, bonding in lanthanide elements is not limited by the availability of metal bonding orbitals. Valence electrons of the lanthanide elements reside in f-orbitals. The 4-f orbitals have three angular nodes and no radial nodes which, through poor shielding and, consequently, a high effective nuclear charge, limits the radial extent of the orbitals. There is little electron density from f-orbitals that extends beyond the core electrons and participation of f-orbitals in lanthanide bonding is usually small, especially in the +3 oxidation state[3]. A consequence of the lack of orbital participation in bonding is the ionic-type bonding of ligands commonly observed for lanthanide elements. The symmetry of the f-orbitals has a minor, if not undetectable, effect on bonding, so no bonding configurations are symmetry forbidden. The lack of orbital geometry restrictions and, in the early lanthanide elements, the large atomic radii contribute to a coordination environment notable for kinetic instability.

Cyclopentadienyl groups are commonly used as spectator ligands, which occupy coordination sites on a metal but do not participate in reactions. The large ionic radii of the early lanthanide elements make inert, spectator ligands particularly useful. Homoleptic alkyl complexes of the lanthanide elements are rare[4] and their kinetic instability is attributed to their low coordination number. Sterically demanding ligands occupy a greater portion of the coordination sphere of a compound and reduce the number of reaction pathways available, thus enhancing its kinetic stability. Cyclopentadienyl compounds of the lanthanide elements were first prepared by Wilkinson in 1954[5]. Despite the fact that three cyclopentadienyl groups occupy the equivalent of nine coordination sites[6], tris(cyclopentadienyl) complexes of the early lanthanides are still coordinatively unsaturated. Lewis base adducts of tris(cyclopentadienyl)lanthanides are common and in the absence of such a base, cyclopentadienyl-bridged oligomers are formed[7-9].

Alkyl substitution of cyclopentadiene is facile and results in more sterically demanding cyclopentadienyl ligands[10-13]. Sterically demanding cyclopentadienyl ligands have been used to occupy a greater portion of the coordination sphere and base free, monomeric tris(cyclopentadienyl) complexes of the early lanthanides have been isolated[14,15].

Sterically demanding bis(cyclopentadienyl)lanthanide alkyl complexes may present an opportunity to examine the chemistry of the lanthanide-carbon bond. The use of cyclopentadienyl complexes of the lanthanides in homogeneous catalysis and in the activation of C-H bonds suggests that a close examination of the chemistry of lanthanide alkyl complexes is merited.

Ligand Redistribution

Previous work in the Anderesen group has shown that $[(Me_3C)C_5H_4]_2CeMe$ and $[(Me_3Si)_2C_5H_3]_2CeMe$ ($Cp"_2CeMe$) and similar compounds with less sterically demanding cyclopentadienyl groups undergo a ligand redistribution process, yielding the corresponding tris(cyclopentadienyl)cerium compound and an uncharacterized, complimentary residue[16].

The half-life of the alkyl complex in solution is increased with the change from mono-*t*-butylcyclopentadienyl groups to bis(trimethylsilyl)cyclopentadienyl groups but the longer half-life is about 100 h and the compound remains impractical for synthetic or mechanistic studies (Table 1).

$$2Cp'_2CeMe \xrightarrow[\text{Half-life in solution}]{} Cp'_3Ce + \text{residue}$$

$[(Me_3C)C_5H_4]_2CeMe$	2-3 h	$[(Me_3C)C_5H_4]_3Ce$
$[(Me_3Si)_2C_5H_3]_2CeMe$	100 h	$[(Me_3Si)_2C_5H_3]_3Ce$
$[(Me_3C)_2C_5H_3]_2CeMe$	?	$[(Me_3C)_2C_5H_3]_3Ce$

Table 1: Half-life in solution of Cp'_2CeMe species

The di-*t*-butylcyclopentadienyl ligand was selected to increase the kinetic stability of the bis(cyclopentadienyl)cerium alkyls. The increase in steric bulk for the di-*t*-butylcyclopentadienyl group over the bis(trimethylsilyl)cyclopentadienyl group is not obvious since the shorter ring-carbon to quaternary carbon bond (compared to the ring-carbon to silicon bond in the trimethylsilyl substituent) dictates a "narrower" ligand (Figure 6). Since, in cerium, the substituent on the ring is unlikely to affect the metal to ring-centroid distance, a narrower ligand would result in decreased steric congestion at the metal atom.

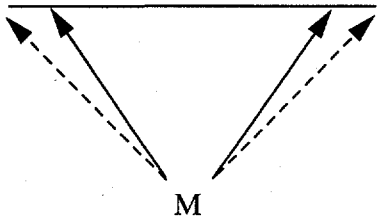

Figure 6: narrower ligand; less steric bulk

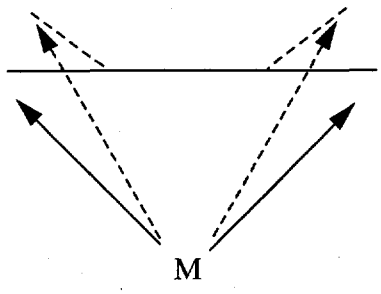

Figure 7: rigid, planar ligand; more steric bulk

However, trimethylsilyl substituents on a cyclopentadienyl ring are more able to bend out of the plane of the ring so that the steric bulk of the ligand is reduced. The ring-carbon to silicon bond is more flexible than the corresponding ring-carbon to quaternary carbon bond (the Si-C bond is less than 10% stronger but is 20% longer, Table 2). *t*-Butyl substituents have a more rigid ring-carbon to quaternary atom bond (Figure 7) and, as a result, the coordination space occupied by the ligand is larger.

	Bond strength (kJ/mol)	Bond length (Å)
Ring-carbon to quaternary carbon	340	1.53
Ring-carbon to quaternary silicon	370	1.89

Table 2: Bond strength and bond length for ring carbon-C and ring carbon-Si bonds[17]

This description of the steric bulk of the ligands amounts to a "cone-angle" type argument[18], which must be used with caution since the ligands are highly anisotropic, but it provides sufficient rationale for examination of the new ligand system.

Preparation of the bis(cyclopentadienyl)cerium alkyls has been accomplished by treating tris(cyclopentadienyl)cerium complexes with alkyl lithium reagents. A reaction solvent was chosen (typically hexane) so that the bis(cyclopentadienyl)cerium alkyl complex was soluble and the byproduct, lithium cyclopentadienide, was not.

$$Cp'_3Ce + MeLi \xrightarrow[\text{hexane}]{} Cp'_2CeMe + Cp'Li\downarrow$$

The tris(cyclopentadienyl)cerium starting material was prepared from cerium tris(bis(trimethylsilyl)amide) and bis(trimethylsilyl)cyclopentadiene.

$$Ce[N(SiMe_3)_2]_3 + 3\ Cp'H \longrightarrow Cp'_3Ce + 3\ HN(SiMe_3)_2$$

The pK_a of bis(trimethylsilyl)amine exceeds the pK_a's of *t*-butylcyclopentadiene and bis(trimethylsilyl)cyclopentadiene and the blue, Cp'_3Ce complexes were formed in high yield. The pK_a of di-*t*-butylcyclopentadiene is also lower than that of bis(trimethylsilyl)amine, and the acid-base reaction is thermodynamically favorable (Table 3).

Brønsted Acid	pK_a
$(C_5H_5)H$	16
$[(Me_3C)C_5H_4]H$	20
$[(Me_3Si)_2C_5H_3]H$	~20
$[(Me_3C)_2C_5H_3]H$	22
$[(Me_3Si)_2N]H$	26

Table 3: pK_a values for substituted cyclopentadienes and bis(trimethylsilyl)amine[17,19,20]

Di-*t*-butylcyclopentadiene ($Cp^{\ddagger}H$) is prepared by a method similar to that reported by Venier and Casserly[12]. Using a concentrated solution of potassium hydroxide, under phase-transfer conditions, cyclopentadiene is deprotonated in the presence of *t*-butylbromide. However, when cerium tris(bis(trimethylsilyl)amide) is treated with di-*t*-butylcyclopentadiene, no tris(di-*t*-butylcyclopentadienyl)cerium is isolated. This presumably kinetic barrier to tri-substitution was encouraging since the impetus for exploring the di-*t*-butylcyclopentadienyl ligand ($Cp^{\ddagger}$) was to impede formation of the tris complex. An alternate route to the $Cp^{\ddagger}_2CeR$ species was investigated. Metathesis reactions between alkali or alkaline-earth metal cyclopentadienides and metal halides are common synthetic methods for preparation of cyclopentadienyl compounds. Magnesium di-*t*-butylcyclopentadienide can be used to prepare $Cp^{\ddagger}_3Ce$ and $Cp^{\ddagger}_2CeCl$ as

potential starting materials for reaction with MeLi to form $Cp^{‡}_2CeMe$. Magnesium di-*t*-butylcyclopentadienide has three primary advantages over other cyclopentadienide salts as a ligand transfer reagent: the compound can be crystallized so that impurities are eliminated and stoichiometric uncertainty is minimized; magnesium salts have a lesser tendency toward formation of metal-halide adducts with the product than, in particular, lithium salts; and magnesium di-*t*-butylcyclopentadienide is very soluble common solvents so reaction rates are not impeded by solubility.

Synthesis of $Cp^{‡}_2Mg$ can be achieved by treating di-*t*-butylcyclopentadiene with "dibutylmagnesium", a mixture of butylmagnesium species, in refluxing heptane for 12 h[21]. Colorless crystals are obtained from cold heptane. The compound sublimes at 100 °C (10^{-3} torr) and melts at 138-141 °C. The ^{1}H NMR spectrum exhibits a single resonance for the *t*-butyl protons and two resonances for the protons bound to the cyclopentadienyl ring. The ring-proton resonances are consistent with the expected A_2B spin system (Figure 8).

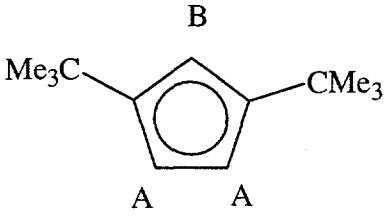

	δ (ppm)	$^4J_{HH}$
Me_3C	1.31	s
A	5.94	d, 2.5 Hz
B	5.88	t, 2.5 Hz

Figure 8: ^{1}H NMR of $Cp^{‡}_2Mg$, 500 MHz

Bis(di-*t*-butylcyclopentadienyl)cerium chloride is prepared from anhydrous cerium chloride and tetra-*t*-butylmagnesocene in tetrahydrofuran. The compound is orange and crystallizes from hexane. The ^{1}H NMR spectrum of the compound exhibits three resonances at 30 °C: a *t*-butyl resonance at –3.89 ppm ($\nu_{1/2}$ = 10 Hz, 36H), and two resonances for protons bound to the cyclopentadienyl ring at 40.1 and 11.6 ppm ($\nu_{1/2}$ =

200 Hz, 2H and $\nu_{1/2}$ = 150 Hz, 4H). For paramagnetic compounds, the chemical shifts are temperature dependent and for a single species, the plot of the chemical shift vs. 1/T is linear [22]. However, the variable temperature ^{1}H NMR spectra of $Cp^{\ddagger}_2CeCl$ indicate that, at low temperatures (<-70 °C), the *t*-butyl substituents on the cyclopentadienyl rings are not magnetically equivalent. The low temperature spectrum consists of two *t*-butyl resonances and one observable ring proton resonance. The ^{1}H NMR spectrum is consistent with a compound in which the two cyclopentadienyl rings are equivalent but the substituents on each ring are no longer magnetically equivalent.

The crystal structure of the compound was determined independently by Bulychev and coworkers[23]. The compound is dimeric and the rings are staggered so that the *t*-butyl environments and the environments of the ring resonances are different (Figure 9).

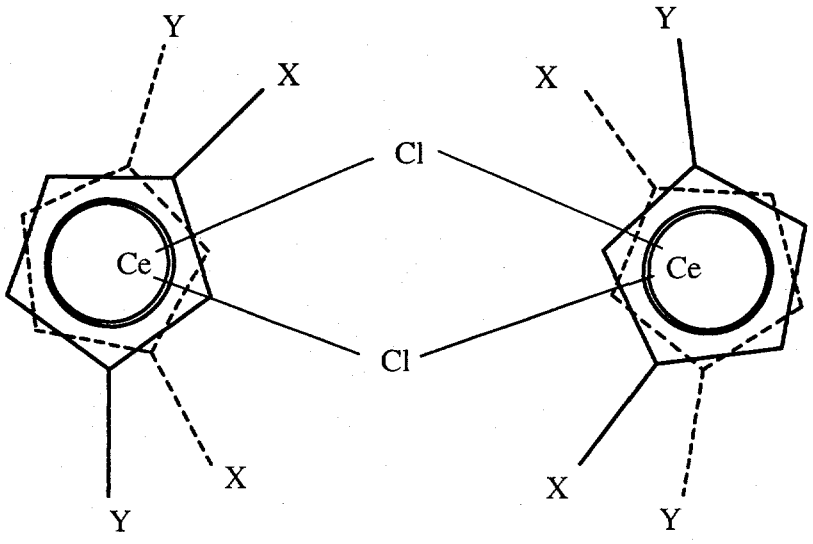

Figure 9: Solid-state symmetry of $[Cp^{\ddagger}_2CeCl]_2$, three perpendicular C_2 axes

In the solid state, the compound has idealized D_2 symmetry but in solution at 30 °C, the ^{1}H NMR spectrum is consistent with the addition of time averaged mirror planes, which make the molecule appear to have D_{2h} symmetry. At room temperature in solution, the

cyclopentadienyl rings rotate sufficiently so that the two *t*-butyl environments exchange rapidly on the NMR time scale (Figure 10).

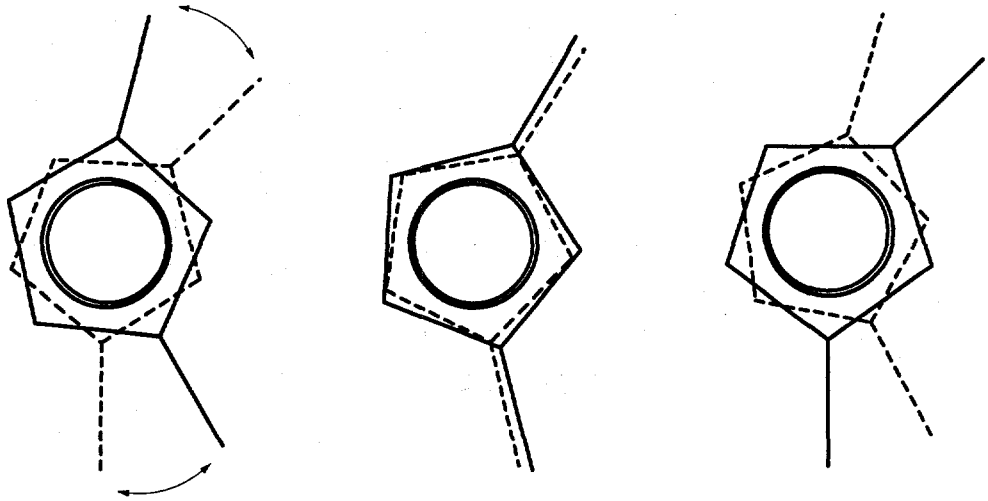

Figure 10: Time averaged equilibration of ring substituents through ring rotation

At lower temperatures, the rate of rotation is slower and the *t*-butyl resonances appear as two, equal area resonances, consistent with molecular D_2 symmetry.

The 30 °C ^{1}H NMR absorptions are the weighted average of the chemical shifts of the resoances that are exchanging on the NMR time scale. The coalescence temperature for the resonances and the difference between the chemical shifts of the species that contribute to the averaged resonance enable the rate of the exchange to be quantified and the energy barrier for the exchange process to be calculated[24]. The exchanging ring resonances coalesce at about –70 °C but they are still too broad to be observed at -100 °C. The *t*-butyl resonances coalesce at -69 °C and the chemical shift difference at the coalescence temperature, extrapolated from the lower temperature data, is 1300 Hz (Figure 11).

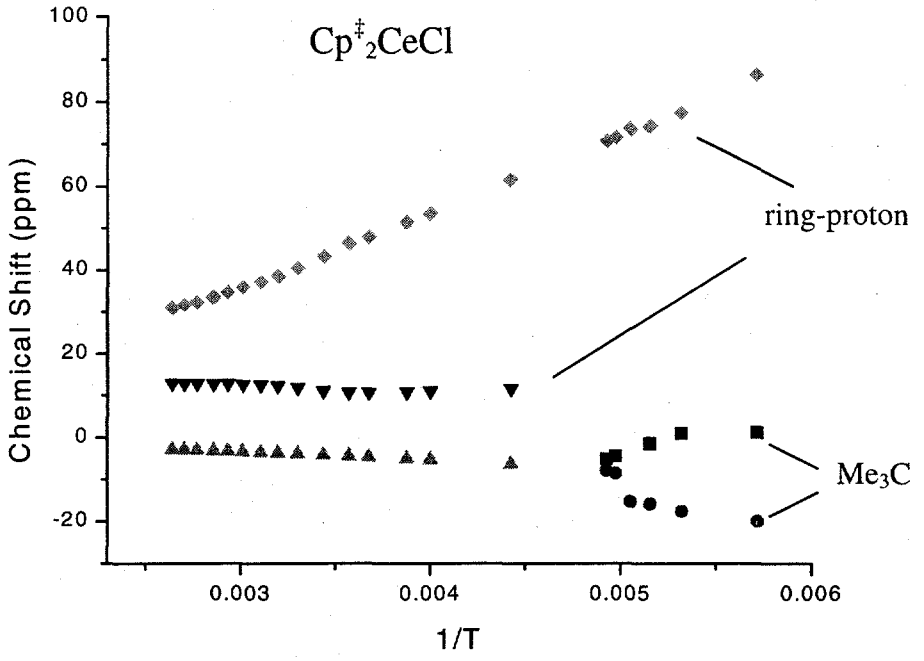

Figure 11: Plot of chemical shifts vs. 1/T, $Cp^{\ddagger}_2CeCl$

The barrier for exchanging the *t*-butyl environments in the compound is 14 kJ/mol (Equation 1).

$$k = \frac{\pi \Delta\delta}{\sqrt{2}} = e^{-\Delta G^{\ddagger} / RT}$$

$$\Delta G^{\ddagger} = -RT \ln k$$

Equation 1: Activation barrier for equal population, two-site exchange

Reaction mixtures with two equivalents of cyclopentadienyl anion and one equivalent of cerium(III) chloride in tetrahydrofuran contain both $Cp^{\ddagger}_2CeCl$ and $Cp^{\ddagger}_3Ce$. Both products are isolable in pure form from reaction mixtures containing two and three cyclopentadienyl groups per cerium atom, respectively, but the yields are low and the second crop of crystals invariably contains *both* species. The chloride ion is competing effectively for the coordination site with the cyclopentadienyl group (Figure 12).

$$Cp^{\ddagger}_2CeCl + \tfrac{1}{2}\, Cp^{\ddagger}_2Mg \underset{THF}{\rightleftharpoons} Cp^{\ddagger}_3Ce + \tfrac{1}{2}\, MgCl_2$$

Figure 12:Chloride ion competes with $Cp^{\ddagger}$ for coordination site

Even when a large excess of cyclopentadienyl ligand is added to the mixture, the reaction is not completely driven to the tris-substituted compound. Using a less polar solvent to encourage precipitation of the magnesium chloride by-product in order to shift the equilibrium toward the product is not practical since cerium chloride is only sparingly soluble in tetrahydrofuran and the reaction does not proceed at an appreciable rate in less polar solvents.

Further inhibiting the utility of the $CeCl_3$ starting material is the fact that Cp'_2CeCl species are of limited value as alkyl precursors due to the propensity of lanthanide elements to form complexes of the type, $Cp'_2Ce(\mu\text{-}Cl)_2Li(solvent)_2$.

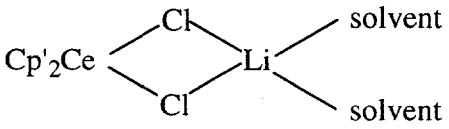

Figure 13: Bonding scheme for lithium chloride adducts of Cp'_2CeCl

If $Cp^{\ddagger}_2CeCl$ is treated with MeLi in ether, multiple extractions and triturations in hexane fail to yield a product that tests negative for Li^+ (flame test) and Cl^- ($AgNO_{3(aq)}$).

The analogous iodide complex was prepared from $Cp^{\ddagger}_2CeCl$ and trimethylsilyl iodide in an attempt to improve the leaving group.

$$[Cp^{\ddagger}_2CeCl]_2 + 2\ Me_3SiI \xrightarrow{Et_2O} [Cp^{\ddagger}_2CeI]_2$$

The iodide anion also competes with the cyclopentadienyl group for coordination to cerium and $Cp^{\ddagger}_2CeI$ cannot be quantitatively converted to $Cp^{\ddagger}_3Ce$. Substitution of $Cp^{\ddagger}_2CeI$ using alkyl- or amidolithium reagents frequently results in formation of lithium

halide complexes, as was observed with $Cp^{‡}_2CeCl$. For example, when $Cp^{‡}_2CeI$ is treated with lithium bis(trimethylsilyl)amide in THF, $Cp^{‡}_2CeI_2Li(THF)_2$ (Figure 14) is isolated in low yield.

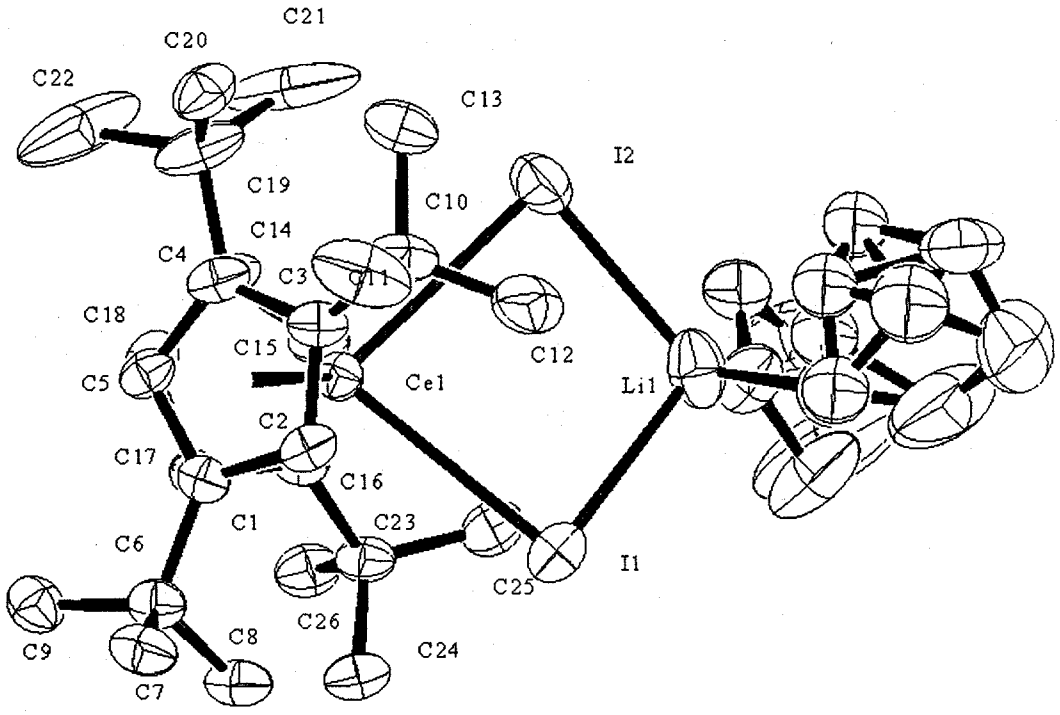

Figure 14: ORTEP diagram of $Cp^{‡}_2CeI_2Li(THF)_2$, 50% thermal elipsoids

Ce-C1	2.808(5)	Ce-ring centroid	2.53, 2.52
Ce-C2	2.821(6)	Ce-I	3.2232(5), 3.2251(5)
Ce-C3	2.845(6)	Ce···Li	4.14(1)
Ce-C4	2.767(6)	Li-I	2.79(1), 2.77(1)
Ce-C5	2.758(6)	Li-O	1.90(1), 1.95(2)
Ce-C14	2.806(6)	ring centroid-Ce-ring centroid	126°
Ce-C15	2.833(6)		
Ce-C16	2.847(6)	angle between cyclopentadienyl planes	60.53(1)°
Ce-C17	2.747(6)		
Ce-C18	2.723(6)	I-Ce-I	82.93(1)°

Table 4:Structural data for $Cp^{‡}_2CeI_2Li(THF)_2$, distances in Å

The tetrahydrofuran complex of cerium iodide[25] is more soluble in tetrahydrofuran than the base-free chloride salt, which significantly increases the reaction rates for preparation

$Cp^{‡}_2CeI$. In addition, the tetrahydrofuran adduct of cerium(III) iodide is sufficiently soluble in toluene that reactions proceed at a practical rate. Preparation of $Cp^{‡}_2CeI$ in tetrahydrofuran results in a mixture of $Cp^{‡}_2CeI$ and $Cp^{‡}_3Ce$ but in toluene solution, no $Cp^{‡}_3Ce$ is formed and the reaction produces $Cp^{‡}_2CeI$ in high yield.

Similar to $Cp^{‡}_2CeCl$, bis(di-*t*-butylcyclopentadienyl)cerium iodide is dimeric. In solution, this is illustrated by a crossover experiment. When a sample of $Cp^{‡}_2CeI$ is mixed with an equimolar amount of $Cp^{‡}_2CeCl$ in benzene-d_6, resonances are observed for $Cp^{‡}_2CeI$, $Cp^{‡}_2CeCl$, and for $[Cp^{‡}_2Ce]_2\mu$-(Cl)μ-(I) in statistically appropriate ratios. The variable temperature NMR spectra of $Cp^{‡}_2CeI$ are similar to those observed for $Cp^{‡}_2CeCl$ and the barrier for cyclopentadienyl ring rotation is 13 kJ/mol.

In an attempt to find a leaving group which would compete less effectively with the di-*t*-butylcyclopentadienyl ligand for the coordination site on cerium, the trifluoromethanesulfonate complex, $Cp^{‡}_2CeOSO_2CF_3$, was prepared from $Cp^{‡}_2CeI$ and trimethylsilyltrifluoromethanesulfonate.

$$[Cp^{‡}_2CeI]_2 + 2\ Me_3Si(OSO_2CF_3) \xrightarrow{Et_2O} 2\ Cp^{‡}_2CeOSO_2CF_3$$

When this compound is treated with one-half an equivalent of $Cp^{‡}_2Mg$, blue, $Cp^{‡}_3Ce$ is formed and no $Cp^{‡}_2CeOSO_2CF_3$ is detected by ^1H NMR spectroscopy either in the crystallized product or in the mother liquor. The anion competition observed with $CeCl_3$ was verified by treating $Cp^{‡}_3Ce$ in tetrahydrofuran with dry KCl or $MgCl_2$. The blue solution changes color to orange and $Cp^{‡}_2CeCl$ is isolated. When $Cp^{‡}_3Ce$ is treated with dry $Mg(OSO_2CF_3)_2$, the blue color remains and no $Cp^{‡}_2CeOS_2CF_3$ is detected.

$$\begin{aligned} Cp^{‡}_2CeCl + \tfrac{1}{2}\ Cp^{‡}_2Mg &\rightleftharpoons Cp^{‡}_3Ce + \tfrac{1}{2}\ MgCl_2 \\ Cp^{‡}_2CeCl + \tfrac{1}{2}\ Cp^{‡}_2Mg &\rightleftharpoons Cp^{‡}_3Ce + \tfrac{1}{2}\ MgI_2 \\ Cp^{‡}_2CeOSO_2CF_3 + \tfrac{1}{2}\ Cp^{‡}_2Mg &\longrightarrow Cp^{‡}_3Ce + \tfrac{1}{2}\ Mg(OSO_2CF_3)_2 \end{aligned}$$

A more direct route to $Cp^{\ddagger}_3Ce$ is to treat cerium(III) trifluoromethanesulfonate[26-29] with a stoichiometric amount of tetra-*t*-butylmagnesocene. Anhydrous cerium(III) trifluoromethanesulfonate ($Ce(OSO_2CF_3)_3$) was prepared from cerium carbonate and aqueous triflic acid, followed by rigorous drying with heat and reduced pressure. When treated with 1-½ equivalents of $Cp^{\ddagger}_2Mg$ in tetrahydrofuran, the reaction proceeds quickly to $Cp^{\ddagger}_3Ce$ in high yield.

$$Ce(OSO_2CF_3)_3 + 3/2\ MgCp^{\ddagger}_2 \xrightarrow{THF} Cp^{\ddagger}_3Ce + 3/2\ Mg(OSO_2CF_3)_2$$

The tris(di-*t*-butylcyclopentadienyl)cerium compound is blue as a solid but is purple in hexane or tetrahydrofuran solution. The melting point is 240-243 °C and the compound sublimes at 120 °C at 10^{-3} torr.

The ^1H NMR spectrum of $Cp^{\ddagger}_3Ce$ at 30 °C exhibits three resonances: a *t*-butyl resonance at –4.63 ppm ($\nu_{1/2}$ = 12 Hz ,54H); and resonances for the ring protons at 17.0 and 25.8 ppm ($\nu_{1/2}$ = 45 Hz , 6H and $\nu_{1/2}$ = 34 Hz , 3H, respectively). The variable temperature ^1H NMR spectra exhibit no broadening attributable to fluxional behavior and the plot of chemical shift vs. 1/T is linear from -100 to 95 °C (Figure 15) indicating that the *t*-butyl substituents and two of the protons on each cyclopentadienyl ring are equivalent on the NMR time scale throughout this temperature range.

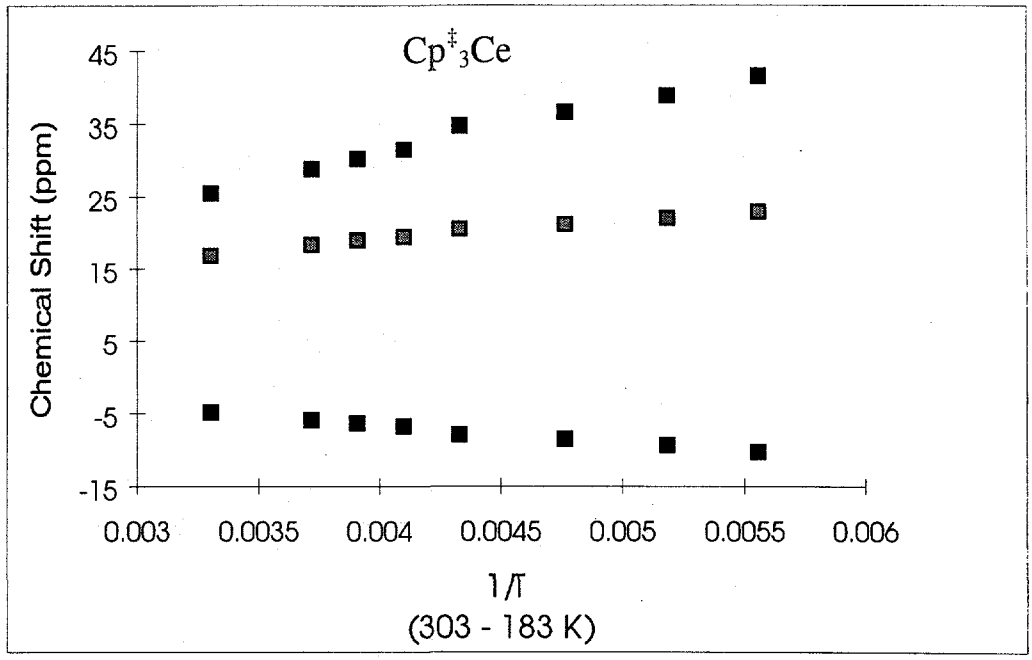

Figure 15: Variable temperature ^{1}H NMR data, $Cp^{\ddagger}_3Ce$

The single crystal X-ray structure of the compound has been solved and molecule has C_{3h} symmetry (Figure 16). In the solid state, $Cp^{\ddagger}_2CeCl$ has magnetically inequivalent *t*-butyl groups that contributed to an averaged resonance in the NMR spectrum at 30 °C. In $Cp^{\ddagger}_3Ce$, however, the *t*-butyl groups are equivalent in the solid state and a single resonance is observable for the protons of the *t*-butyl groups at all temperatures. It is impossible to distinguish between a fluxional process with a low barrier, which makes the substituents equivalent on the NMR time scale, and a compound that maintains the C_{3h} configuration in solution, without rotation of the cyclopentadienyl rings.

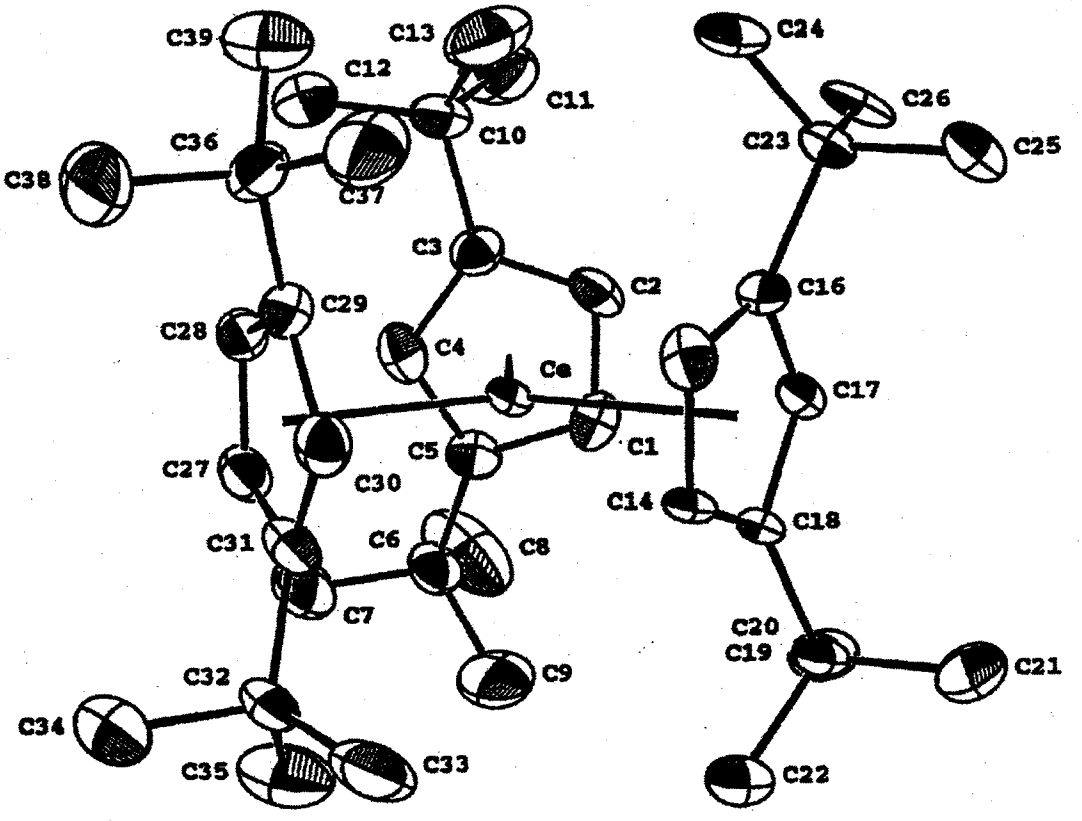

Figure 16:ORTEP diagram of $Cp^{‡}_3Ce$, 50% thermal ellipsoids

$Cp^{‡}_3Ce$		$[(Me_3Si)_2C_5H_3]_3Ce$ [14]	
Ce-ring centroid (avg.)	2.59	Ce-centroid (avg.)	2.57
Ce-C (avg.)	2.86 (2.75-2.95)	Ce-C (avg.)	2.83 (2.75-2.92)
ring centroid-Ce-ring centroid (avg.)	120°	ring centroid-Ce-ring centroid (avg.)	120°

Table 5: Structural comparison of $Cp^{‡}_3Ce$ and $[(Me_3Si)_2C_5H_3]_3Ce$, distances in Å

Bis(di-*t*-butylcyclopentadienyl)cerium methyl can be prepared from methyllithium and $Cp^{‡}_3Ce$ or $Cp^{‡}_2CeOSO_2CF_3$. The compound is orange and decomposes before melting at ~250 °C. The methyl resonance in the ^1H NMR spectrum was not observed between 100 and –100 ppm. It is possible that the contact shift lies outside this window or that the resonance is too broad to observe. Crystals of the complex, suitable for analysis by X-ray

diffraction were not obtained, but elemental analysis and mass spectrometry support the characterization as $Cp^{\ddagger}_2CeMe$.

In solution, $Cp^{\ddagger}_2CeMe$ is only slightly more kinetically stable than Cp''_2CeMe. The compound undergoes a ligand redistribution reaction to form $Cp^{\ddagger}_3Ce$ with a half-life of 7 days at 25 °C. Although longer than the half-life of the bis(trimethylsilyl)cyclopentadienyl compound, the spontaneous decomposition in solution will complicate mechanistic and reactivity studies. Other cyclopentadienyl groups were examined with regard to their utility in kinetic stabilization of the Cp'_2CeR species.

Tri-*t*-butylcyclopentadiene has been prepared using various methods including phase transfer methods[12], metathesis [10], Grignard methods[13], and ring expansion of tri-*t*-butylcyclopropene[30]. In addition to these preparations, $(Me_3C)_3C_5H_3$ can be prepared from $Cp^{\ddagger}_2Mg$ and *t*-butylbromide. Substitution rates for cyclopentadienes decrease as the degree of substitution increases and as a result, none of these preparations is ideal. All, however, produce tri-*t*-butylcyclopentadiene and purification is easily achieved by distillation (140 °C, 10^{-3} torr).

Magnesium tri-*t*-butylcyclopentadienide is prepared from "dibutylmagnesium" and tri-*t*-butylcyclopentadiene in heptane. Metallation of tri-*t*-butylcyclopentadiene is considerably slower than metallation of the disubstituted cyclopentadiene and requires 5-7 days at reflux (55 mmol). Concentrating and cooling the heptane solution (-20 °C) yields colorless crystals of $[(Me_3C)_3C_5H_2]_2Mg$. The ^1H NMR spectrum shows two *t*-butyl resonances with relative intensities of 2:1, and a single ring resonance. These data are consistent with two equivalent cyclopentadienyl rings with 1,2,4-tri-*t*-butyl

substitution. No evidence for the 1,2,3-substituted isomer was detected. The magnesocene melts at 187-189 °C and sublimes at 120 °C (10^{-3} torr). The single crystal X-ray structure confirms that the compound is 1,1',2,2',4,4'-hexa-*t*-butylmagnesocene and the ring are oriented to minimized repulsions between the *t*-butyl substituents (Figure 17).

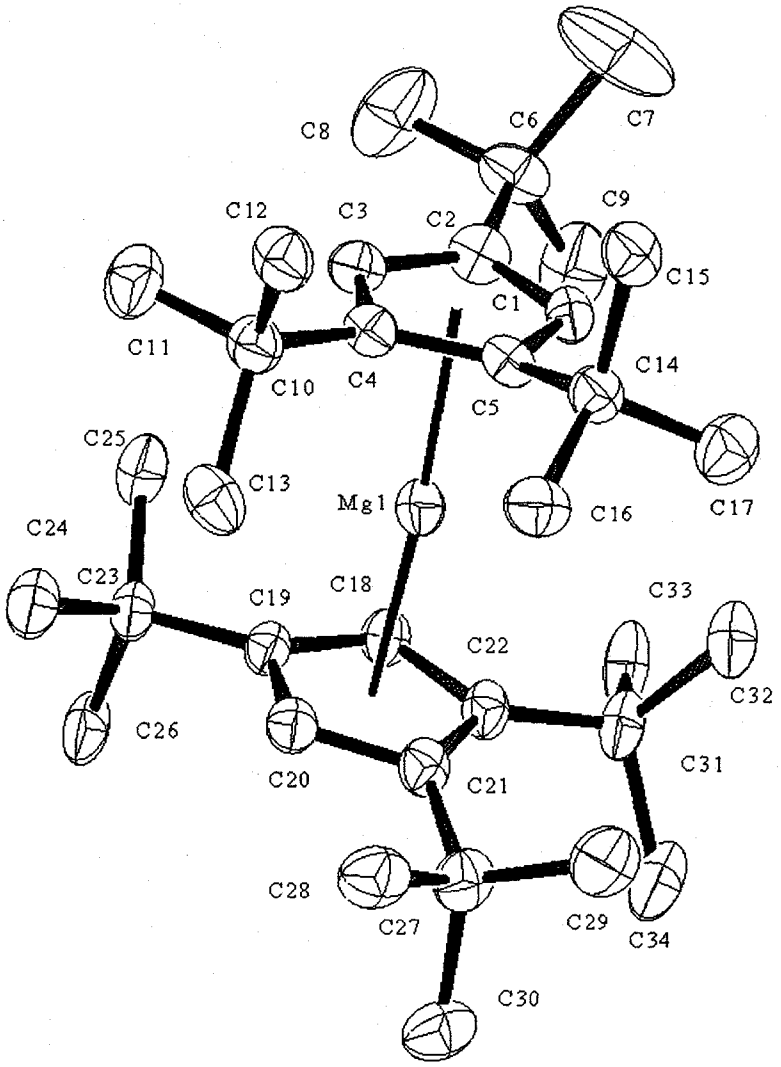

Figure 17: ORTEP diagram of $[(Me_3C)_3C_5H_2]_2Mg$, 50% thermal ellipsoids

Mg-C1	2.450(4)	Mg-ring centroid	2.18, 2.18
Mg-C2	2.545(4)	ring centroid-M-ring centroid	174°
Mg-C3	2.459(4)		
Mg-C4	2.480(4)	angle between cyclopentadienyl planes	7.9°
Mg-C5	2.462(4)		
Mg-C18	2.427(4)		
Mg-C19	2.421(4)		
Mg-C20	2.486(4)		
Mg-C21	2.548(4)		
Mg-C22	2.509(4)		

Table 6: Structural data for $[(Me_3C)_3C_5H_2]_2Mg$, distances in Å

The rate of reaction between hexa-*t*-butylmagnesocene and either the tetrahydrofuran adduct of cerium iodide or anhydrous cerium triflate, under conditions comparable to those used for the preparation of $Cp^{\ddagger}{}_3Ce$, is infinitesimal. Development of the chemistry of bis(tri-*t*-butylcyclopentadienyl)cerium complexes is in progress by another member of this research group[31].

ansa-Cyclopentadienes

Linking two cyclopentadienyl ligands and coordinating them to the same metal is another potentially useful method of preventing ligand redistribution in cerium compounds. Linked cyclopentadienyl ligands, in the form of *ansa*-cyclopentadienyl groups, have experienced dramatic recent growth in applications primarily in the field of catalysis[32-36]. In addition to being relatively inert spectator ligands, *ansa*-cyclopentadienyl groups are commonly used to restrict the coordination environment of the complex, for example, to decrease the ring centroid-metal-ring centroid angle (Figure 18).

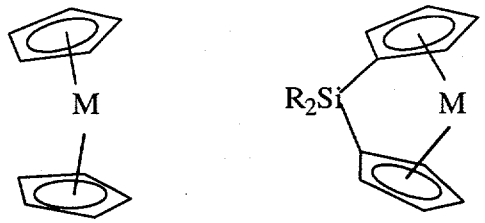

Figure 18: *ansa*-metallocenes have smaller centroid-M-centroid angles

Aside from the steric bulk of substituted *ansa*-cyclopentadienyl groups, the linked-ring ligands have two additional advantages applicable to Cp'_2CeR chemistry. The chelate effect[6] adds kinetic stabilization to the bis-cyclopentadienyl complex, which will decrease the rate of ligand redistribution. Also, formation of a tris-cyclopentadienyl complex would require a dimeric, or larger, structure, which is entropically unfavorable (Figure 19).

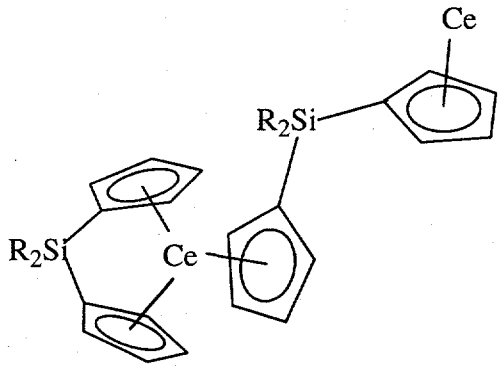

Figure 19: Entropically unfavorable *ansa*-cyclopentadienyl oligamer

The linked cyclopentadiene, $[(Me_3C)_2C_5H_4]_2SiMe_2$, was prepared from $Cp_2^{\ddagger}Mg$ and Br_2SiMe_2[37] in tetrahydrofuran.

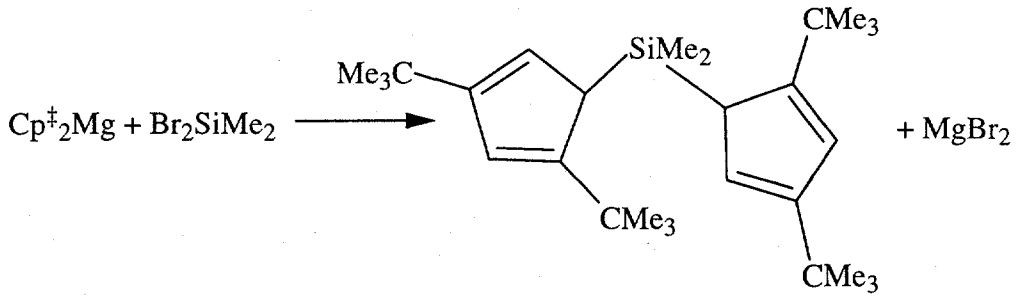

Figure 20: Preparation scheme for a-$Cp^{‡}_2H_2$

The compound forms colorless crystals from hexane in relatively poor yield, presumably due to its high solubility. The compound was treated with "dibutylmagnesium" in a procedure similar to the one used to synthesize the other substituted magnesocenes. The reaction mixture was heated to reflux and stirred for five days. The solvent was removed leaving a colorless solid, but attempts to crystallize the compound from hexane, toluene, or diethylether were unsuccessful. Upon attempted sublimation, the compound decomposes at ~250 °C in dynamic vacuum.

The solid, presumed to be a-$Cp^{‡}_2Mg$, was combined with $FeBr_2$·2THF in tetrahydrofuran. The reaction mixture was stirred for 48 hours at 25 °C and the dark-red product was crystallized from hexane. The compound melts at 140-142 °C and the 500 MHz ^1H NMR spectrum exhibits two resonances for the *t*-butyl protons, one resonance for the methyl groups on the bridging silicon atom, and two resonances for protons bound to the cyclopentadienyl rings. The structure was determined by X-ray crystallography.

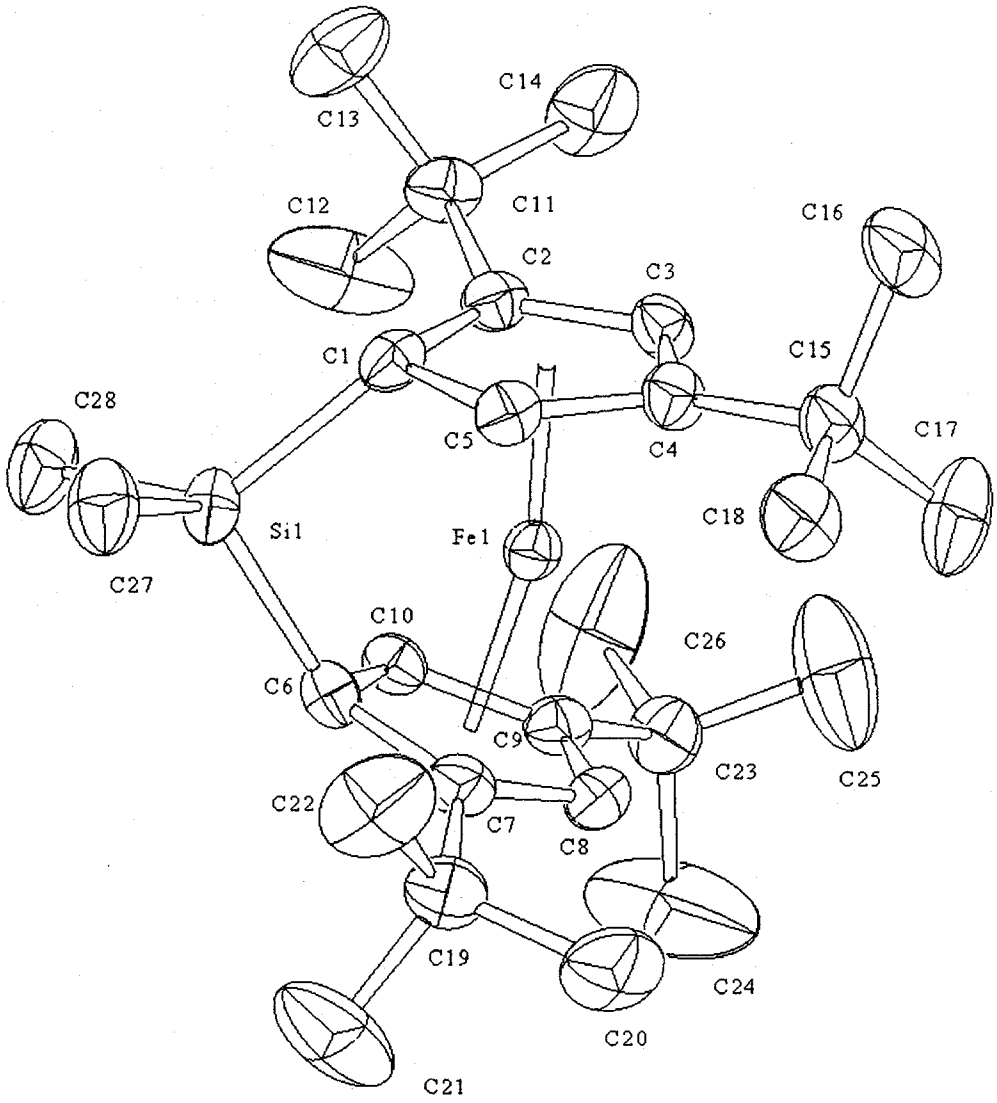

Figure 21: ORTEP diagram of a-Cp$^{‡}_{2}$Fe

Fe-C1	2.021(3)	Fe-ring centroid	1.66, 1.66
Fe-C2	2.086(3)	ring centroid-Fe-ring centroid	166°
Fe-C3	2.093(3)		
Fe-C4	2.091(3)		
Fe-C5	2.034(3)	angle between cyclopentadienyl planes	20.21°
Fe-C6	2.14(3)		
Fe-C7	2.086(3)		
Fe-C8	2.096(3)		
Fe-C9	2.095(3)		
Fe-C10	2.022(3)		

Table 7: Structural data for a-Cp$^{‡}_{2}$Fe, distances in Å

Attempts to synthesize other compounds using the uncharacterized a-$Cp^{\ddagger}_2Mg$ starting material were unsuccessful. Reactions in tetrahydrofuran between "a-$Cp^{\ddagger}_2Mg$" and $MnI_2 \cdot 2THF$, $CeI_3 \cdot 3THF$, $Ce(OSO_2CF_3)_3$, and $TiCl_3 \cdot 3THF$ produced mixtures of products, none of which was isolated in pure form.

Parallel preparations using *t*-butyl and trimethylsilyl substituted cyclopentadienyl ligands show that reaction rates for the formation of cyclopentadienyl complexes are considerably faster for the trimethylsilyl substituted cyclopentadienyl ligands than for the *t*-butyl substituted ligands. Speculation that increased reaction rates may facilitate the preparation of other metallocenes led to the preparation of the tetra-trimethylsilyl *ansa*-cyclopentadiene, a-$(Cp"H)_2$. $Cp"_2Mg$ was treated with Br_2SiMe_2 to generate a-$Cp"_2H_2$. The "tetraene" was isolated as a pale yellow oil by distillation (140 °C, 10^{-4} torr). The tetraene was treated with "dibutylmagnesium" in refluxing heptanes for seven days. As was observed with the *t*-butyl analog, attempts to crystallize the magnesocene were unsuccessful and the compound decomposes upon attempted sublimation.

a-$Cp"_2Fe$ is prepared from the uncharacterized a-$Cp"_2Mg$ product in a preparation analogous to that used to prepare a-$Cp^{\ddagger}_2Fe$. The compound is magenta and melts at 203-205 °C. In contrast to the *t*-butyl substituted *ansa*-compound, the ^1H NMR spectrum of a-$Cp"_2Fe$ exhibits a *single* trimethylsilyl resonance, a resonance for the methyl groups on the bridging silicon atom, and a *single* resonance for the protons bound to the cyclopentadienyl ring. It is notable that a single ring-proton resonance is observed whereas in the analogous tetra-*t*-butyl substituted compound, two ring-proton resonances and two substituent resonances are observed.

The single crystal X-ray structure of the compound shows that the trimethylsilyl groups are at the 3 and 4 positions of the cyclopentadienyl rings (Figure 22).

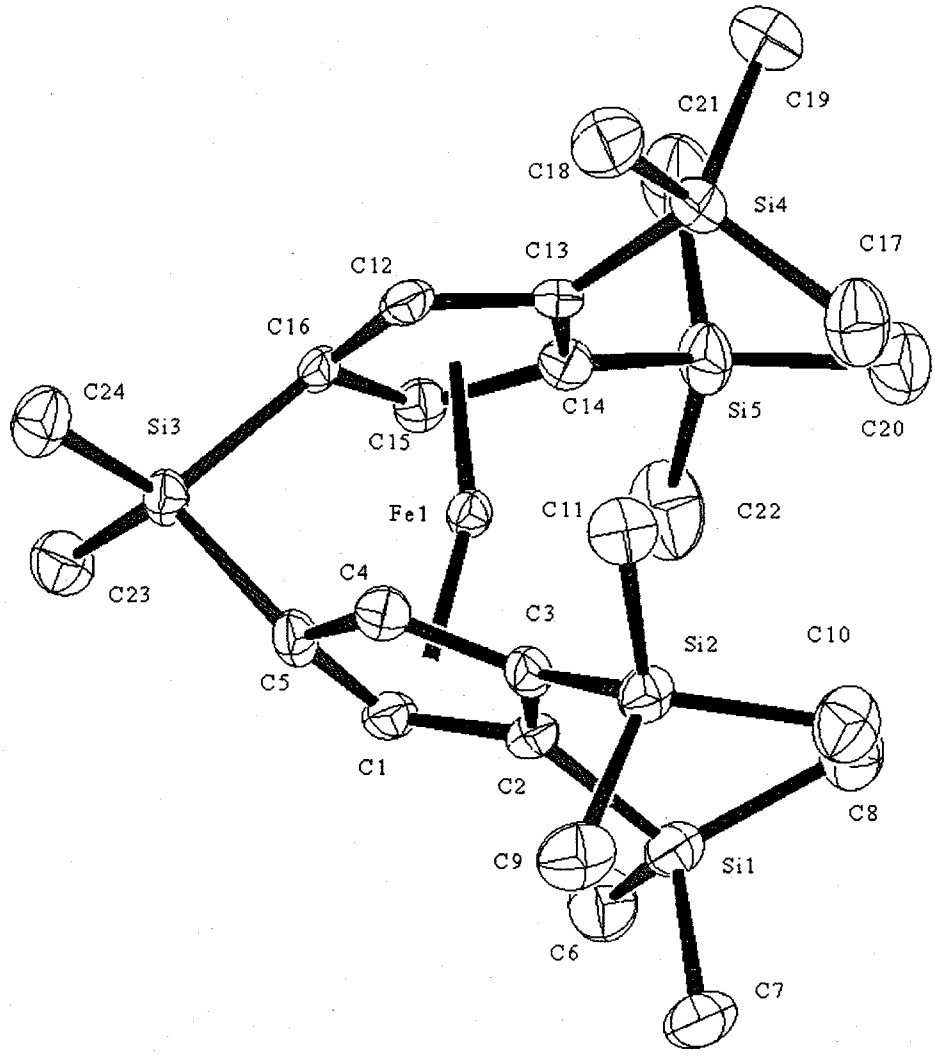

Figure 22:ORTEP diagram of a-Cp"Fe

Fe-C1	2.041(5)	Fe-ring centroid	1.66, 1.67
Fe-C2	2.121(5)	ring centroid-Fe-ring centroid	161°
Fe-C3	2.126(5)	angle between cyclopentadienyl planes	26.06°
Fe-C4	2.039(4)		
Fe-C5	2.025(4)	Fe-C14	2.130(4)
Fe-C12	2.041(5)	Fe-C15	2.033(5)
Fe-C13	2.124(5)	Fe-C16	2.026(4)

Figure 23:Structural data for a-Cp"Fe

The corresponding *t*-butyl substituents in a-$Cp^{\ddagger}_2Fe$ are at the 2 and 4 positions. Since the starting material was not properly characterized, it is impossible to know when the trimethylsilyl group shifted. NMR studies of bis- and tris(trimethylsilyl)-cyclopentadiene have shown that the trimethylsilyl group shifts to form several isomers of the diene[38-40]. Presumably, the trimethylsilyl groups of the dimethylsilyl-bridged bis(trimethylsilyl)cyclopentadienes also shift positions and, upon metallation, form the less strained 3,4-isomer. Analogous shifts for *t*-butyl groups on cyclopentadienes have not been observed and are unlikely based on the fact that 1,2,3-tri-*t*-butylcyclopentadiene can be prepared and does not isomerize to the less sterically hindered, 1,2,4-configuration[30].

Repeated attempts to prepare other transition metal or cerium complexes with the tetrasubstituted *ansa*-cyclopentadienyl ligands were unsuccessful. The uncharacterized a-Cp''_2Mg and a-$Cp^{\ddagger}_2Mg$ and their unpredictable reactivity suggest that alternative starting materials should be investigated. The unsuccessful attempts to crystallize the starting materials may indicate that they are not homogeneous magnesium cyclopentadienides. It is possible that the colorless powder is a mixture of partially metallated ligand and some remaining "dibutylmagnesium". Rather than a metathesis reaction, the iron compounds may be formed from "butyl"iron intermediates or by reduction of iron to form a reactive metallic iron, which oxidatively reacts with the substituted cyclopentadiene. Such a reaction was used by Miller and coworkers to prepare ferrocene[41]. It would not be surprising if the, essentially, *in situ* reaction is not transferable to other metals. New starting materials and the chemistry of *ansa*-Cp'_2CeR compounds are topics for further study.

Fulvalenes

Cyclopentadienyl rings bound directly to each other with a single bond were also explored. Fulvalene compounds have been reported for many early transition metals but the study of fulvalenes has been complicated by the instability of the ligand and its problematic preparation[42]. The dihydrotetra-*t*-butylfulvalene, however is isolable and has been used to synthesize fulvalene compounds[43].

On cerium, the fulvalene ligand is unlikely to form a complex of the type Cp'_2CeR but a bis(fulvalene) bridged dimer is an appealing possibility (Figure 24).

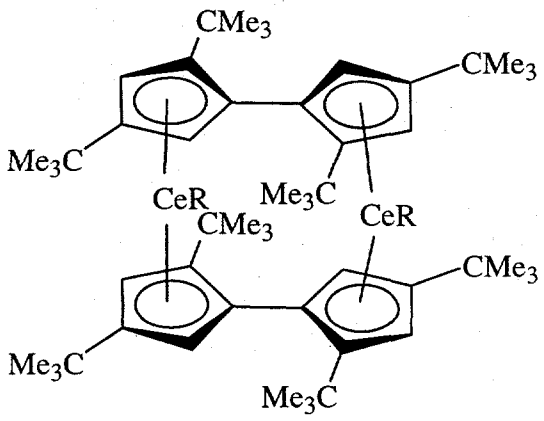

Figure 24: Proposed cerium bis(fulvalene) dimer

Dihydrotetra-*t*-butylpentafulvalene was prepared from $LiCp^{\ddagger}$ and iodine in tetrahydrofuran at –78 °C[42]. The dihydrofulvalene can also be prepared from $Cp^{\ddagger}_2Mg$ and iodine under similar conditions. The product crystallizes from hexane as straw-colored crystals. The tetra-*t*-butyldihydrofulvalene was treated with "dibutylmagnesium" in refluxing heptane for 5 days. The colorless product crystallized when the reaction mixture was concentrated and cooled to –20 °C.

The melting point is greater than 350 °C but the product is soluble in hexane, which suggests that it is not a polymer. The product sublimes at 270 °C at 10^{-3} torr. The ^1H NMR spectrum of the product at 30 °C exhibits two *t*-butyl resonances and two ring proton resonances, which is consistent with a single fulvalene environment. The mass spectrum indicates that the compound is a dimer and the single crystal X-ray structure shows that, in the solid state, the compound is twisted, like a small fragment of a helix, presumably to reduce steric interactions between the *t*-butyl substituents.

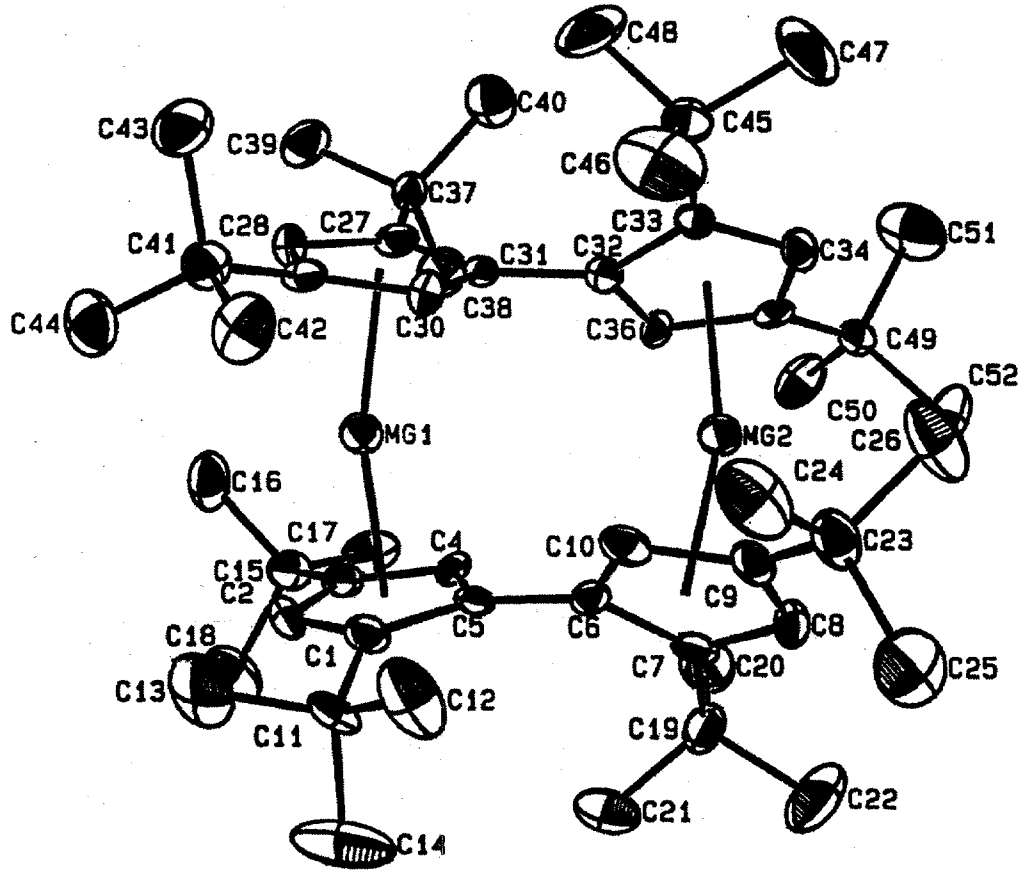

Figure 25:ORTEP diagram of $Fv^{t}_{2}Mg_2$, 50% thermal ellipsoids

Treatment of $FeBr_2 \cdot 2THF$ with $Fv^{\ddagger}{}_2Mg_2$ in tetrahydrofuran yields a dark-red solution. The dark red compound is crystallized from hexane. The ^1H NMR spectrum is similar to that of the magnesium analog. The *t*-butyl resonances are at 1.40 and 1.42 ppm and the ring proton resonances are doublets at 6.36 and 6.15 ppm. The single crystal X-ray structure of the compound was solved and indicates that the compound is isostructural with the bis(tetra-*t*-butylfulvalene)magnesium.

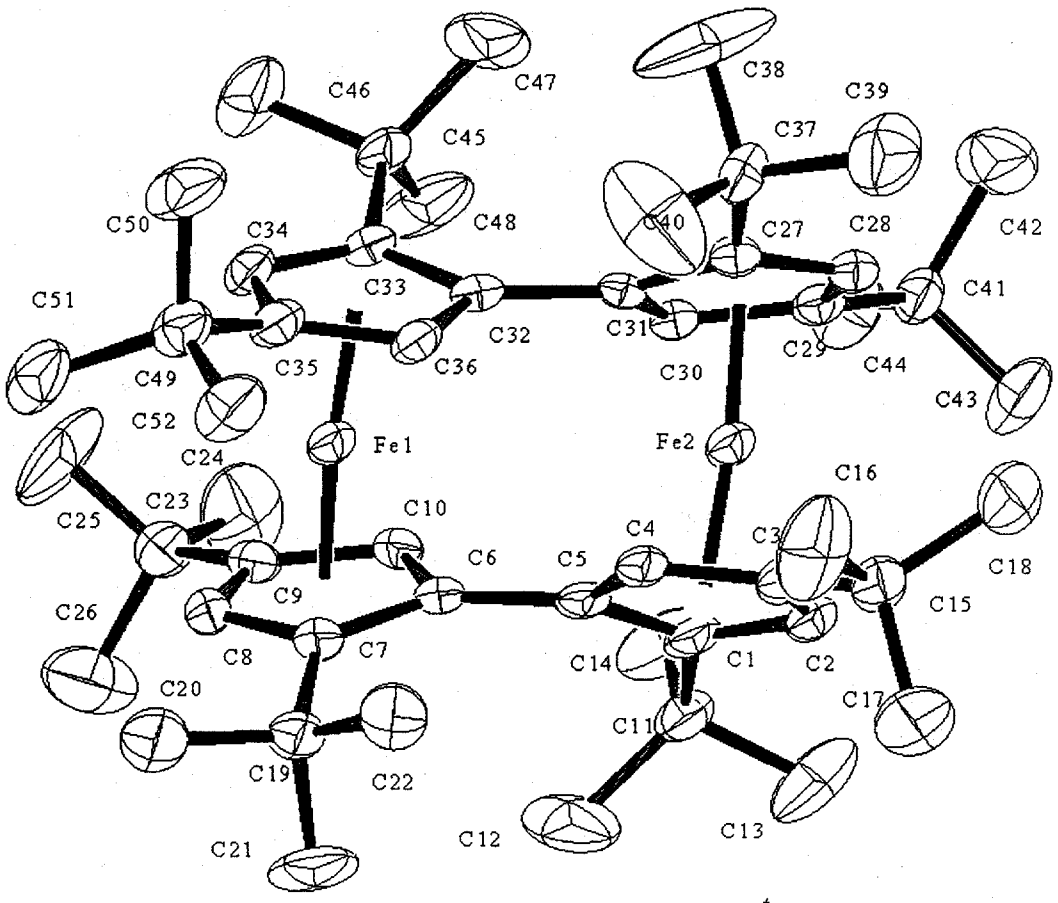

Figure 26:ORTEP diagram of $Fv^{\ddagger}{}_2Fe_2$, 50% thermal elipsoids

Treatment of $MnI_2 \cdot 2THF$ with $Fv^{\ddagger}{}_2Mg_2$ in tetrahydrofuran results in the formation of isostructural $Fv^{\ddagger}{}_2Mn_2$ (Figure 27). The ^1H NMR spectrum of the paramagnetic manganese compound exhibits a single very broad resonance consistent with similar

manganocenes (Chapter 4). Preliminary magnetic susceptibility measurements suggest that the dimer exhibits antiferromagnetic coupling at low temperature.

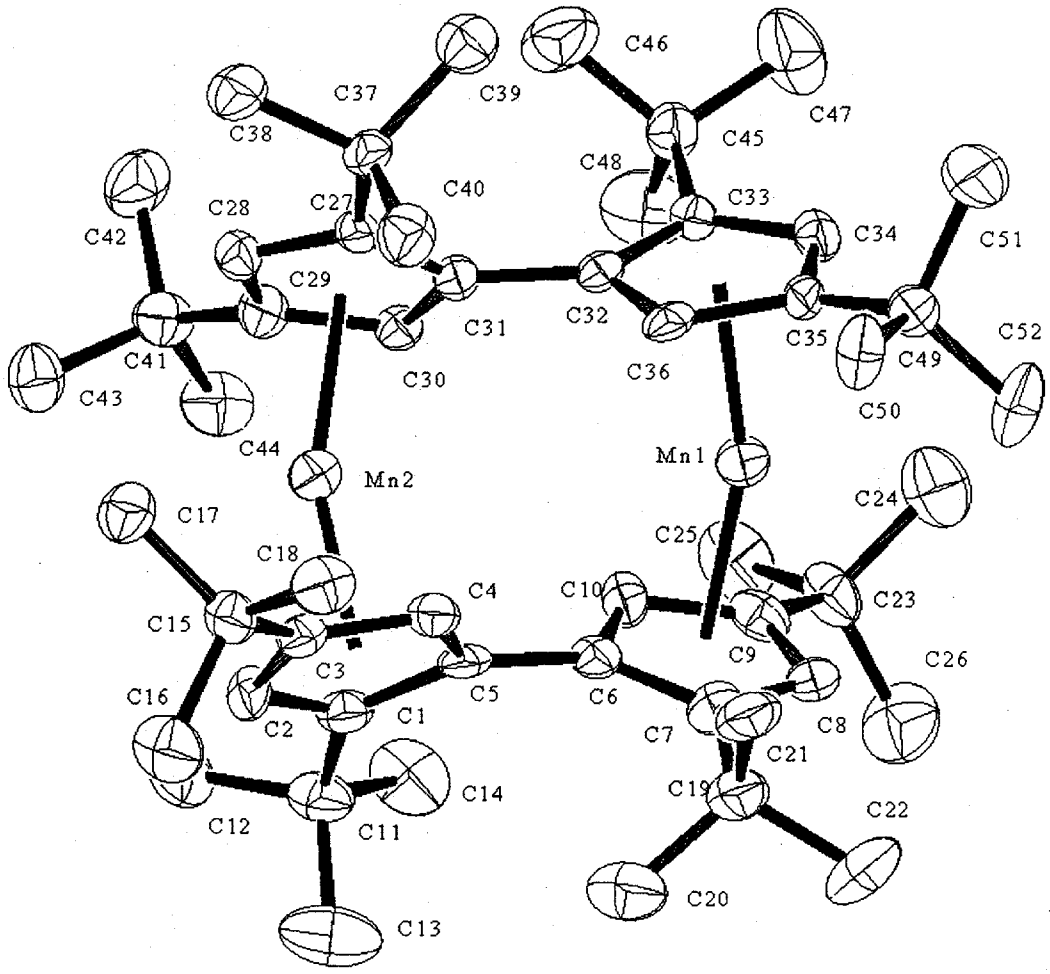

Figure 27:ORTEP diagram of $Fv^{\ddagger}_2Mn_2$, 50% thermal elipsoids

	$Fv^{‡}_2Mg_2$	$Fv^{‡}_2Fe_2$	$Fv^{‡}_2Mn_2$
space group	Pbca (#61)	Pbca	Pbca
cell dimensions	17.637(5)	17.6942 (2)	17.6225(4)
	27.920(5)	27.9725 (4)	27.8231(7)
	19.761(6)	19.3540 (2)	19.9242(4)
cell volume	9731(5) $Å^3$	9579.3 (4) $Å^3$	9769.1 (7) $Å^3$
Z	8	8	8
metal-metal distance	4.232(2)	4.00(1)	4.44(1)
metal-ring centroid distances	2.02, 2.03, 2.10, 2.03	1.70, 1.72, 1.61, 1.59	2.10, 2.11, 2.11, 2.07
average metal-C distance	2.38	2.05	2.40
ring centroid-M-ring centroid angles		174°, 174°	161°, 159°
angle between cyclopentadienyl planes in fulvalene	49°, 48°	39°, 39°	54°,52°

Table 8:Structural comparison of tetra-*t*-butylfulvalene compounds, distances in Å

Attempts to prepare a cerium compound containing the tetra-*t*-butylfulvalene ligand were unsuccessful but the observed structures suggest that a dimer with two reactive sites may be accessible for a large +3 metal ion such as cerium. Synthetic difficulties may be a result of slow substitution rates for sterically demanding cyclopentadienyl ligands as was observed in attempts to prepare a cerium compound from $[(Me_3C)_3C_5H_2]_2Mg$ and cerium salts.

References

1)Collman, J. P.; Hegedus, L. S.; Norton, J. R.; Finke, R. G. *Principles and Applications of Organotransition Metal Chemistry*; University Science Books: Mill Valley, CA, 1987.

2)Cotton, F. A.; Wilkinson, G. *Advanced Inorganic Chemistry*; 6th ed.; John Wiley and Sons: New York, 1999, pp 959.

3)Bagnall, K. W. *Organometallics of the f-Elements*; Marks, T. J. and Fischer, R. D., Ed.; D. Reidel Publishing Co.: Boston, 1978; Vol. 44, pp 221-248.

4)P.B.Hitchcock; M.F.Lappert; R.G.Smith; R.A.Bartlett; P.P.Power *J. Chem. Soc., Chem. Comm.*, **1988**, 1007.

5)Wilkinson, G.; Birmingham, J. M. *J. Am. Chem. Soc.*, **1954**, *76*, 6210.

6)Crabtree, R. H. *The Organometallic Chemistry of the Transition Metals*; 2 nd ed.; John Wiley and Sons: New York, 1994, p.36.

7)Rogers, R. D.; Atwood, J. L. *J. Organomet. Chem.*, **1981**, *216*, 383.

8)Wasserman, H. J.; Zozulin, A. J.; Ryan, R. R.; Salazar, K. V. *J. Organomet. Chem.*, **1983**, *254*, 305.

9)Ni, C.; Deng, D.; Qian, C. *Inorg. Chim. Acta*, **1985**, *110*, L7.

10)Dehmlow, E. V.; Bollmann, C. *Z. Naturforsch. B*, **1993**, *48*, 457.

11)Threlkel, R. S.; Bercaw, J. E. *J. Organomet. Chem.*, **1977**, *136*, 1-5.

12)Venier, C. G.; Casserly, E. W. *J. Am. Chem. Soc*, **1990**, *112*, 2808.

13)Herrmann, W. A. ; Herrmann, W. A., Ed.; Georg Thieme Verlag: New York, 1996; Vol. 1, pp 56-57.

14)Stults, S. D.; Andersen, R. A.; Zalkin, A. *Organometallics*, **1990**, *9*, 115-122.

15)Evans, W. J.; Forrestal, K. J.; Leman, J. T.; Ziller, J. W. *Organometallics*, **1996**, *15*, 527-531.

16)Stults, S. D. *Tris(cyclopentadienyl)cerium and -uranium: Relative Basicity, Structure, and Reactions*; Univerity of California: Berkeley, CA, 1988.

17)Streitwieser, A., Jr.; Heathcock, C. H. *Introduction to Organic Chemistry*; 3rd ed. ed.; Macmillan Publishing Co.: New York, 1985.

18)Tolmann, C. A. *Chem. Rev.*, **1977**, *77*, 313.

19)Kinoshita, T.; Murata, N.; Fujita, R.; Yanagi, Y.; Takeuchi, K. *J. Organomet. Chem.*, **1994**, *471*, 19-21.

20)Fraser, R. R.; Mansour, T. S.; Savard, S. *J. Org. Chem.*, **1985**, *50*, 3232-3234.

21)Duff, A. W.; Hitchcock, P. B.; Lappert, M. F.; Taylor, R. G. *J. Organomet. Chem*, **1985**, *293*, 271-283.

22)Fischer, R. D. *Organometallics of the f-Elements*; Marks, T. J. and Fischer, R. D., Ed.; D. Reidel Publishing Co.: Boston, 1978; Vol. 44, pp 337-377.

23)Lobkovsky, E. B.; Gunko, Y. K.; Bulychev, B. M.; Belsky, V. K.; Soloveichik, G. L.; Antipin, M. Y. *J. Organomet. Chem.*, **1991**, *406*, 343-352.

24)Sandstrom, J. *Dynamic NMR Spectroscopy*; Academic Press: New York, 1982.

25)Hazin, P. N.; Huffman, J. C.; Bruno, J. W. *Organometallics*, **1987**, *6*, 23.-27.

26)Forsberg, J. H.; Spaziano, V. T.; Balasubramanian, T. M.; Liu, G. K.; Kinsley, S. A.; Duckworth, C. A.; Poteruca, J. J.; Brown, P. S.; Miller, J. L. *J. Org. Chem*, **1987**, *52*, 1017.

27)Hahn, F. E.; Mohr, J. , **1990**.

28)Dixon, N. E.; Lawrance, G. A.; Lay, P. A.; Sargeson, A. M.; Taube, H. *Inorg. Synth.*, , *24*, 243-249.

29)Lawrance, G. A. *Chem. Rev.*, **1986**, *86*, 17-33.

30)Donovan, B. T.; Hughes, R. P.; Trujillo, H. A.; Rheingold, A. L. *Organometallics*, **1992**, *11*, 64-69.

31)Werkema, E. L. *Unpublished results.*

32)Christopher, J. N.; Diamond, G. M.; Jordan, R. F.; Petersen, J. L. *Organometallics*, **1996**, *15*, 4038-4044.

33)Christopher, J. N.; Jordan, R. F.; Petersen, J. L.; Young, V. G. *Organometallics*, **1997**, *16*, 3044-3050.

34)Miyake, S.; Bercaw, J. E. *J. Mol. Cat.*, **1998**, *128*, 29-39.

35)Miyake, S.; Henling, L. M.; Bercaw, J. E. *Organometallics*, **1998**, *17*, 5528-5533.

36)Schmidt, K.; Reinmuth, A.; Reif, U.; Diebold, J.; Brintzinger, H. H. *Organometallics*, **1997**, *16*, 1724-1728.

37)Leffler, A. J. *Inorg. Chem.*, **1968**, *7*, 2651-2652.

38)Ashe III, A. J. *J. Am. Chem. Soc.*, **1970**, *92*, 1233-1235.

39)Ustynyuk, Y. A.; Kisin, A. V.; Pribytkova, I. M.; Antonova, N. D. *J. Organomet. Chem.*, **1972**, *42*, 47-63.

40)Ustynyuk, Y. A.; Luzikov, Y. N.; Mstislavsky, V. I.; Azizov, A. A.; Pribytkova, I. M. *J. Organomet. Chem.*, **1975**, *96*, 335-353.

41)Miller, S. A.; Tebboth, J. A.; Tremaine, J. F. *J. Chem. Soc.*, **1952**, 623-635.

42)Brand, R.; Krimmer, H.-P.; Linder, H.-J.; Sturm, V.; Hafner, K. *Tetrahedron Lett.*, **1982**, *23*, 5131-5134.

43)Jutzi, P.; Schnittger, J.; Hursthouse, M. B. *Chem. Ber.*, **1991**, *124*, 1693-1697.

Chapter 3

Stereochemically Labeled Cyclopentadienyl Ligands

Asymmetrically substituted cyclopentadienyl ligands have attracted attention recently as supporting ligands for stereoregular reactive sites on catalysts[1-10]. Examples of catalysts or catalyst models containing cyclopentadienyl ligands that define the stereospecific coordination site have been reviewed[11,12].

The asymmetrically substituted, (trimethylsilyl)(*t*-butyl)cyclopentadienyl ligand (Figure 28) does not form enantiomerically pure compounds or define a stereospecific reactive site on a catalyst but it does provide a stereochemical label that facilitates observation of dynamic processes.

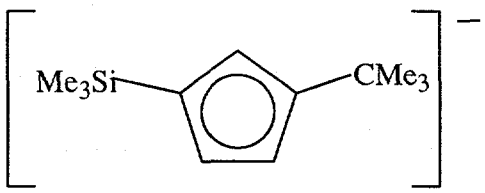

Figure 28: (Trimethylsilyl)(*t*-butyl)cyclopentadienyl ligand, Cp^{tt}.

Trimethylsilyl(*t*-butyl)cyclopentadiene is prepared from cyclopentadiene, which is first substituted with a *t*-butyl group and then with a trimethylsilyl group. Mono-*t*-butylcyclopentadiene has been prepared from fulvene and methyllithium[13], from cyclopentadienyl Grignard and *t*-butyl chloride [14], and from sodium cyclopentadienide and *t*-butyl bromide [15]. It is also collected as a byproduct of the synthesis of di-*t*-butylcyclopentadiene (chapter 2) and can be prepared using the phase transfer method described by Venier and Casserly[16] with appropriate stoichiometric adjustments. The colorless *t*-butylcyclopentadiene is distilled at atmospheric pressure (bp 140 °C) and

again under reduced pressure (40 °C at ~ 8 torr) in order to remove di-*t*-butylcyclopentadiene. Product purity was monitored by gas chromatography and the distillations were repeated until no detectable di-*t*-butylcyclopentadiene remained. *t*-Butylcyclopentadiene is treated with "dibutylmagnesium" in heptane to form 1,1'-di-*t*-butylmagnesocene. The compound is obtained as colorless crystals from heptane. The compound melts at 93-95 °C and sublimes at 80 °C (10^{-3} torr)*. The ^{1}H NMR spectrum exhibits a single *t*-butyl resonance and an AA'BB' set of resonances for the ring protons.

1,1'-Di-*t*-butylmagnesocene reacts with trimethylsilyl chloride in tetrahydrofuran at 25 °C to form (trimethylsilyl)(*t*-butyl)cyclopentadiene ($Cp^{tt}H$). The disubstituted cyclopentadiene is distilled at reduced pressure (40 °C at 10^{-2} torr). The corresponding magnesocene is prepared from $Cp^{tt}H$ and "dibutylmagnesium" in refluxing heptane. After concentrating and cooling the reaction mixture, colorless crystals of Cp^{tt}_2Mg are obtained. The compound melts at 107-108 °C and sublimes at 100 °C (10^{-3} torr). Resonances for two trimethylsilyl groups, two *t*-butyl groups, and two sets of three, ring proton resonances are observed in the 500 MHz ^{1}H NMR spectrum, indicating that there are two different cyclopentadienyl environments (Table 9).

---

* The compound has been prepared by another method but was reported as a liquid at 25 °C [17].

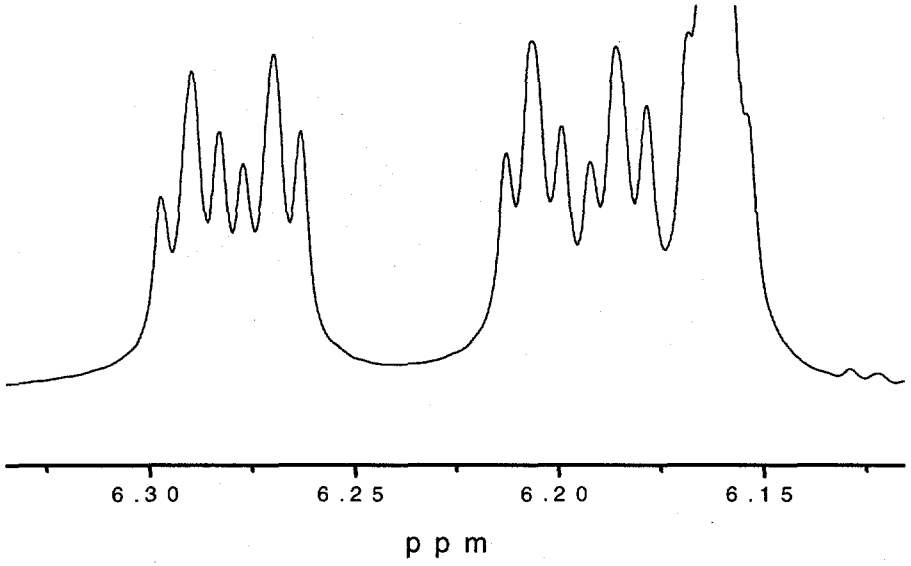

Figure 29: 500 MHz ^{1}H NMR spectrum of Cp^{tt}_2Mg, ring proton region

integration	chemical shift (ppm)	coupling (Hz)		integration	chemical shift (ppm)	coupling (Hz)
9H	0.301	s		9H	0.308	s
9H	1.30	s		9H	1.31	s
1H	6.28	d,d (10,2)		1H	6.28	d,d (10,2)
1H	6.21	d,d (10,2)		1H	6.20	d,d (10,2)
1H	6.16	d,d (2,2)		1H	6.16	d,d (2,2)

Table 9: 500 MHz ^{1}H NMR chemical shifts for Cp^{tt}_2Mg

Compounds containing both an η^1- and an η^5-cyclopenatienyl group have been observed[18-20] and would account for the two cyclopentadienyl environments, but the observed chemical shifts of the two cyclopentadienyl environments in Cp^{tt}_2Mg are very similar (Table 9). It is unlikely that the η^1-and η^5-cyclopentadienyl groups would exhibit such similar resonances. Literature examples of η^1-, η^5-biscyclopentadienyl complexes often show fluxional behavior[21]and references cited therein. The variable temperature ^{1}H NMR spectrum of Cp^{tt}_2Mg shows no changes on the NMR time scale between 30 and 120 °C and no fluxional behavior is observed.

1,1',3,3'-Tetra-*t*-butylmagnesocene ($Cp^{\ddagger}_2Mg$), which is presumed to be isostructural with Cp^{tt}_2Mg, exhibits a single *t*-butyl resonance and an A_2B set of ring resonances in its 500 MHz ^1H NMR spectrum, indicating that the cyclopentadienyl groups are either frozen in a symmetric orientation, or undergoing a fluxional process so that the *t*-butyl substituents are equivalent on the NMR time scale (see chapter 2)(Figure 30). The variable temperature ^1H NMR spectrum of $Cp^{\ddagger}_2Mg$ shows no changes on the NMR time scale between 30 and 100 °C and no fluxional behavior is observed, suggesting that the compound has idealized C_2v symmetry and symmetry operations (a C_2 axis and a two orthogonal mirror planes) equate both of the cyclopentadienyl rings within the molecule.

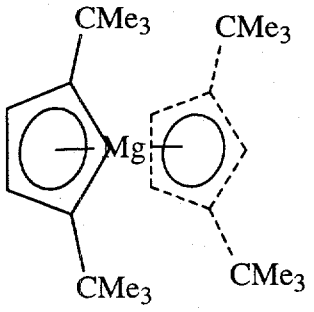

C_{2v}

Figure 30: One *t*-butyl environment, $Cp^{\ddagger}_2Mg$

For Cp^{tt}_2Mg, there are two inequivalent orientations that the two cyclopentadienyl rings in the molecule can assume due to the lower symmetry of the asymmetrically substituted cyclopentadienyl rings. The cyclopentadienyl rings may be oriented so that Cp^{tt}_2Mg attains idealized C_2 symmetry (a C_2 axis relates the top and bottom cyclopentadienyl ligands) or C_S symmetry (a horizontal mirror plane relates the top and bottom cyclopentadienyl ligands). (Figure 31).

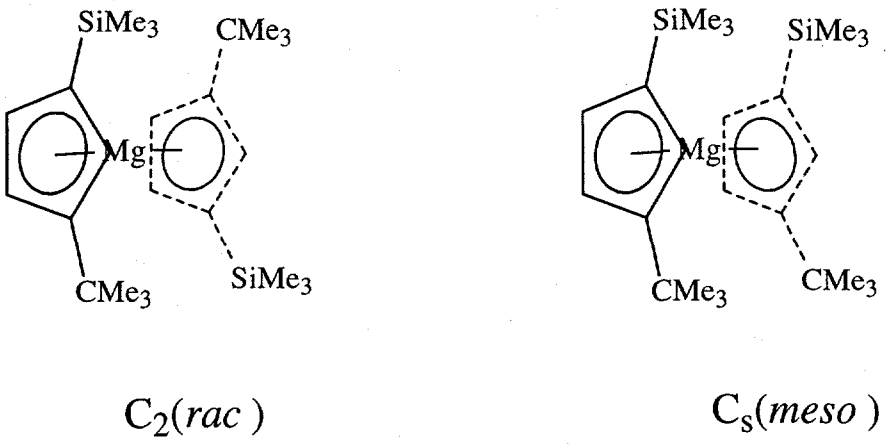

$C_2(rac)$ $C_s(meso)$

Figure 31: Two *t*-butyl and two trimethylsilyl environments, Cp^{tt}_2Mg

For both the C_2 and C_S symmetry molecules, the *t*-butyl and trimethylsilyl substituents and analogous ring protons on each of the two cyclopentadienyl ligands in each molecule are chemically and magnetically equivalent, so that a single *t*-butyl resonance, a single trimethylsilyl resonance and an ABC ring proton spin system should be observed in the ^{1}H NMR spectrum of either molecule. However, the C_2 and C_S symmetry molecules are not chemically equivalent, they are diastereomers, which have different free energies, and would be expected to display different chemical shifts in the absence of chemical exchange. If both the C_2 and C_S symmetry molecules were present in the same sample, two *t*-butyl resonances, two trimethylsilyl resonances and two ABC ring proton spin systems, one resonance for each chemically and magnetically inequivalent group for each of the molecules, should be observed in the ^{1}H NMR spectrum of the mixture. This prediction, based on the symmetry analysis of the magnesocene containing two asymmetrically substituted cyclopentadienyl ligands, is consistent with the observed ^{1}H NMR spectrum of Cp^{tt}_2Mg. The difference in chemical

shift for the two diastereomers is small (Figure 29, Table 9), suggesting that the chemical and magnetic environments in the two diastereomers is quite similar, and the relative ratio of the population of the isomers is 1:1, suggesting that there is little difference in the ground state free energy of the diastereomers.

Right-handed and Left-handed Ligands

Careful consideration of the full symmetry of the (trimethylsilyl)(*t*-butyl)cyclopentadienyl ring reveals that the asymmetrically substituted cyclopentadienyl ring bound in an η^5 fashion to a metal constitutes a chiral center. Three vectors in Figure 32 describe the stereocenter: vector "A" is from the ring-centroid to the trimethylsilyl group, vector "B" is from the ring centroid to the *t*-butyl group, and vector "C" is from the ring centroid to the metal atom. The three vectors, in Figure 32, comprise a *right-hand triple*[22]. The ligands in Figure 32 are both right-handed cyclopentadienyl ligands. Rotation of the ring about its metal-centroid axis does not convert a right-handed ring to a left-handed ring.

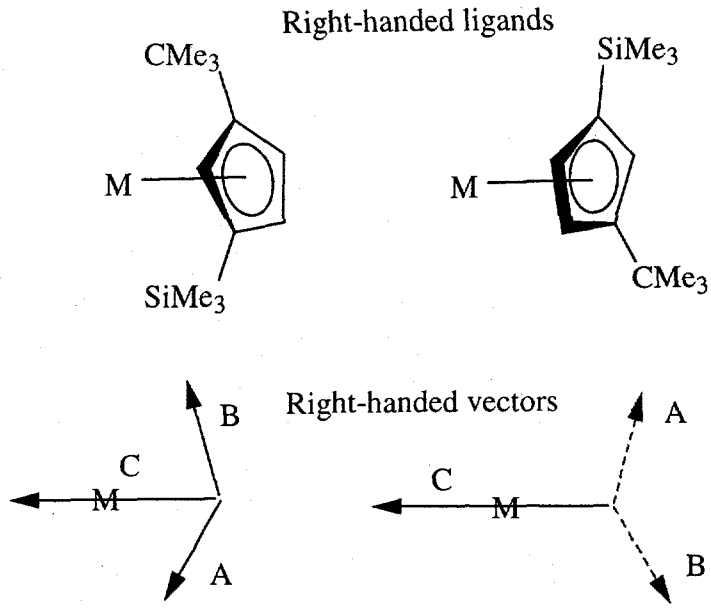

Figure 32; Right-handed cyclopentadienyl groups

If the vectors, A, B, and C, form a *left-hand triple*, the ligand is a left-handed cyclopentadienyl group (Figure 33).

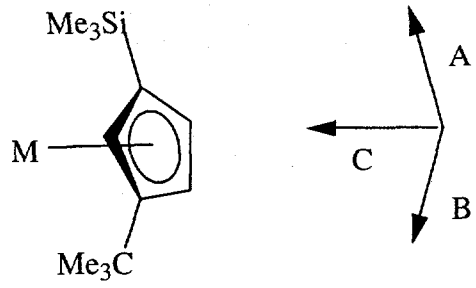

Figure 33: Left-handed cyclopentadienyl ligand

Conversion between a right-handed cyclopentadienyl ring and a left-handed cyclopentadienyl ring can be accomplished by changing the face of the cyclopentadienyl ligand to which the metal is bound. Using a right-hand triple, the metal atom now lies in the negative domain of axis "C", constituting a left-hand triple(Figure 34).

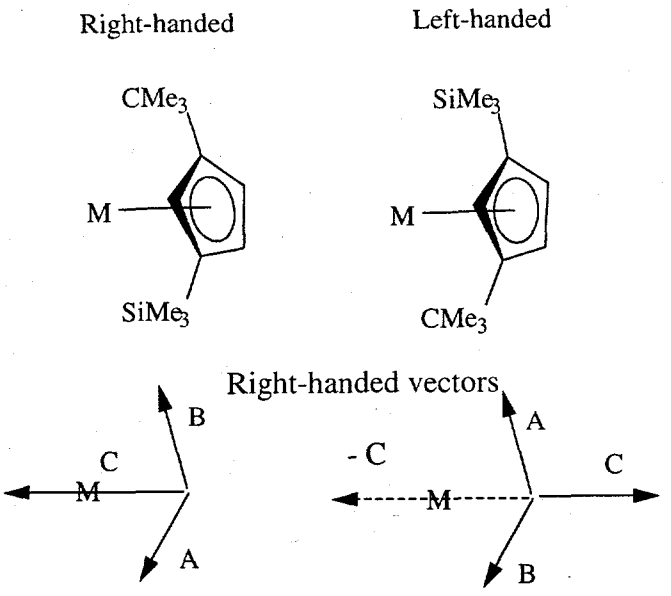

Figure 34; Right-handed coordinate system

The right- and left-handed cyclopentadienyl ligands generate four isomers of Cp^{tt}_2Mg. The relationships between the four isomers are summarized in Figure 35. The right/right and left/left isomers are enantiomers with C_2 symmetry. The right/left and left/right isomers are enantiomers with C_S symmetry.

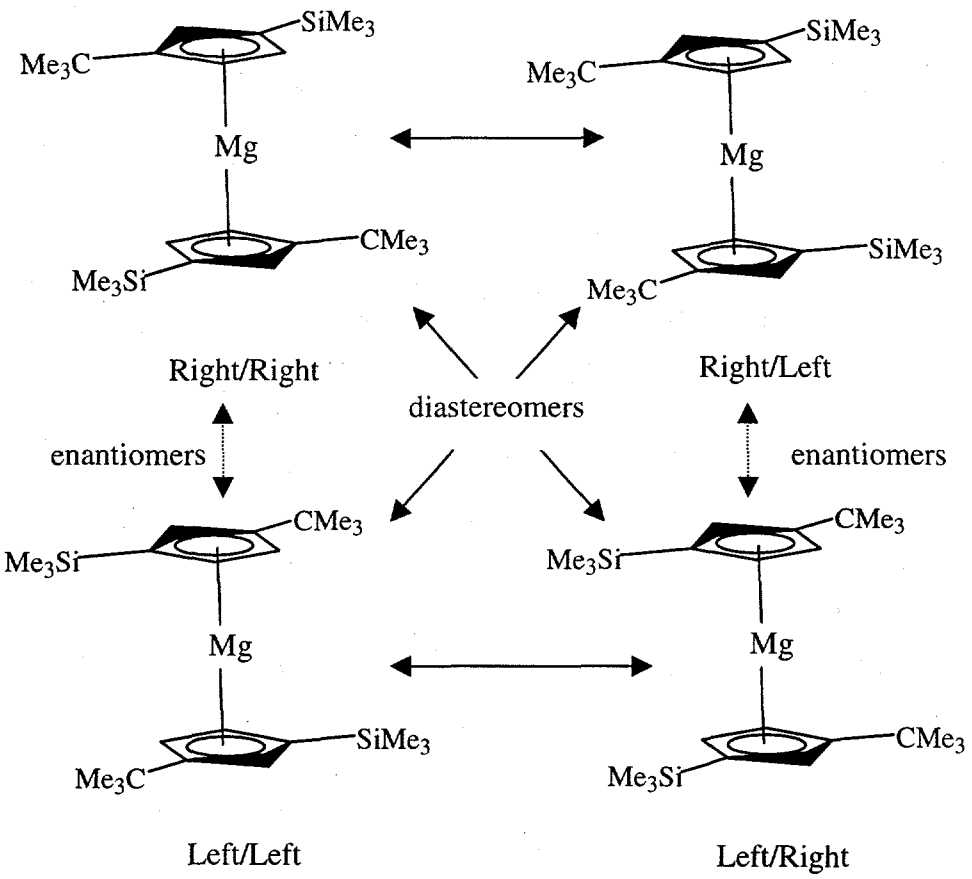

Figure 35: Four isomers of Cp^{tt}_2Mg, enantiomeric and diastereomeric relationships

Enantiomers have identical physical and chemical properties in an achiral environment, except for the direction that each enantiomer would rotate plane-polarized light. Consequently, the enantiomers cannot be resolved in the ^1H NMR spectra of Cp^{tt}_2Mg, which is presumably a racemic mixture of all of the isomers depicted in Figure 35. Pure samples of either of the C_2 enantiomers would exhibit optical activity[23] but no efforts were made to resolve the racemic mixtures. The C_S enantiomers would not display optical activity, since the rotation of plane polarized light effected by one of the chiral (trimethylsilyl)(*t*-butyl)cyclopentadienyl ligands would be identical in magnitude and opposite in direction to that caused by the other (trimethylsilyl)(*t*-

butyl)cyclopentadienyl ligand with the opposite handedness within the same molecule. The C_S isomers are *meso* in that the right/left and left/right isomers are mirror images of each other and are related by rotation. Rotating the right/left isomer in Figure 35 about an axis perpendicular to the ring centroid-ring centroid axis, produces the left/right isomer. The right/right and left/left isomers are not related by rotation.

The C_2 enantiomers (right/right and left/left) are diastereomers of the C_S enantiomers (right/left and left/right). Only the two sets of diastereomers are distinguishable by NMR spectroscopy (Table 10). Each preparation of Cp^{tt}_2Mg results in a 1:1 ratio of diastereomers in solution. It is possible that the ratio of isomers is set during synthesis and the handedness of Cp^{tt}_2Mg ligands is preserved under all conditions. Alternatively, the diastereomers may be in equilibrium and the C_2 and C_S isomers are interconverting at some rate.

conformational isomers	right-right	left-left	left-right	right-left
optically active isomers	✓	✓	X	X
isomers resolvable by NMR	C_2	C_2	C_S	C_S

Table 10: Conformational isomers of Cp^{tt}_2Mg

If the Cp^{tt}_2Mg diastereomers are interconverting rapidly on the NMR timescale, broadening followed by coalescence of the analogous resonances for each of the diastereomers would be observed in the variable temperature NMR spectra. However, no broadening is observed of any of the ^1H NMR resonances of the mixture of diastereomers at temperatures of up to 120 °C.

If the diastereomers were in equilibrium but interconverting on a somewhat slower time scale, changing the temperature of the mixture would be expected to change

the relative populations of the species, however, attempts to change the populations of the Cp^{tt}_2Mg diastereomers thermally failed. Presumably, the ground state free energy difference between the diastereomers is very small, and it is, therefore, not be possible to perturb the diastereomer populations measurably at these temperatures.

Diastereomers have different physical properties and separation of diastereomers is frequently possible. If the diastereomers could be separated, regeneration of a mixture of diastereomers from a single isolated diastereomer would verify that the C_2 and C_S isomers interconvert on the laboratory time scale. Attempts at separation of the isomers by differential crystallization or sublimation have been unsuccessful. Separation of diastereomers has been accomplished in many systems, often by derivatization with an enantiomerically pure substituent followed by chromatography, however, this process is time consuming and expensive. The asymmetrically substituted cyclopentadienyl ring in Cp^{tt}_2Mg provides a spectroscopic alternative for detecting interconversion of the C_2 and C_S diastereomers.

Exchange Spectroscopy

If the Cp^{tt}_2Mg diastereomers are interconverting on the laboratory time scale, their interconversion may be observable using magnetization transfer NMR experiments. Interconversion of the diastereomers would result in magnetization transfer between the analogous resonances in the C_2 and C_S isomers. Since the cyclopentadienyl environments are quite similar, there is only a small difference in chemical shift between analogous resonances in the C_2 and C_S diastereomers. Because the difference in chemical shift is small, a one dimensional spin saturation transfer experiment is impractical; it is not

possible to selectively irradiate a resonance for a single diastereomer without also irradiating the nearby resonance of the other diastereomer. A two dimensional EXSY (EXchange SpectroscopY) experiment[24-26], in which all of the resonances are irradiated simultaneously, can be used to trace the magnetization exchange pathways in a sample with small separation of chemical shifts.

The same NMR experiment provides nOe (Nuclear Overhauser effect) magnetization transfer information that can be used to unambiguously assign the chemical shifts of the ring resonances of the cyclopentadienyl ligands. For small molecules, like Cp^{tt}_2Mg, the nOe and EXSY magnetization transfer resonances would have opposite phases, and are therefore, distinguishable from each other.

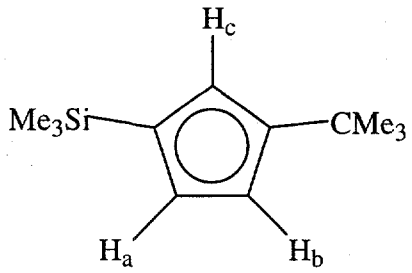

Strong antiphase nOe cross peaks are observed between the trimethylsilyl resonance for each isomer and the cyclopentadienyl ring proton resonances at 6.28 and 6.16 ppm. Strong antiphase nOe cross peaks are also observed between the *t*-butyl resonance for each isomer and the cyclopentadienyl ring proton resonances at 6.19 and 6.16 ppm. Since nOe cross peaks are observed between the upfield cyclopentadienyl ring resonance (6.16 ppm) and both the trimethylsilyl resonance and the *t*-butyl resonance, this absorption corresponds to the hydrogen atom that is located between the trimethylsilyl and the *t*-butyl groups on the cyclopentadienyl ring (H_c). This assignment is consistent with the observation that the proton coupling observed for this resonance is

quite small ($^4J_{HH}$ = 3 Hz) consistent with the four-bond H-H coupling that would be expected for the hydrogen in this position on the cyclopentadienyl ring. The downfield proton resonance (6.28 ppm) experiences nOe only from the trimethylsilyl substituent and is therefore located adjacent to the trimethylsilyl group (H_a). The proton resonance at 6.19 ppm experiences nOe only from the *t*-butyl substituent and is therefore located adjacent to the *t*-butyl group (H_b). Both of these resonances exhibit stronger H-H coupling ($^3J_{HH}$ = 10 Hz), consistent with three-bond coupling between these two protons as well as the smaller ($^4J_{HH}$ = 3 Hz) four-bond H-H coupling to the hydrogen located between the trimethylsilyl and *t*-butyl substituents on the cyclopentadieyl ring. With these assignments completed, the EXSY experiment can be considered in greater detail.

The threshold of detection using EXSY requires that 1% of the sample undergoes conversion between diastereomers during the longitudinal spin relaxation time (T_1) for the exchanging resonances and optimization of the EXSY experiment parameters requires accurate measurements of the T_1's for each of the resonances of the sample. Since the longitudinal relaxation times for NMR resonances of organometallic compounds vary significantly as a function of many parameters including magnetic environment, solvent, and temperature, the T_1's for Cp^{tt}_2Mg were measured and are listed in Table 11.

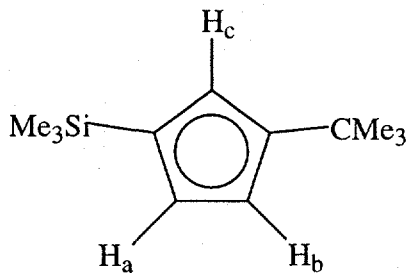

	Chemical shift (ppm)	Longitudinal relaxation times (T_1) (s) 90 °C a	120 °C b
Me_3Si	0.30	3.82	8.11
Me_3C	1.31	2.30	4.20
H_a	6.28	4.46	12.1
H_b	6.19	4.00	11.3
H_c	6.16	4.61	12.2
500 MHz, H_a is distinguishable from H_b using nOe information, a) in toluene-d_8, b) in mesitylene-d_{12}, viscosity increase also contributes to longer T_1's			

Table 11:Spin-lattice relaxation times for Cp^{tt}_2Mg

The T_1's for organometallic compounds are generally longer than those observed for organic compounds and are proportional to the temperature at which they are measured. At higher temperatures, the T_1's are longer, rendering slow exchange easier to detect. Additionally, the interconversion rate of the diastereomers is expected to be proportional to the temperature so the optimum temperature for detecting a slow exchange process is the maximum temperature tolerated by the molecule without decomposition.

Information about the mechanism of the diastereomer interconversion is theoretically accessible, based on analysis of the magnetization transfer pathway. Interconversion of the diastereomers requires that the handedness of one of the (trimethylsilyl)(*t*-butyl)cyclopentadienyl ligands on the $Cptt_2Mg$ molecule be changed. The simplest mechanism which converts a right-handed cyclopentadienyl ring to a left-

handed cyclopentadienyl ring involves changing the face of the ring to which the metal is bound (Figure 36).

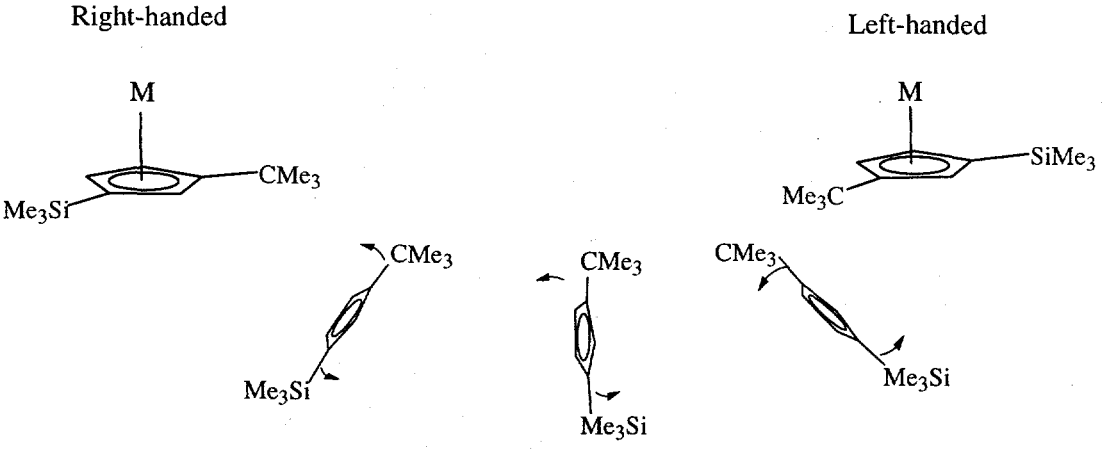

Figure 36:Right-handed to left-handed "ring flip"

An alternative mechanism for diastereomer interconversion involves no face change of the cyclopentadienyl ring but rather a shift of the trimethylsilyl group on the ring. A 1,5-silatropic shift of a trimethylsilyl group on a cyclopentadienyl ligand will convert a right-handed ligand to left without breaking the metal-ligand bond.

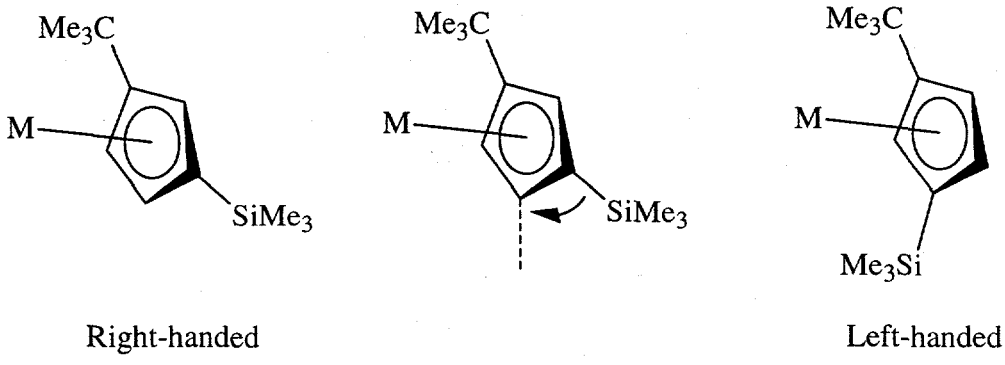

Figure 37: 1,5-Silatropic shift converts right-handed ring to left-handed ring

Trimethylsilyl shifts on cyclopentadienes have been demonstrated and occur in solution at room temperature[27-30](Figure 38).

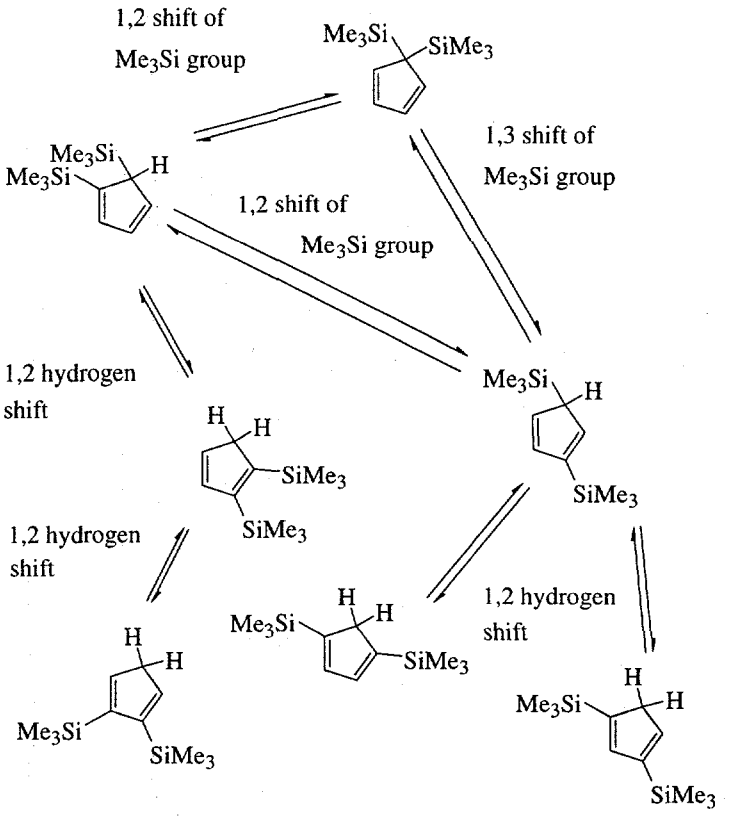

Figure 38: Silatropic shifts in $(Me_3Si)_2C_5H_4$

1,2-Hydrogen shifts have also been detected at somewhat higher temperatures.

It is unlikely that the *t*-butyl group is undergoing a similar ring-walking phenomenon since the barrier to migration of the *t*-butyl substituent is higher than the barrier for silyl or H-atom shifts[30,31]. Hughes and coworkers have prepared complexes with 1,2- and 1,2,3-substituted cyclopentadienyl ligands with *t*-butyl groups and have observed no redistribution to 1,3- or 1,2,4-substituted rings[32-35].

These two methods of converting a right-handed ligand to a left-handed ligand have different exchange characteristics which may be distinguished using NMR. In the

"face change" process, the proton at the 2-position of the cyclopentadienyl ring, remains at the 2-position after the face change so that, during exchange, magnetization transfer could be expected between the 2-position protons of the two isomers (Figure 39).

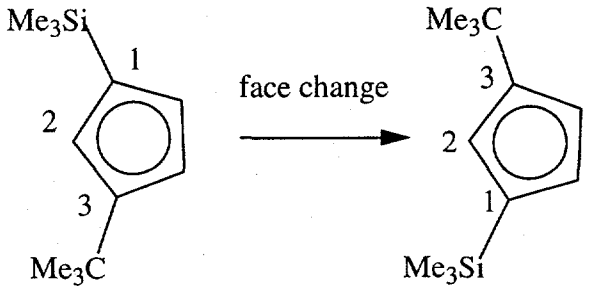

Figure 39: 2-position proton is unchanged during face change

If the handedness of the cyclopentadienyl ring is changed by a silatropic shift, however, the 2-position proton becomes the 4-position proton of the other NMR isomer. Magnetization transfer would demonstrate a correlation between the 2- and 4-position protons of the NMR isomers as shown in Figure 40 and Table 12.

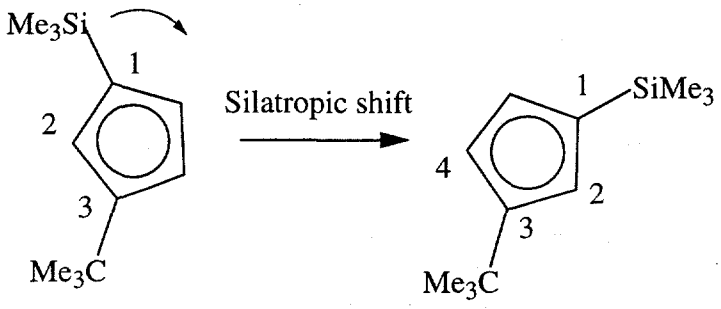

Figure 40: 2-position becomes 4-position during silatropic shift

The small difference in chemical shift between the 2-position resonances of the ligands would make EXSY resonances between them difficult to resolve, but similar mechanism-specific exchanges can be identified in the other ^{1}H resonances, which have chemical shifts that are more easily resolved, or in the ^{13}C resonances.

C_2 isomer	C_S isomer		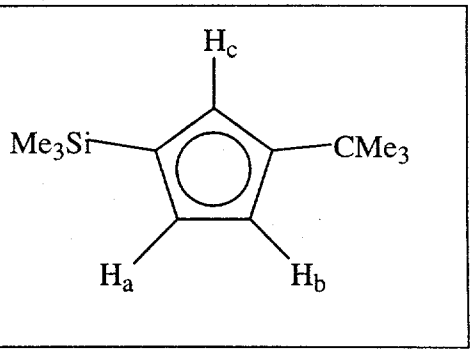
^{1}H NMR Resonance	after face change	after trimethylsilyl shift	
Me_3Si	Me_3Si	Me_3Si	
Me_3C	Me_3C	Me_3C	
H_a	H_a	**H_c**	
H_b	H_b	H_b	
H_c	H_c	**H_a**	

Table 12: ^{1}H NMR resonance correlation table

No magnetization exchange has been detected in samples at 30, 90, and 120 °C indicating that the diastereomers do not interconvert in this temperature range or that the exchange rate is slower than 3 x 10^{-5} mol/s at 120 °C. Efforts are underway to improve the detection limit of the experiment[36].

The analogous ferrocene complex is prepared by mixing Cp^{tt}_2Mg with $FeBr_2$·2THF in tetrahydrofuran. The red-orange, Cp^{tt}_2Fe is crystallized from hexane and melts at 137-139 °C. The ^{1}H NMR spectrum exhibits resonances consistent with a C_2 isomer and a C_S isomer. Similar to the corresponding magnesocene, the variable temperature NMR spectra exhibit equal concentrations of the two NMR observable isomers and no exchange is detected. Ferrocenes have a low-spin d^6 electronic configuration and are kinetically inert. It is unclear what effect the metal atom might have on silatropic shifts, since this phenomenon has not been observed with a cyclopentadienyl ligand on *any* metal. Unfortunately, no magnetization transfer has been detected in Cp^{tt}_2Fe at 90 °C in toluene.

Sandwich complexes of other metals were considered in an effort to locate a system in which the isomer conversion might be easier to detect. In an early description

of manganocene, Wilkinson and coworkers characterized the compound as an "ionic" complex, which exhibited reactions not observed in other first-row metallocenes[37]. It is possible that a similar ligand-metal interaction, specifically a lower bond order between the cyclopentadienyl group and the metal, might accelerate the interconversion, either by making the ligand more labile to facilitate a ring-slip or dissociative mechanism, or by a lesser interaction with the π-electrons of the cyclopentadienyl ligands, which could facilitate a silatropic shift. Bis[(trimethylsilyl)(*t*-butyl)cyclopentadienyl]manganese was prepared (chapter 4) but, since this metallocene is high spin-d^5 and paramagnetic, the ^{1}H NMR resonances are too broad to allow productive study of the exchange by NMR spectroscopy.

Tris(cyclopentadienyl)cerium and Uranium

The ^{1}H NMR resonances for paramagnetic cerium(III) compounds, although broader than the analogous diamagnetic resonances, are easily observable by ^{1}H NMR spectroscopy. The bonding in lanthanide compounds, which is often referred to as "ionic" bonding[38], may facilitate the interconversion of the isomers. The tris[(trimethylsilyl)(*t*-butyl)cyclopentadienyl]cerium compound is prepared in a procedure analogous to that used for $Cp^{\ddagger}_3Ce$ (Chapter 2). The compound is purple and crystallizes from hexane. The ^{1}H NMR spectrum of the reaction mixture at 30 °C shows three *t*-butyl resonances, three trimethylsilyl resonances, and eight resonances attributable to ring protons (Figure 41)*.

---

* eight resonances are resolvable at 30 °C and 90 MHz, all nine are identifiable during VT ^{1}H NMR.

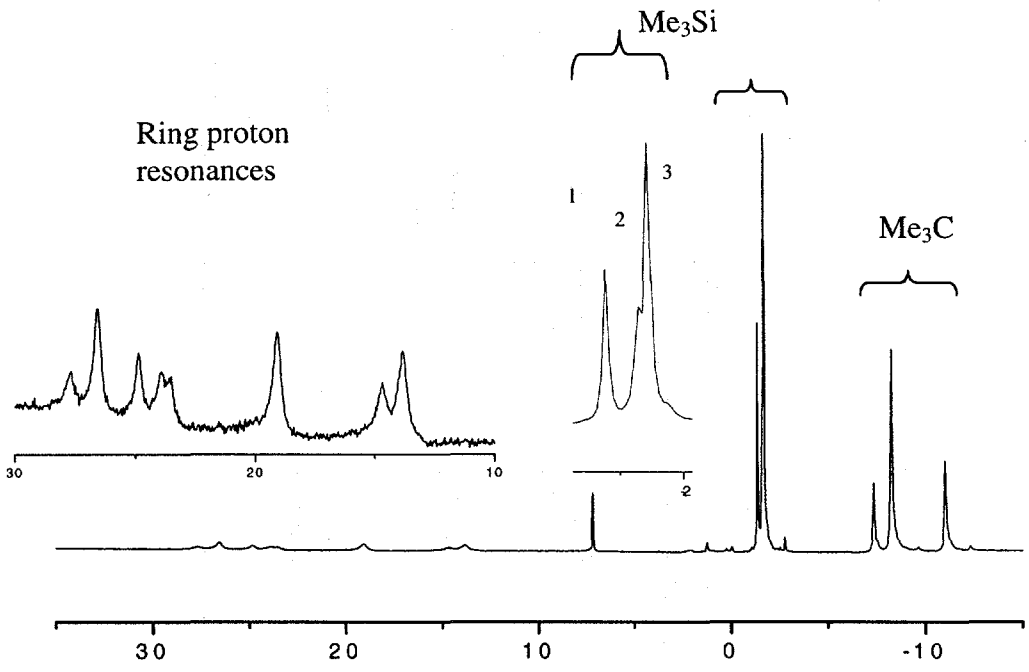

Figure 41: 90MHz ^{1}H NMR spectrum of Cp^{tt}_3Ce, C_1 and C_3 isomers, 30 °C

If the product is crystallized slowly (over a period of weeks) from hexane, the ^{1}H NMR spectrum exhibits two *t*-butyl resonances, two trimethylsilyl resonances, and six ring proton resonances (Figure 42).

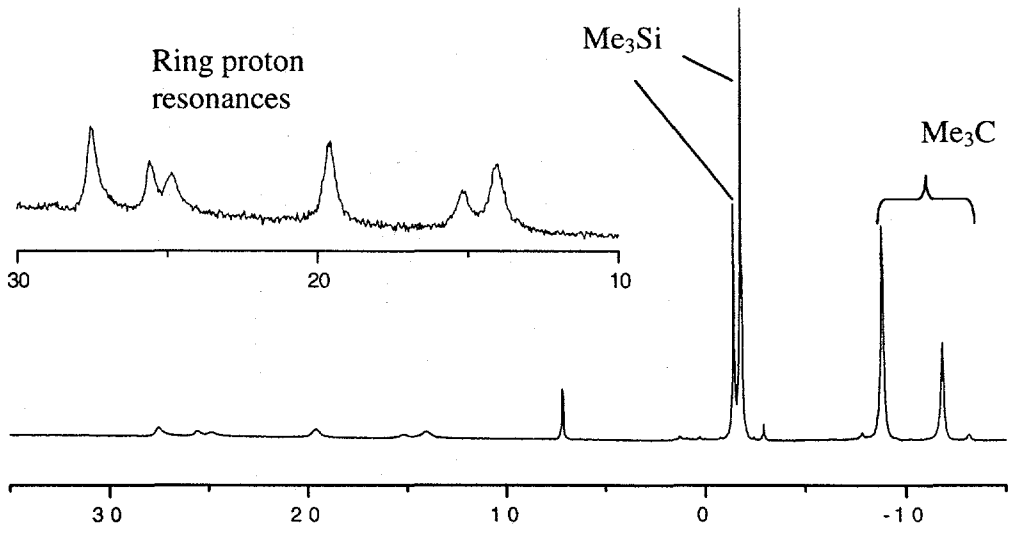

Figure 42: 90 MHz ^{1}H NMR spectrum of Cp^{tt}_3Ce, C_1 isomer, 30 °C

If the NMR sample is heated to 50 °C for several hours, the relative areas of the resonances in Figure 42 decrease and new resonances appear until the spectrum resembles the spectrum observed for the reaction mixture.

Examination of the symmetry elements of Cp^{tt}_3Ce reveals enantiomers and diastereomers similar to those observed for Cp^{tt}_2Mg. If three (trimethylsilyl)(*t*-butyl)cyclopentadienyl groups are coordinated to the same metal, as in Cp^{tt}_3Ce, eight isomers are possible and the isomers are described in Table 13.

conformational isomers	R,R,R	L,L,L	R,R,L	R,L,R	L,R,R	R,L,L	L,R,L	L,L,R
optically active isomers	✓	✓	✓	✓	✓	✓	✓	✓
isomers resolvable by NMR	C_3	C_3	C_1	C_1	C_1	C_1	C_1	C_1

Table 13: Confirmational isomers of Cp^{tt}_3Ce

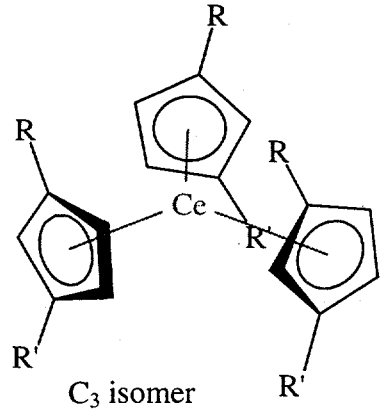

C_3 isomer

Figure 43: C_3 isomer of Cp^{tt}_3Ce

The isomer with three right-handed (or three left-handed) cyclopentadienyl rings has an idealized C_3 axis and no other symmetry elements. The 1H NMR spectrum has a single trimethylsilyl resonance, a single *t*-butyl resonance, and three resonances for ring protons (Table 14).

	chemical shift (ppm)	number of protons
Me_3Si	-1.65	27
Me_3C	-7.37	27
ring-protons	27.7, 23.7, 18.7	3,3,3

Table 14: ^{1}H NMR resonances of Cp^{tt}_3Ce, C_3 isomer, 30 °C

The isomer with two right-handed and one left-handed (or two left- and one right-handed) cyclopentadienyl ligands has no symmetry elements (C_1) (Figure 44).

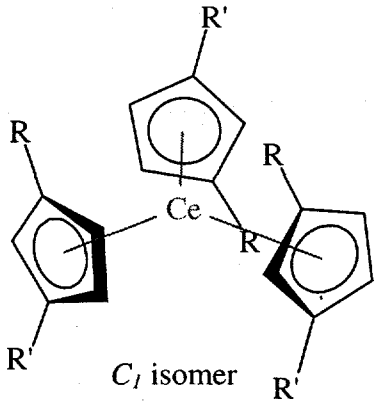

Figure 44: Cp^{tt}_3Ce, C_1 isomer

The ^{1}H NMR spectrum is expected to have three trimethylsilyl resonances, three *t*-butyl, and nine ring proton resonances. The observed spectrum at 30 °C, however, exhibits fewer resonances (Table 15).

	chemical shift (ppm)	number of protons
Me_3Si	-1.78, -1.42	18, 9
Me_3C	-8.80, -11.81	18, 9
ring-protons	27.6, 19.6, 14.1, 25.6, 24.9, 15.2	2, 2, 2, 1, 1, 1

Table 15: ^{1}H NMR resonances of Cp^{tt}_3Ce, C_1 isomer, 30 °C

The 2:1 ratios for the set of NMR resonances suggest that two of the cyclopentadienyl rings are contributing to a single set of resonances on the NMR time scale.

An illustration of a single case makes this clearer and the exchange scheme can be applied to other ring orientations. Consider the case in which a right/right/left isomer is

situated so that the 2-positions of each cyclopentadienyl ring and the cerium atom all share a single plane. Moreover, if the rings are considered arrows, the 2-positions of the rings are the "point" of the arrow and each arrow is pointed in the clockwise direction* (Figure 45).

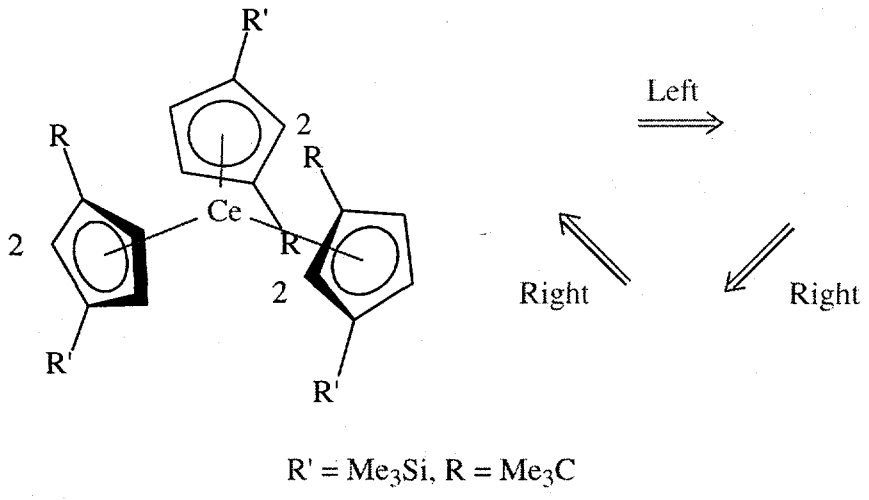

R' = Me_3Si, R = Me_3C

Figure 45: The "2" positions of the cyclopentadienyl rings and cerium lie in one plane

If the three rings are "following" each other around the cerium atom, one right-handed ring is "leading" the left-handed ring and the other is "following" the left-handed ring (Figure 46).

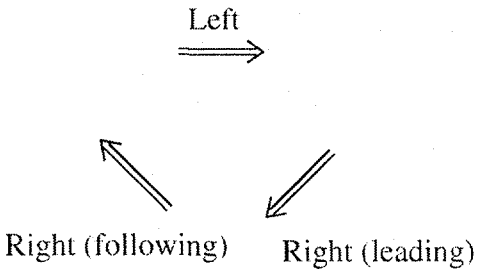

Figure 46: Idealized orientation for analysis of fluxional process

---

* The frame of reference is arbitrary and need only be consistent throughout this example.

If each ring then undergoes a rotation of 180° about its metal/ring-centroid axis so that the arrows are pointed in the counterclockwise direction, the left-handed ring remains left-handed and the two right-handed rings remain right-handed, but the leading ring has become the following and the following ring has become the leading (Figure 47).

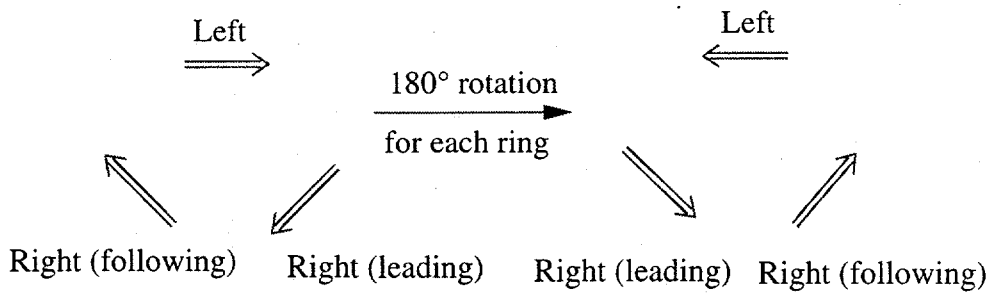

Figure 47: Chemical exchange of the "leading" and "following" cyclopentadienyl groups

If the rotation described above occurs rapidly on the NMR time scale, the pairs of resonances that are exchanging will each appear as one, averaged resonance in the NMR spectrum.

At room temperature, the two rings with the same handedness are exchanging rapidly on the NMR time scale and the observed spectrum has two trimethylsilyl resonances, two *t*-butyl resonances and six ring resonances (Figure 42).

When the sample is cooled below -40 °C, the exchange becomes slow relative to the NMR time scale and all fifteen resonances expected for the C_1 species are observable (Figure 48).

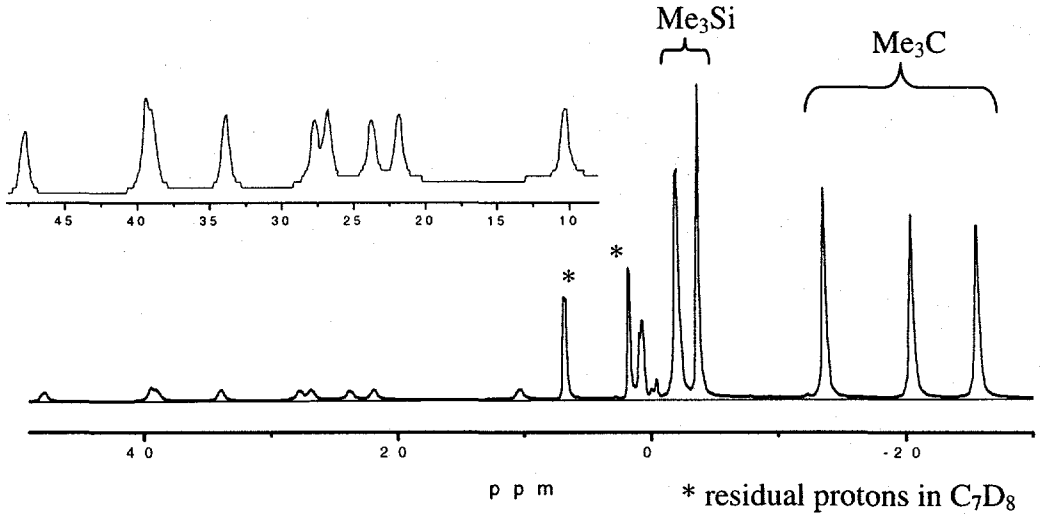

Figure 48: 500 MHz ^{1}H NMR spectrum of Cp$^{tt}_3$Ce, *C$_1$* isomer, -83 °C

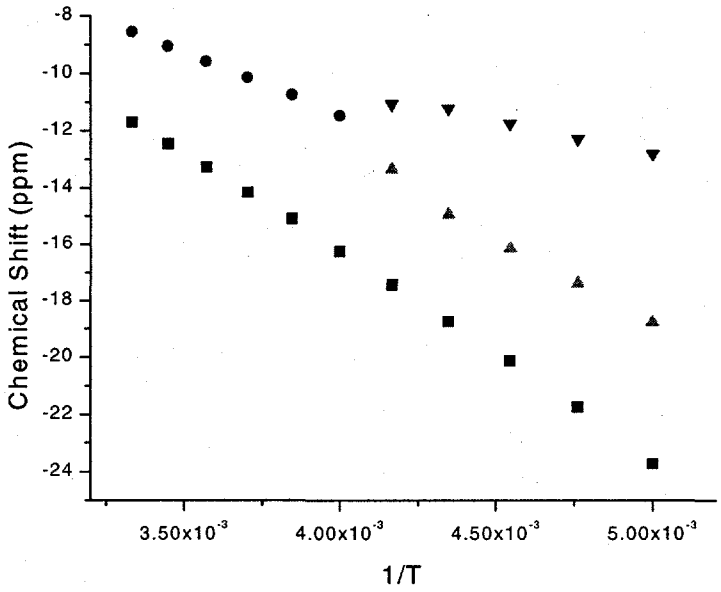

Figure 49: Variable temperature NMR, *t*-butyl resonances of Cp$^{tt}_3$Ce, *C$_1$* isomer

The energy barrier associated with the interconversion of the two, cyclopentadienyl rings is 16 kJ/mol, which was calculated from this coalescence behavior (Equation 2).

$$k = \frac{\pi \Delta\delta}{\sqrt{2}} = e^{-\Delta G^{\ddagger} / RT}$$

$$\Delta G^{\ddagger} = -RT \ln k$$

Equation 2: Gutowsky-Holm equation, equal population two-site exchange

The symmetry analysis explains the origins of each of the resonances in the reaction mixture and we have seen that rotation of the cyclopentadienyl rings about the metal/ring-centroid axes does not change a left-handed ring to a right-handed ring. Recall that the C_1 isomer can be crystallized from a mixture of the two isomers and the ^{1}H NMR spectrum has ten resonances. Heating the sample to temperatures greater than 60 °C in benzene causes a decrease in the integrals for the C_1 resonances and resonances of the C_3 isomer appear and increase with time until equilibrium is reached.

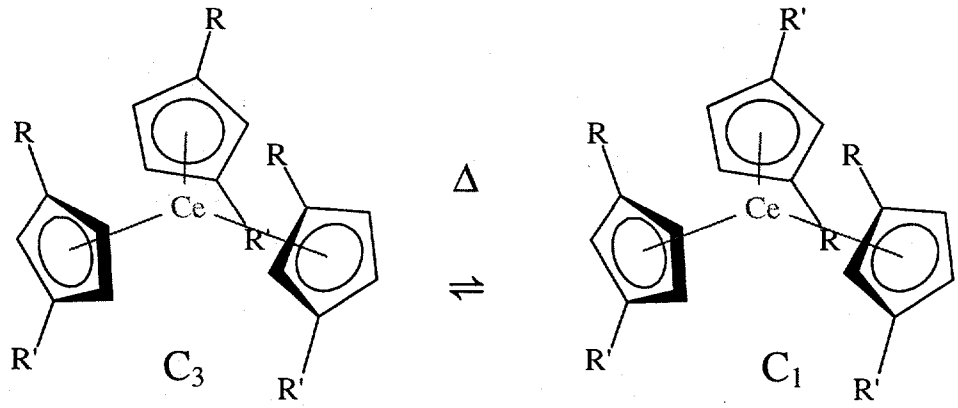

Since the C_1 isomer can be selectively crystallized from the reaction mixture and the resonances for the C_3 isomer are observed to grow into the ^{1}H NMR spectrum of the pure C_1 isomer at the same rate that the resonances for the C_1 isomer decrease in intensity, there is no doubt that the C_1 and C_3 diastereomers of Cp^{tt}_3Ce interconvert on the slow, laboratory time scale. There is no evidence in the variable temperature NMR

spectrum to indicate that the C_1 and C_3 diastereomers are interconverted on the faster NMR timescale at temperature of up to 110 °C.

The correlation between C_1 isomer resonances and C_3 isomer resonance is slightly more complicated since a face change or trimethylsilyl shift does not always result in interconversion between isomers (Table 16, Table 17).

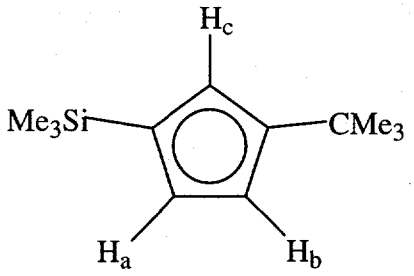

C_3 isomer	C_1 isomer	
	after face change	after Me_3Si shift
Me_3Si	Me_3Si	Me_3Si
Me_3C	Me_3C	Me_3C
H_A	H_A	H_C
H_B	H_B	H_B
H_C	H_C	H_A
Correlation is always between C_3 resonances and the "odd" ring of the C_1 isomer		

Table 16: Correlation table for C_3 isomer

C_1 isomer	C_1 isomer	
	after face change	after Me_3Si shift
Me_3Si	Me_3Si	Me_3Si
Me_3C	Me_3C	Me_3C
H_A	H_A	H_C
H_B	H_B	H_B
H_C	H_C	H_A
Correlation is always between the resonances of the C_1 isomer related by a fluxional process (i.e. always between R and R for R,R,L)		

Table 17: Correlation table for C_1 isomer

The separation between resonances is much larger for two isomers of the paramagnetic $Cp^{tt}{}_3Ce$, which facilitates resolution of the EXSY resonances, but the

experiment is complicated by the longitudinal relaxation times of the resonances (Table 18). The T_1's of Cp^{tt}_3Ce are measured in milliseconds and are typically 2-3 orders of magnitude shorter than the T_1's of the diamagnetic compounds discussed above. Since 1% of the sample must have undergone chemical exchange during the mixing time of the EXSY experiment in order for the exchange resonance to be detectable, the shorter T_1's of the paramagnetic complex require that the exchange occur at a rate 2-3 orders of magnitude faster in order to have a comparable signal in the EXSY spectrum. No exchange resonances have, as yet, been detected.

	Chemical shifts (ppm)	longitudinal relaxation time (T1) (s) 90 °C
Me_3C	-7.8- -5.4	62-70 ms
Me_3Si	-1.5- -1.2	211-235 ms
$H_{a,b,c}$	12.8-22.3	13-20 ms

Table 18: Chemical shifts and spin-lattice relaxation times, Cp^{tt}_3Ce

The NMR time scale experiments have only provided an upper limit on the rate of exchange between the C_1 and C_3 isomers. Laboratory time scale experiments can provide thermodynamic data about the equilibrium. If a mixture of isomers is heated to temperatures greater than 50 °C, the system reaches equilibrium in a few hours or less. The equilibrium populations are not a statistical mixture indicating that there is an energy difference between the two isomers.

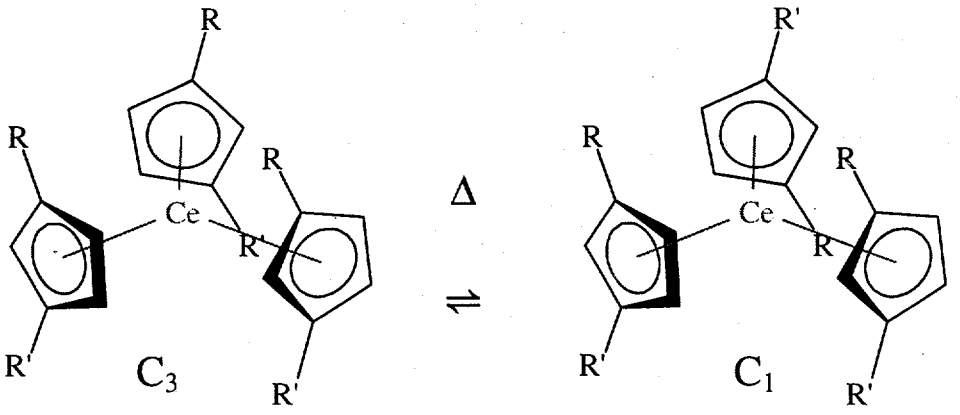

If the equilibrium is evaluated at different temperatures, the enthalpy and entropy change between the isomers can be derived from the change in the equilibrium concentrations with temperature.

$$K = \frac{[C_1 \text{ isomer}]}{[C_3 \text{ isomer}]}$$

Equation 3

$$\ln K = -\Delta H/RT + \Delta S/R$$

The tranformation from the C_3 to the C_1 isomer is exothermic, $\Delta H = 7.0$ kJ/mol, and results in an entropy increase, $\Delta S = 10$ J/mol K.

Since population changes of the two isomers are detectable, the energy barrier and the rate of the interconversion between isomers can also be determined from laboratory time scale experiments. The pure C_1 isomer is obtained by differential crystallization and samples of the isomer can be monitored by ^{1}H NMR spectroscopy to measure the rate at which the concentrations of the C_1 and C_3 isomers approach the equilibrium values at a given temperature.

The analogous uranium tris(cyclopentadienyl) compound, Cp^{tt}_3U, has also been prepared[36]. The C_1 isomer of the uranium compound can also be obtained in pure form

by differential crystallization. The barrier for interconversion of the isomers is slightly higher than the barrier for Cp^{tt}_3Ce (Table 19).

	$\Delta G^{\ddagger}$ for interconversion of isomers (kJ/mol)	ΔG_{rxn} $C_3 \rightleftharpoons C_1$ (kJ/mol)
Cp^{tt}_3Ce		4.5
Cp^{tt}_3U	120	3.0

Table 19: Comparison of thermodynamic values for Cp^{tt}_3Ce and Cp^{tt}_3U

Laboratory time scale experiments can also be used to probe the mechanism of the exchange. A dissociative mechanism involving the loss of a cyclopentadienyl group followed by coordination to a different cyclopentadienyl face is unlikely based on the tendency of the lanthanide elements to maximize their coordination number, which would discourage dissociative mechanisms. Experimental results cast doubt on this scheme as well. If Cp''_3Ce and $Cp^{\ddagger}_3Ce$ are mixed, dissolved in benzene or tetrahydrofuran, and heated to 80 °C, no new species are detected.

$$Cp^{\ddagger}_3Ce + Cp''_3Ce \not\rightleftharpoons Cp^{\ddagger}_2CeCp'' + Cp''_2CeCp^{\ddagger}$$

If the cyclopentadienyl rings were labile, $Cp^{\ddagger}_2CeCp''$ and $Cp''_2CeCp^{\ddagger}$ would be formed. It was possible that the resonances for the mixed species were obscured by or averaged with the resonances of the homoleptic compounds. If the chemical shift differences between the parent compounds and the mixed species are small, the coalescence temperature for the exchange process could be low compared to a process requiring similar energy for species with very different chemical shifts.

To eliminate these possibilities, the mixed species, $Cp^{\ddagger}_2CeCp''$, was prepared from $Cp^{\ddagger}_2CeOSO_2CF_3$ and Cp''_2Mg in tetrahydrofuran.

$$Cp‡_2CeOSO_2CF_3 + ½\ Cp"_2Mg \longrightarrow Cp‡_2CeCp" + ½\ Mg(OTf)_2$$

The compound is purple and has a single trimethylsilyl resonance, a single *t*-butyl resonance, and six ring-resonances in the ^1H NMR spectrum (Table 20).

	$Cp"_3Ce$	$Cp^‡_3Ce$	$Cp^‡_2CeCp"$
Me_3Si	4.47		-2.30
Me_3C		-4.63	-6.55
ring protons	17.1, 26.8	17.0, 28.5	29.55, 23.86, 21.11, 9.50

Table 20: ^1H NMR chemical shifts at 30 °C

If a sample of the mixed species is combined with $Cp^‡_3Ce$ and $Cp"_3Ce$ in an NMR sample, all species are observed without exchange.

Conclusions

Although experiments are ongoing to detect magnetization transfer in an effort to describe the mechanism of isomerization, it is quite possible that the rate of magnetization exchange is too slow to be detected for each of the examples examined here. Future work in this system will undoubtedly include synthesis of the corresponding diamagnetic lanthanum compound, Cp^{tt}_3La. In addition to the possibility of separating diastereomers by differential crystallization analogous to the cerium and uranium results, lanthanum(III) compounds are diamagnetic have much longer longitudinal relaxation times than the paramagnetic tris(cyclopentadienyl) compounds. In the bis(cyclopentadienyl)metal systems, the ring centroid-metal-ring centroid angles are large and the interaction between ring substituents is small. Three cyclopentadienyl groups on the same metal require that the ring centroid-metal-ring centroid angles average 120° and

the substituents on the rings are closer to one another, causing a greater perturbation of the magnetic environment. The chemical shifts differences between isomers should be larger than those observed for the Cp^{tt}_2Mg and Cp^{tt}_2Fe.

References

1)Hultzsch, K. C.; Spaniol, T. P.; Okuda, J. *Organometallics*, **1997**, *16*, 4845-4856.

2)Giardello, M. A.; Yamamoto, Y.; Brard, L.; Marks, T. J. *J. Am. Chem. Soc.*, **1995**, *117*, 3276-3277.

3)Giardello, M. A.; Eisen, M. S.; Stern, C. L.; Marks, T. J. *J. Am. Chem. Soc.*, **1993**, *115*, 3326-3327.

4)Giardello, M. A.; Conticello, V. P.; Brard, L.; Sabat, M.; Rheingold, A. L.; Stern, C. L.; Marks, T. J. *J. Am. Chem. Soc.*, **1994**, *116*, 10212-10240.

5)Giardello, M. A.; Conticello, V. P.; Brard, L.; Gagne, M. R.; Marks, T. J. *J. Am. Chem. Soc.*, **1994**, *116*, 10241-10254.

6)Giardello, M. A.; Eisen, M. S.; Stern, C. L.; Marks, T. J. *J. Am. Chem. Soc.*, **1995**, *117*, 12114-12129.

7)Yoder, J. C.; Day, M. W.; Bercaw, J. E. *Organometallics*, **1998**, *17*, 4946-4958.

8)Miyake, S.; Henling, L. M.; Bercaw, J. E. *Organometallics*, **1998**, *17*, 5528-5533.

9)Schmidt, K.; Reinmuth, A.; Reif, U.; Diebold, J.; Brintzinger, H. H. *Organometallics*, **1997**, *16*, 1724-1728.

10)Christopher, J. N.; Jordan, R. F.; Petersen, J. L.; Young, V. G. *Organometallics*, **1997**, *16*, 3044-3050.

11)Halterman, R. L. *Chem. Rev.*, **1992**, *92*, 965-994.

12)Schlögl, K. *J. Organomet. Chem.*, **1986**, *300*, 219-248.

13)Knox, G. R.; Pauson, P. L. *J. Chem. Soc.*, **1961**, 4610-4615.

14)Leigh, T. *J. Chem. Soc.*, **1964**, 3294-3302.

15)Riemschneider, R.; Reisch, A.; Horak, H. *Monatsh. Chem.*, **1960**, *91*, 805-811.

16)Venier, C. G.; Casserly, E. W. *J. Am. Chem. Soc*, **1990**, *112*, 2808.

17)Burkey, D. J.; Hanusa, T. P. *Comments Inorg. Chem.*, **1995**, *17*, 41-77.

18)Guggenberger, L. J.; Tebbe, F. N. *J. Am. Chem. Soc.*, **1971**, *93*, 5924-5925.

19)Tebbe, F. N.; Parshall, G. W. *J. Am. Chem. Soc.*, **1971**, *93*, 3793-3795.

20)Cooper, N. J.; Green, M. L. H.; Couldwell, C.; Prout, K. *J. Chem. Soc., Chem. Comm.*, **1977**, 145-146.

21)Cotton, F. A. *J. Organomet. Chem.*, **1975**, *100*, 29-41.

22)Kleppner, D.; Kolenkow, R. J. *An Introduction to Mechanics*; McGraw-Hill Book Company: New York, 1973.

23)Sokolov, V. I. *Chirality and Optical Activity in Organometallic Compounds*; Gordon and Breach Science Publishers: New York, 1990.

24)Abel, E. W.; Coston, T. P. J.; Orrell, K. G.; Sik, V. *J. Mag. Res.*, **1986**, *70*, 34-53.

25)Derome, A. E. *Modern NMR Techniques for Chemistry Research*; Pergamon Press: New York, 1987; Vol. 6.

26)Perrin, C. L.; Dwyer, T. J. *Chem. Rev.*, **1990**, *90*, 935-967.

27)Ashe III, A. J. *J. Am. Chem. Soc.*, **1970**, *92*, 1233-1235.

28)Ustynyuk, Y. A.; Kisin, A. V.; Pribytkova, I. M.; Antonova, N. D. *J. Organomet. Chem.*, **1972**, *42*, 47-63.

29)Ustynyuk, Y. A.; Luzikov, Y. N.; Mstislavsky, V. I.; Azizov, A. A.; Pribytkova, I. M. *J. Organomet. Chem.*, **1975**, *96*, 335-353.

30)Jutzi, P. *Chem. Rev.*, **1986**, *86*, 983-996.

31)Childs, R. F. *Tetrahedron*, **1982**, *38*, 567-608.

32)Hughes, R. P.; Lomprey, J. R. *Inorg. Chim. Acta*, **1995**, *240*, 653-656.

33)Hughes, R. P.; Kowalski, A. S.; Neithamer, D. R. *J. Org. Chem.*, **1996**, *61*, 401-404.

34)Hughes, R. P.; Lomprey, J. R.; Rheingold, A. L.; Haggerty, B. S.; Yap, G. P. A. *J. Organomet. Chem.*, **1996**, *517*, 89-99.

35)Donovan, B. T.; Hughes, R. P.; Trujillo, H. A.; Rheingold, A. L. *Organometallics*, **1992**, *11*, 64-69.

36)Blosch, L. L. unpublished results.

37)Wilkinson, G.; Cotton, F. A.; Birmingham, J. M. *J. Inorg. Nucl. Chem.*, **1956**, 2, 95-113.

38)Raymond, K. N. *Organometallics of the f-Elements*; Fischer, R. D. and Marks, T. J., Ed.; D. Reidel Publishing Co.: Boston, 1978; Vol. 44, pp 249-280.

Chapter 4

The Effect of Substituted Cyclopentadienyl Ligands On the Electronic State of Manganocene

The characterization of manganese compounds invariably includes data about the magnetic and electronic properties of the compound. Manganese compounds are the subjects of a disproportionate number of papers on molecular magnetism, in part because of the large number of stable oxidation states available in manganese chemistry, and also because manganese commonly forms high-spin complexes, which are rare for the first-row transition elements. Discussion of the chemistry of manganese is invariably accompanied by analysis of the electronic and magnetic properties of the molecules.

Manganocenes represent a small class of Mn(II) compounds which share an idealized orbital scheme (Figure 50).

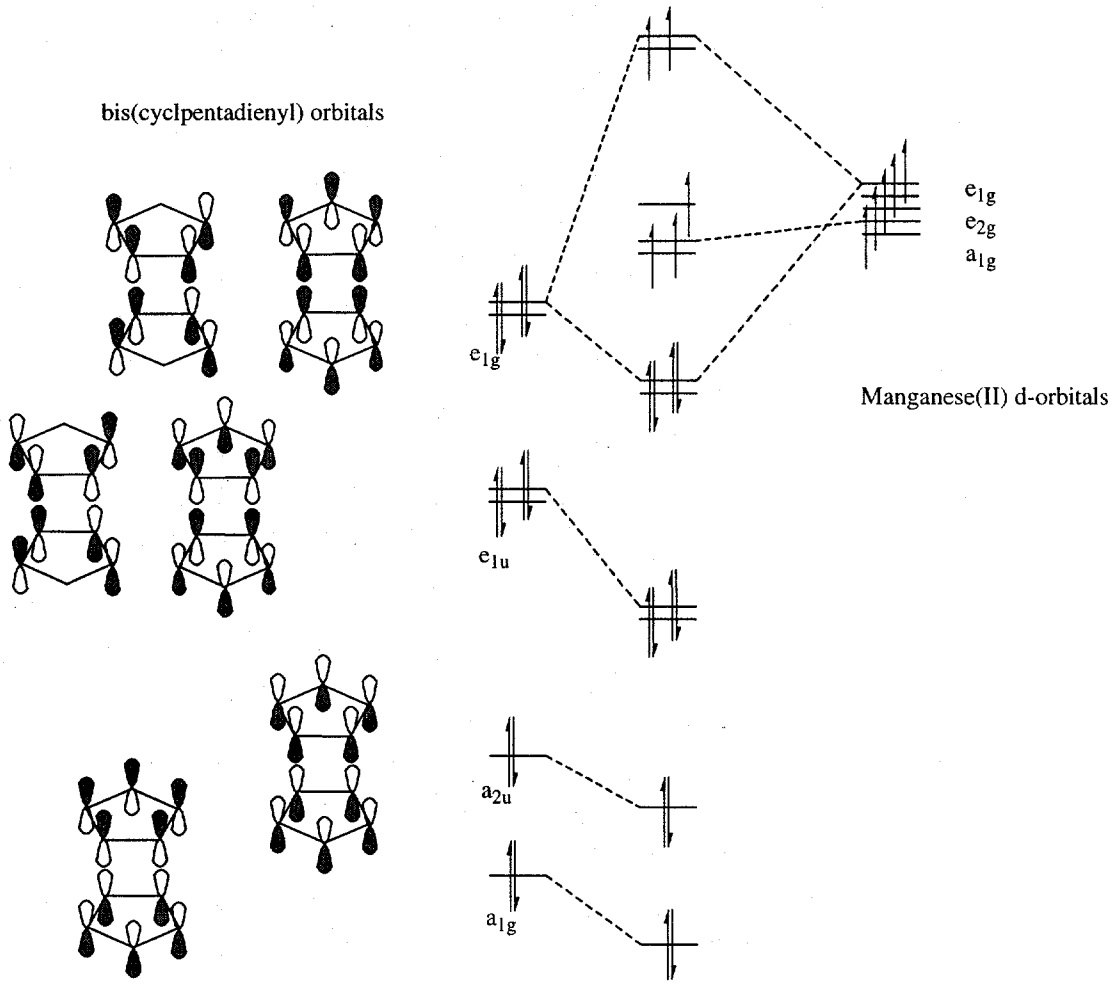

Figure 50: Idealized D_{5d} manganocene orbital scheme[1]

The strength of the interaction between the e_{1g} ligand orbitals and the metal orbitals of the same symmetry will govern the magnitude of the energy difference between the frontier molecular orbitals. The magnetism of the substituted manganocenes can illustrate the influence that subtle changes in the ligand environment have on the electronic configuration of a complex. Substituted cyclopentadienyl groups have been used to prepare manganocenes that have high-spin electronic configurations, low-spin configurations, and manganocenes that exhibit both high- and low-spin states simultaneously, in equilibrium. A variety of techniques has been used to determine the

spin-states of substituted manganocenes and to evaluate the thermodynamics of spin-state equilibria.

Manganocene

Manganocene [$(C_5H_5)_2Mn$] was first prepared in Wilkinson's laboratory from NaC_5H_5 and $MnBr_2$ in 1954[2]. Substituted manganocenes have been prepared using the same reaction scheme and analogous reagents (Figure 51).

$$2\ MCp' + MnX_2 \xrightarrow[THF]{} MnCp'_2$$

M = Na, Li, K; X = Cl, Br

Figure 51: A general scheme for preparation of manganocenes

Anhydrous manganese salts are insoluble in most aprotic solvents but are soluble enough in tetrahydrofuran to achieve reasonable reaction rates at room temperature. The tetrahydrofuran adducts of $MnCl_2$ and MnI_2 have been described[3,4] and, in addition to having increased kinetic solubility, these adducts can be crystallized from tetrahydrofuran.

Wilkinson and coworkers prepared 1,1'-Dimethylmanganocene [$(MeC_5H_4)_2Mn$] from $NaMeC_5H_4$ and $MnCl_2$ in 1959[5]. Decamethylmanganocene was prepared from LiC_5Me_5 and $MnCl_2$ by Smart and Robbins in 1978[6]. Di-*t*-butylmanganocene was prepared by Ammeter and coworkers but details of the preparation were not published in a journal[7]. Groups of alkylated manganocenes were prepared by Sitzmann and coworkers[8] using $MnCl_2$ and sodium or lithium cyclopentadienides and by Köhler and coworkers[9] using $MnCl_2$ and potasium cyclopentadienides. All of the preparations were

conducted in tetrahydrofuran and the products were purified by sublimation, crystallization or distillation (Table 21). The colors of the complexes were not reported in all cases but orange and red figure prominently.

	Color	mp (°C)	electronic configuration Solid	Soln.	Vapor	Mn-ring centroid distance (Å)
$(C_5H_5)_2Mn$	amber	172-173	^6A	^6A, ^2E	^6A	2.10[a]
$(MeC_5H_4)_2Mn$	dark-brown	61-63	^6A, ^2E	^6A, ^2E	^6A, ^2E	2.10[a]
$(Me_5C_5)_2Mn$[10-13]	red-orange	292	^2E	^6A, ^2E	^2E	1.73
$(Me_3CC_5H_4)_2Mn$[7]	orange	< 25	^6A, ^2E	^6A, ^2E		
$(EtC_5H_4)_2Mn$[9]		< 25				
$(iPrC_5H_4)_2Mn$[14]	orange-red	< 25	^6A, ^2E			
$(Me_3SiC_5H_4)_2Mn$[9]		27-28	^6A			2.05
$(Me_2C_5H_3)_2Mn$[9]		69-71		^6A, ^2E		
$(Me_4C_5H)_2Mn$[9]		144-146		^2E		
$(EtMe_4C_5)_2Mn$[9]		100-101		^2E		
$(iPr_4C_5H)_2Mn$[8]	orange-brown			^6A		
$[(Me_3C)_3C_5H_2]_2Mn$[8]	brownish-yellow			^6A		
$(iPr_3Me_2C_5)_2Mn$[8]	brownish			^6A, ^2E		
$(iPrMe_4C_5)_2Mn$[8]	yellow-brown			^2E		

a. Mn-Cp distance for the η^5-cyclopentadienyl ring

Table 21: Physical data for manganocenes

In the solid state, manganocene is not a monomer. The single crystal X-ray structure of manganocene was published in 1978[15] showing that manganocene was not structurally analogous to ferrocene but had one bridging, η^2-cyclopentadienyl group and one terminal, η^5-cyclopentadienyl group. The structure of $(MeC_5H_4)_2Mn$ is shown to be similar (Figure 52, Table 22).

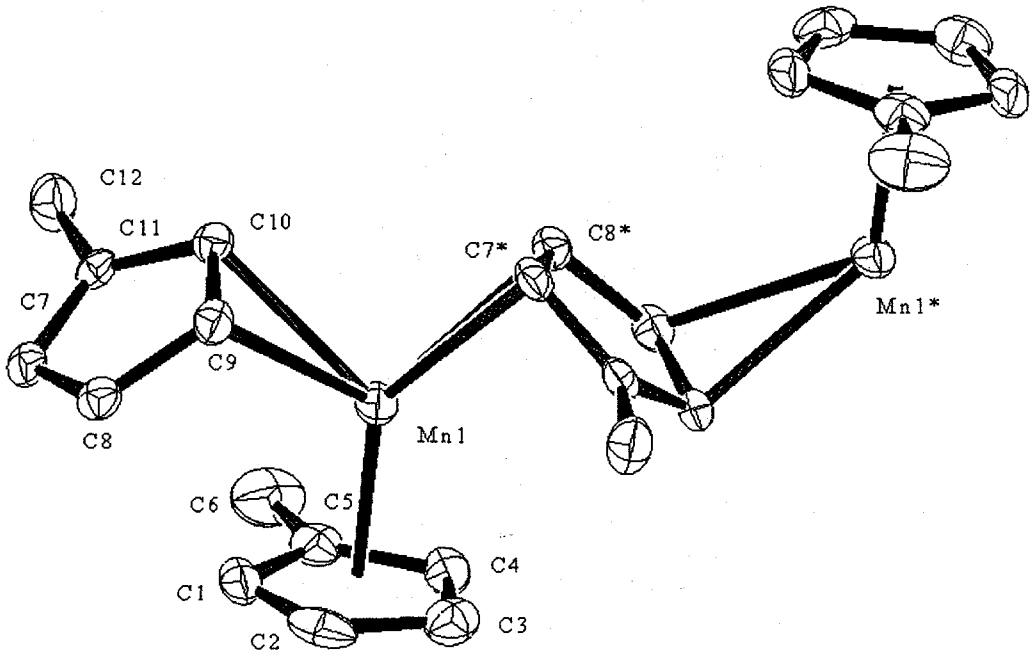

Figure 52: ORTEP diagram of $(MeC_5H_4)_2Mn$, 50% thermal elipsoids

	Cp_2Mn[15]	$(MeC_5H_4)_2Mn$
Mn-C1	2.24	2.43
Mn-C2	2.42	2.37
Mn-C3	2.40	2.28
Mn-C4	2.40	2.43
Mn-C5	2.43	2.47
Mn-ring centroid	2.10	2.10
Mn-C7	3.09	3.63
Mn-C8	3.30	3.31
Mn-C9	2.37	3.01
Mn-C10	2.51	2.41
Mn-C11	2.81	3.00
Mn-C7*	2.62	2.41
Mn-C8*	2.44	2.41
Mn···Mn*	5.38	5.32

Table 22: Comparison of structural data for Cp_2Mn and $(MeC_5H_4)_2Mn$, distances in Å

The X-ray crystal structure and gas phase electron diffraction data for decamethylmanganocene[10,11] show that the molecule is monomeric and the metal-ring centroid distance is considerably shorter than that observed for the η^5-cyclopentadienyl

groups on manganocene and dimethylmanganocene. The single crystal X-ray structure of $(Me_3SiC_5H_4)_2Mn$ indicates that the compound is also monomeric, but the metal-ring centroid distances are comparable to those observed for manganocene and dimethylmanganocene(Table 21).

Magnetism of Manganocenes

Measurement of molecular magnetism is a diagnostic tool for probing the electronic structure of molecules. To a first approximation, the magnetic moment of an isolated compound with no intermolecular interactions is dependent upon the number of unpaired electrons in the compound (Equation 4).

$$\mu = 2\sqrt{S(S+1)}$$

$$S = \frac{\text{number of unpaired electrons}}{2}$$

Equation 4

The number of unpaired electrons for a given metal complex is dictated by the magnitude of the energy difference between molecular orbitals and the energy required to pair electrons. The energy difference between molecular orbitals is a function of the relative energies of ligand and metal atomic orbitals and the overlap between the two.

Weak Orbital Overlap Strong Orbital Overlap

Figure 53: Frontier orbital scheme for a d^5-metallocene with D_{5d} symmetry

For a d^5-complex with idealized D_{5d} symmetry and weak overlap between the metal d-orbitals and the ligand frontier orbitals, a high-spin species (S = 5/2) is favored. If the orbital overlap is strong, the energy gap between the orbitals is larger than the energy required pair the electrons and a low-spin species (S = 1/2) results[1] (Figure 53). When the measured magnetic moment corresponds to the high- or low-spin value, the molecules are behaving as isolated paramagnets, that is, there are no intermolecular interactions which affect the magnetic moment. When this condition is met, the compound is *magnetically dilute*. Intermolecular interactions, which affect the magnetic moment of the sample, for example, ferromagnetic coupling, will result in a measured magnetic moment that is not consistent with the value predicted by the number of unpaired electrons.

The molar or gram magnetic susceptibility of a compound is determined by dividing the magnetism of the sample by the number of moles or grams, respectively, of compound in the sample. If the susceptibility of a magnetically dilute sample is measured as a function of temperature, the plot of the inverse of susceptibility vs. temperature is linear and the slope of the line is a function of the magnetic moment (Equation 5).

$$\chi = \frac{N\mu^2}{3kT}$$

Equation 5

χ = susceptibility, N = Avagadro's number, μ = magnetic moment, and k = Boltzmann constant

The linear relationship between temperature and the inverse of susceptibility is known as Curie Law. Often a constant term attributed to small intermolecular interactions is added and the sum is known as Curie-Weiss behavior (Equation 6).

$$\chi = \frac{C}{T + \theta} \quad \text{Curie-Weiss Law}$$

$$C = 0.454 \text{ emu K/mol}$$

Equation 6

If the sample is not magnetically dilute, the data will not follow Curie-Weiss law but can provide an indication of the type and magnitude of intermolecular interactions.

For the parent manganocene, high-temperature, magnetic susceptibility studies revealed an observed magnetic moment of 5.9 B.M. indicating that the sample had five unpaired electrons (Table 23), consistent with high-spin manganese (II)[16]. At lower temperatures (200- 420 K) an unspecified intermolecular interaction caused a deviation from Curie-Weiss behavior and the low temperature magnetism (< 134 K) exhibited antiferromagnetic coupling. The intermolecular interactions indicate that the manganese atoms are not in a magnetically dilute environment. Dissolving the compound in a solvent or a diamagnetic host-compound are common methods used to achieve a magnetically dilute environment. When the susceptibility of manganocene was measured in ether or benzene solution or as a solid solution of $(C_5H_5)_2Mn$ in $(C_5H_5)_2Mg$, the compound exhibited Curie-Weiss behavior and the observed moment was 5.8 B.M.

Dimethylmanganocene[5] was examined under similar conditions and the susceptibility data suggested that the sample was not magnetically dilute. The neat sample exhibited intermolecular effects at all temperatures at which the susceptibility was

measured, from 196 to 365 K. A tetrahydrofuran solution of the compound was the only sample to obey Curie law (μ_{eff} = 5.83 B.M.). The cyclopentadienyl bridge (Figure 52) is thought to be responsible for the magnetic interactions in the neat samples.

The spin equilibrium of dimethylmanganocene was probed by Rettig and coworkers using solution magnetic susceptibility, UV-vis spectroscopy, and EPR spectroscopy[17]. The variable temperature magnetic susceptibility data are consistent with an equilibrium between a ^{2}E ground state and a ^{6}A excited state that is thermally accessible (Figure 54).

$$(MeC_5H_4)_2Mn \text{ (low-spin)} \rightleftharpoons (MeC_5H_4)_2Mn \text{ (high-spin)}$$

$$\Delta H = 7.4 \text{ kJ/mol}, \Delta S = 24 \text{ J/mol K}$$

Figure 54: Spin-equilibrium in dimethylmanganocene

Ammeter and coworkers demonstrated that the ground state electronic configuration for manganocene and dimethylmanganocene was dependent upon the molecular environment[18]. Manganocene, diluted in solid magnesocene ($[C_5H_5]_2Mg$) has a *high*-spin ground state whereas manganocene diluted in solid ferrocene has a *low*-spin ground state. Dimethylmanganocene, diluted in either dimethylmagnesocene or dimethylferrocene exhibited a low-spin ground state.

Smart and Robbins noted that manganocene appeared to be near the high-spin/low-spin crossover point and postulated that more electron donating groups might favor the low-spin configuration. Magnetic susceptibility measurements of decamethylmanganocene[6], both in solution (Evans Method[19]) and in the solid state (4-116 K), describe a low-spin compound that obeys simple Curie Law (Table 23).

	μ (B.M.)
Cp_2Mn	5.8-5.9
$(MeC_5H_4)_2Mn$	5.8
$(C_5Me_5)_2Mn$[6]	1.97-2.16
5 unpaired, 1 unpaired electron (spin only)	5.92, 1.73

Table 23: Magnetic moments for manganocenes

Spin-state changes have been reported for hundreds of compounds and often the energy difference between the high- and low-spin species is small enough that conversion between the two species is observed thermally. Typically the magnetic moment is measured as a function of temperature to determine the equilibrium constant, and the free energy change for the conversion between spin-states can be calculated (Equation 7).

Ammeter and coworkers have measured the temperature dependence of the magnetism of 1,1'-di-t-butylmanganocene by variable temperature UV-vis spectroscopy and by the Evans NMR method[19] and determined that the enthalpy change for the low-spin to high-spin transition is 12.7 kJ/mol and the entropy change is 44 J/mol K[7].

$$Cp'_2Mn(\text{Low-spin}) \rightleftharpoons Cp'_2Mn(\text{High-spin})$$

$$Cp' = (Me_3C)C_5H_4$$

$$K = e^{-\Delta G/RT}$$

Equation 7

For molecules with intermediate-strength metal-ligand interactions the electron pairing energy is comparable to the energy difference between orbitals and both high- and low-spin states can exist in equilibrium. Subtle changes in the metal environment, such as modifying a substituent on a ligand, can perturb the relative populations of the high- and low-spin species.

The electronic states of manganocene and dimethylmanganocene have been evaluated using photoelectron spectroscopy[20,21]. The photoelectron spectrum of manganocene indicates that the molecule is high-spin in the gas phase. Dimethylmanganocene exhibits a complex photoelectron spectrum indicating that the high-spin configuration is in equilibrium with the low spin configuration.

A Series of Tetrasubstituted Manganocenes

A series of closely related manganocenes, 1,1',3,3'-tetra-t-butylmanganocene, 1,1',3,3'-tetratrimethylsilylmanganocene, and 1,1'-di-trimethylsilyl-3,3'-di-t-butylmanganocene, was prepared in order to examine the effect of the cyclopentadienyl substituents on the variable temperature magnetic susceptibility of manganocenes. The tetrahydrofuran adduct of manganese iodide (MnI_2·2THF) [3,4] was treated with magnesium cyclopentadienides in tetrahydrofuran at room temperature to yield the substituted manganocenes (Figure 55, Table 24).

$$MnI_2\cdot 2THF + Cp'_2Mg \xrightarrow{THF,\ 25^\circ C} Cp'_2Mn$$

$Cp' = (Me_3Si)_2C_5H_3$, $(Me_3Si)(Me_3C)C_5H_3$, $(Me_3C)_2C_5H_3$

Figure 55: General synthesis of manganocenes.

	Color	mp	^{1}H NMR
Cp''_2Mn $[(Me_3Si)_2C_5H_3]_2Mn$	pale straw	90-91° C	11.1 ppm, ($\nu_{1/2}$ =500 Hz)
Cp^{tt}_2Mn $[(Me_3Si)(Me_3C)C_5H_3]_2Mn$	orange	106-107° C	12.5 ppm, ($\nu_{1/2}$ =700Hz)
$Cp^{\ddagger}_2Mn$ $[(Me_3C)_2C_5H_3]_2Mn$	red-orange	145-146° C	14.5 ppm, ($\nu_{1/2}$ =700 Hz)

Table 24: Characterization data for substituted manganocenes

The only signals observed by ^{1}H NMR are those of the trimethylsilyl groups and t-butyl groups. Only a single resonance is observed for Cp^{tt}_2Mn, the trimethylsilyl resonance and t-butyl resonances are too close together to be resolved. The observed resonances are very broad, a consequence of the short longitudinal relaxation time (T_2) for the paramagnetic compounds[22], and the other resonances are presumably broadened into the baseline.

The single crystal X-ray structures of $Cp^{\ddagger}_2Mn$ and Cp''_2Mn have been solved and indicate that the molecules are monomers in the solid-state (Figure 56, Table 25, Figure 57). The X-ray structure of Cp^{tt}_2Mn has not been attempted since disorder between Me_3C- groups and Me_3Si- groups is likely but the general structural feautures are presumed to be analogous.

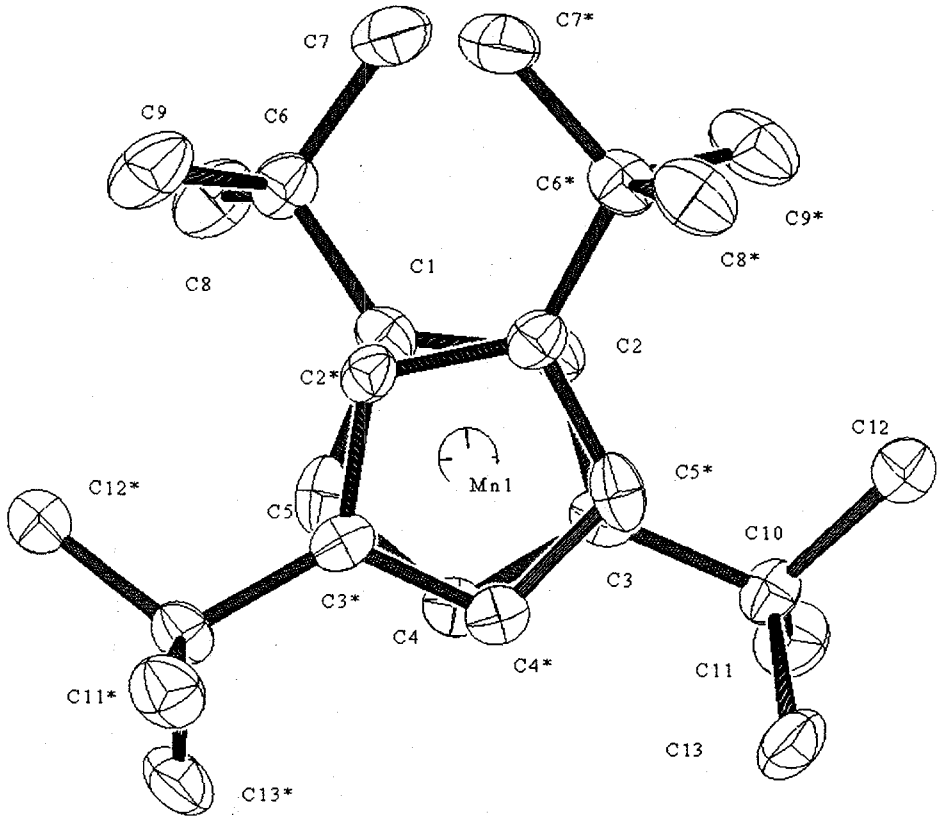

Figure 56: ORTEP diagram of $Cp^{\ddagger}_2Mn$, 50% thermal elipsoids

	$Cp^{‡}_2Mn$	Cp''_2Mn
Mn-ring centroid	1.75	2.04
Mn-C1	2.18	2.36
Mn-C2	2.17	2.32
Mn-C3	2.12	2.38
Mn-C4	2.06	2.41
Mn-C5	2.09	2.39
centroid-Mn-centroid	175°	166°
angle between Cp planes	12°	10°

Table 25: Comparison of structural data for $Cp^{‡}_2Mn$ and Cp''_2Mn, distances in Å, angles in deg.

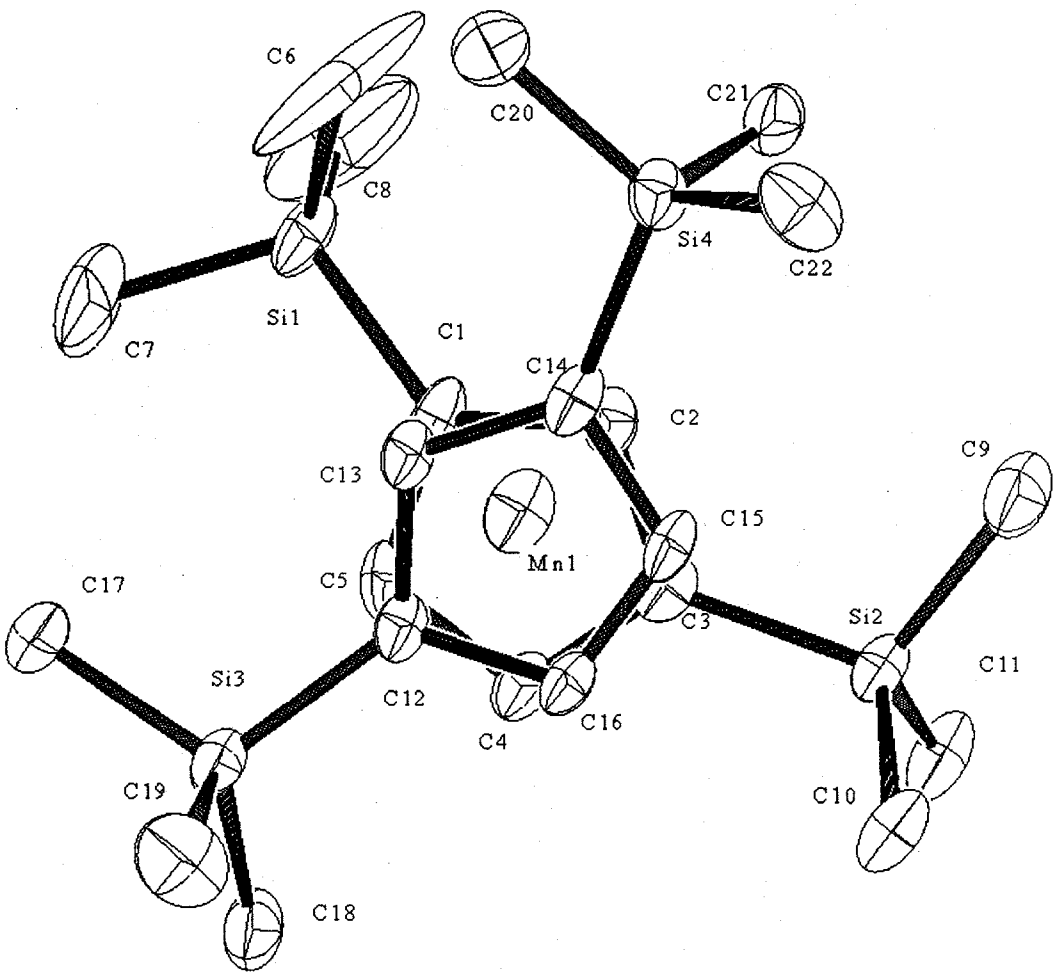

Figure 57: ORTEP diagram of Cp''_2Mn, 50% thermal elipsoids

The crystals of the tetrasubstituted manganocenes are not isomorphous. 1,1',3,3'-Tetra-t-butylmanganocene crystallized in the orthorhombic space group Pccn (#56) and the molecule contains a crystallographic C_2-axis whereas the 1,1',3,3'-tetratrimethylsilylmanganocene formed monoclinic crystals, $P2_1/c$ (#14). The most significant structural difference between the two metallocenes is that the metal-ring centroid distance in Cp''_2Mn is, on average, 0.3 Å longer than the metal-ring centroid distance in $Cp^{\ddagger}_2Mn$.

Solid State Magnetic Susceptibility

The tetra(trimethylsilyl)manganocene exhibited typical Curie-Weiss behavior (Figure 58).

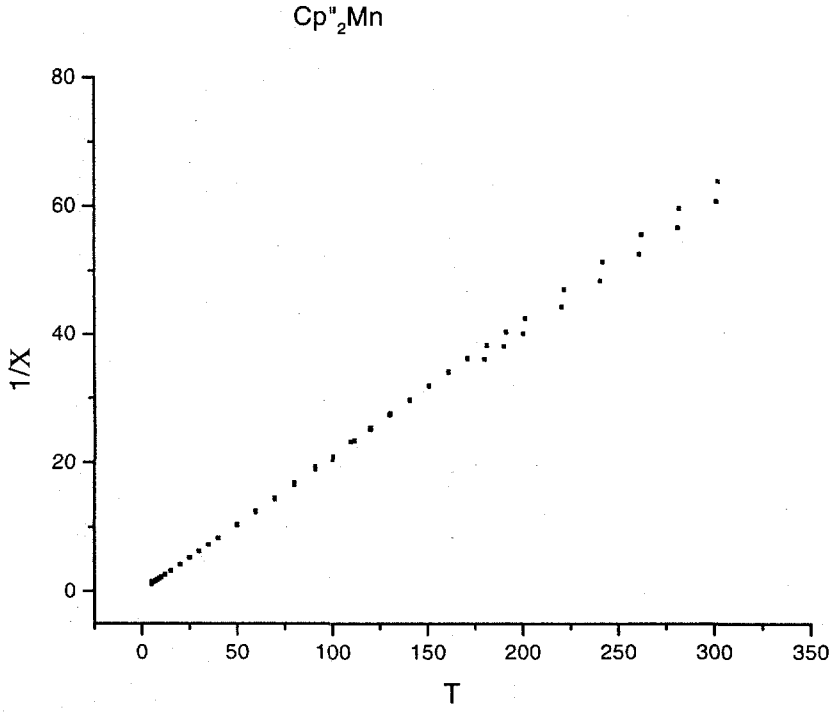

Figure 58: Plot of χ^{-1} vs. T, Cp''_2Mn

The observed magnetic moment of 6.2 BM is slightly higher than predicted by the spin only (Equation 4) magnetic moment for S = 5/2 of 5.92 BM. Orbital angular momentum can contribute to the magnetic moment of a sample but for high-spin d_5-compounds, the orbital angular momentum is zero (the sum of the angular momentum quantum numbers is zero) and does not contribute to the observed moment. An additional term results from mixing of the ground-state with higher energy states that do have orbital angular moments greater than zero, but this *spin-orbit coupling* is a minor contributor to the magnetic moment when the ground-state, as in this case, has half-filled shells [23]. The plot of μ_{eff} vs. temperature shows no variation in the spin-state over the temperature range of 25–300K indicating that the molecule is high-spin Mn(II) at all these temperatures (Figure 59).

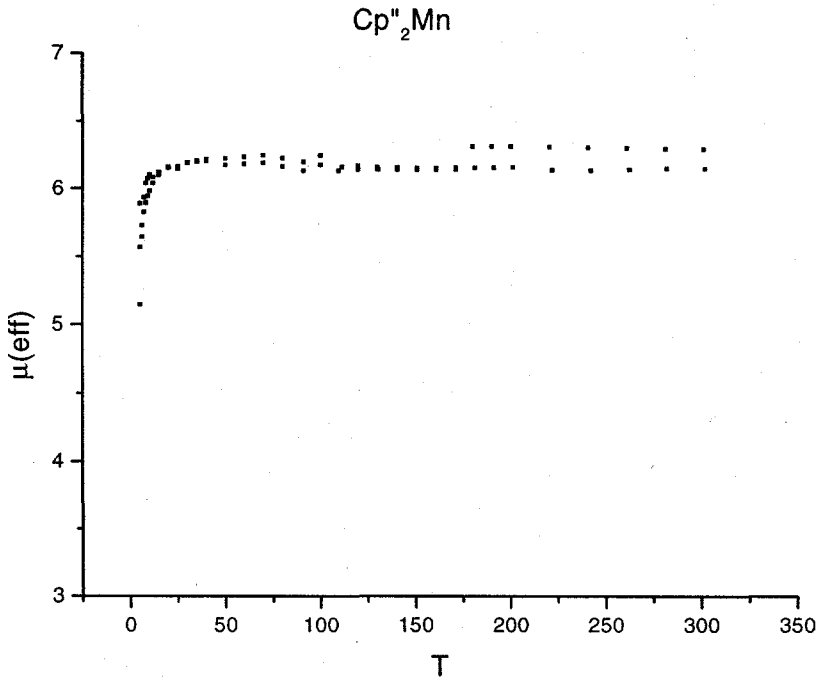

Figure 59: Plot of μ_{eff} vs. T, Cp"$_2$Mn

Following molecular orbital theory arguments[24,25], Wilkinson concluded that the five unpaired electrons exceeded the maximum number permissible for a "sandwich bonded" Cp_2Mn. Chemical reactions and the characterization of the complex showed that the cyclopentadienyl group was more labile in manganocene than in other first-row metallocenes. This led to the conclusion that the bonding in manganocene is ionic, rather than the product of overlapping orbitals, and the compound is more properly named "manganese(II) cyclopentadienide", akin to alkali-metal complexes of the same ligand[16].

The X-ray crystal structure of $Cp"_2Mn$ indicates that it is unmistakably "sandwich bonded" and the solid-state magnetic susceptibility shows that the complex is high-spin, but these results contradict the earlier conclusion that such a combination is forbidden by molecular orbital theory. In the molecular orbital treatment by Albright, Burdett, and Whangbo[1], five unpaired electrons is not forbidden, but requires that two electrons occupy the e_{1g}^* antibonding orbitals (Figure 53). The two electrons in antibonding orbitals in manganocene reduce the bond order between the cyclopentadienyl groups and the metal and account for the increased lability of the cyclopentadienyl ligand in manganocene compared to other first-row metallocenes.

The solid-state magnetic susceptibility of $Cp^{\ddagger}_2Mn$ is shown in Figure 60. The plot of χ^{-1} vs. T has a much steeper slope indicating a smaller magnetic moment and there is a significant deviation from Curie behavior as the sample is warmed above 250 K.

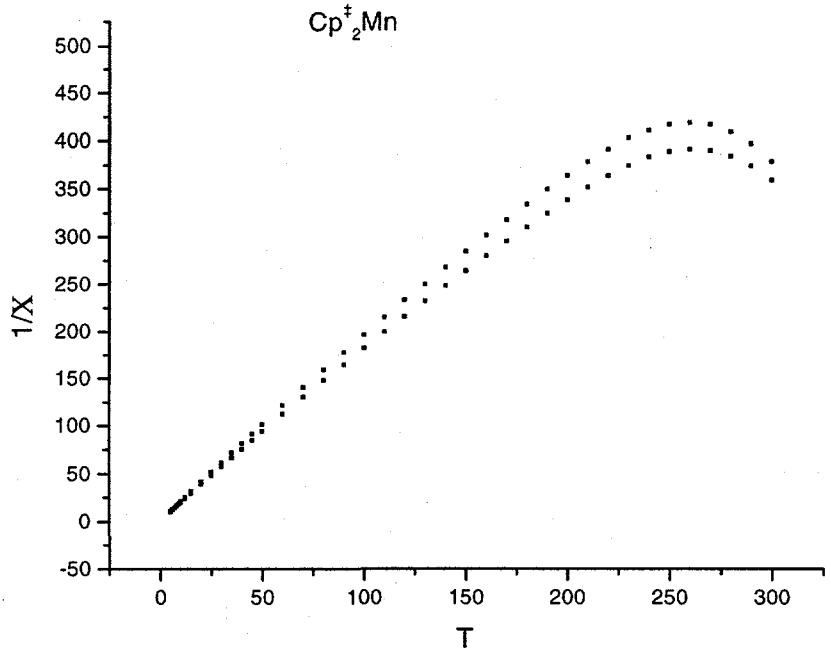

Figure 60: Plot of χ^{-1} vs. T, $Cp^{\ddagger}_2Mn$

Below 250 K, the plot of μ_{eff} vs. temperature indicates that the magnetic moment (2.1 B.M.) is consistent with low-spin Mn(II) The predicted moment based on the number of unpaired electrons is 1.73 BM but observed moments for low-spin d^5-complexes are slightly higher due to the orbital contribution to the magnetic moment. The moment begins to increase sharply at higher temperatures, reaching 2.6 BM at 300 K (Figure 61).

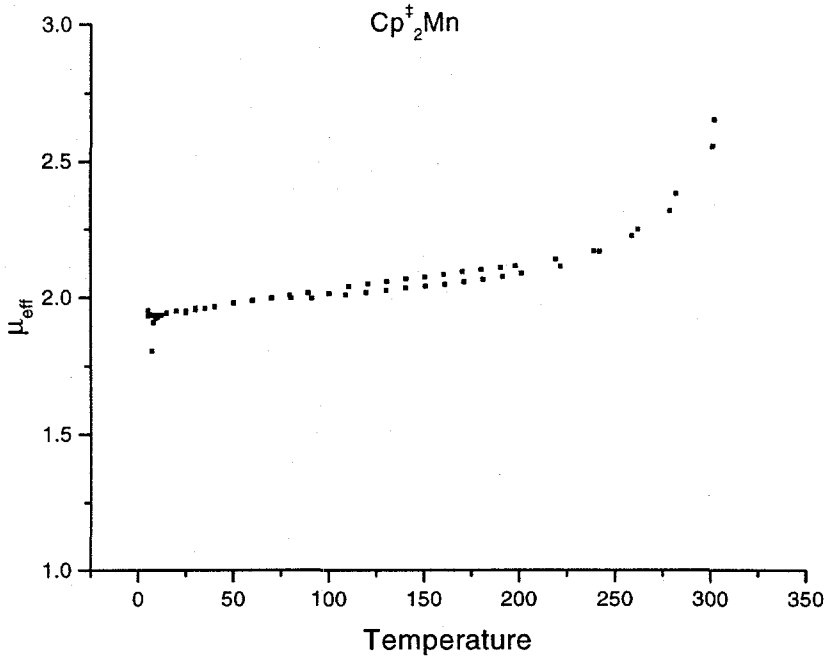

Figure 61: Plot of μ_{eff} vs. T, $Cp^{\ddagger}_2Mn$

The difference in ring centroid to Mn distances between Cp''_2Mn and $Cp^{\ddagger}_2Mn$ can be attributed to the difference observed in spin-state. The longer metal/ring-centroid distance for the high-spin compound, Cp''_2Mn (Table 26), is consistent with the reduced bond order. The long, bond distances are shared by the other high-spin complexes mentioned earlier. In unsubstituted manganocene, the metal/ring-centroid distance for the pentahapto-cyclopentadienyl ring is 2.10 Å and the metal/carbon distances for the nearest carbon atoms in the bridging cyclopentadienyl group is 2.41 Å[15]. These distances are equivalent to the corresponding bond lengths observed in $(MeC_5H_4)_2Mn$ (Table 26).

Low-spin		High-spin			
$Cp^{\ddagger}_2Mn$	$(C_5Me_5)_2Mn$[1 0,11]	$(MeCp)_2Mn$	Cp''_2Mn	Cp_2Mn[15]	$(Me_3SiC_5H_4)_2Mn$[9]
1.75	1.73	2.10	2.04	2.10	2.10

Table 26: Metal-ring centroid distances in low-spin and high-spin manganocenes (Å)

As predicted, the magnetic susceptibility of Cp^{tt}_2Mn is highly temperature dependent (Figure 62).

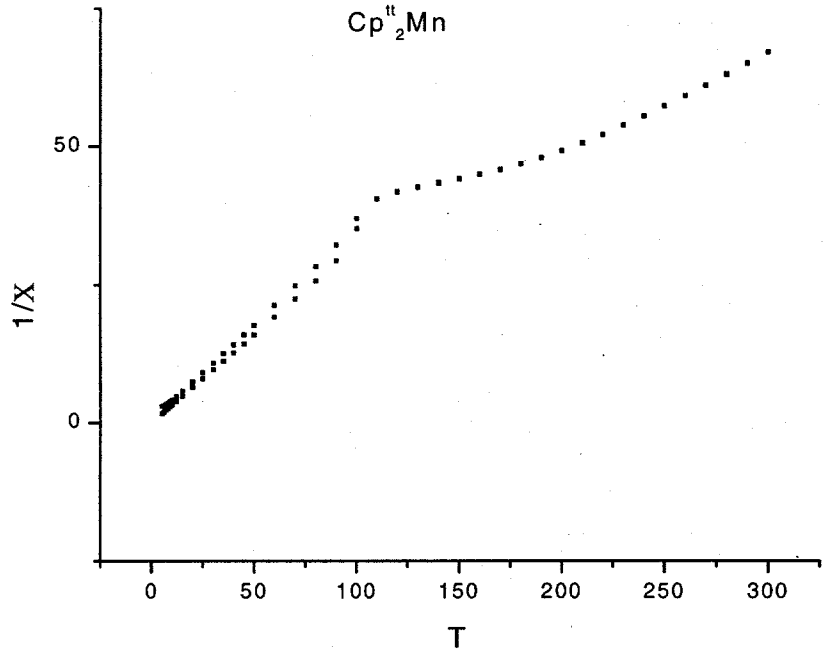

Figure 62: Plot of χ^{-1} vs. T, Cp^{tt}_2Mn

At room temperature, the complex has a magnetic moment consistent with high-spin Mn(II) (μ_{eff} = 5.9 B.M.) but μ_{eff} falls as the temperature decreases and abruptly reaches a minimum (4.6 B.M.) at ~120 K.

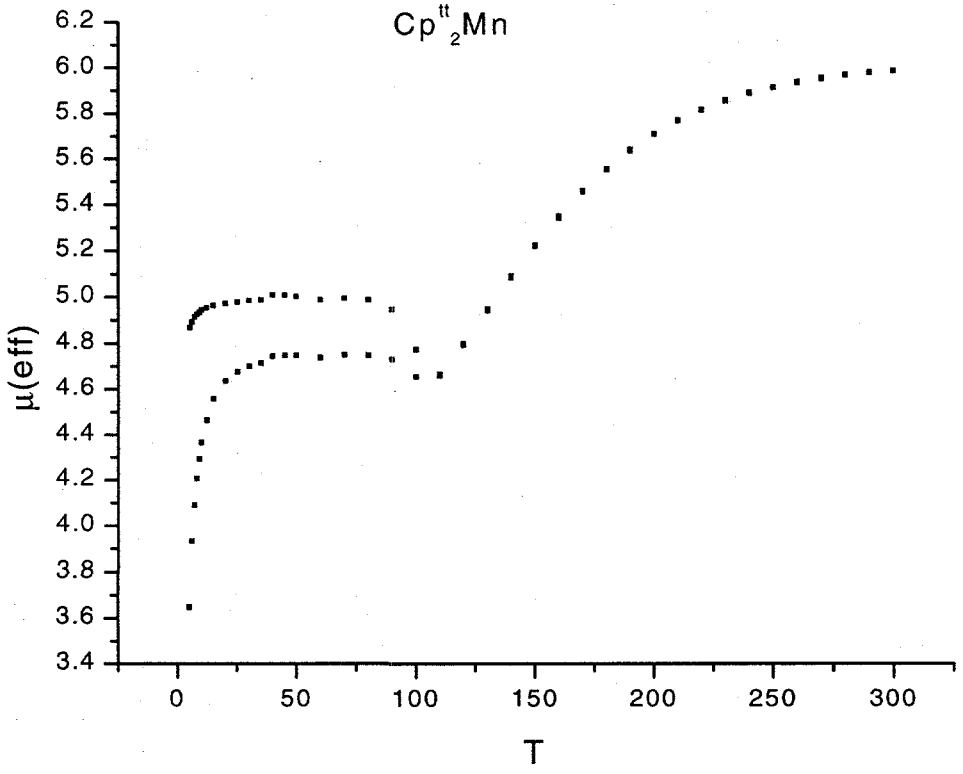

Figure 63: Plot of μ_{eff} vs. T, Cp''_2Mn

The low-temperature magnetic moment suggests an either an improbable, intermediate-spin ground state or a mixture of the high-spin and low-spin species. The intermediate-spin ground state is unsupported by theoretical treatments and would require a significant geometric distortion to split the degenerate, e_{1g}^* orbitals to such a degree that the energy difference between the two orbitals is larger than the electron pairing energy. If the cyclopentadienyl rings are distorted from a periplanar configuration, the molecule has idealized C_{2V} symmetry and the degeneracy of the e_{1g}^* orbitals is lost, but the X-ray crystal structures of the analogous and presumably isostructural, $Cp^{\ddagger}_2Mn$ and Cp''_2Mn indicate only a *minor* C_{2V} distortion (Table 25), and the quartet ground state, which would result from three unpaired and two paired electrons, is unlikely. Since magnetic susceptibility is a bulk property of a given sample it is impossible to distinguish between

a sample consisting of spin 3/2 molecules and a sample consisting of equal populations of spin 1/2 and spin 5/2 species. Electron paramagnetic resonance (EPR) spectroscopy, however, exhibits discrete signals for each paramagnetic contributor present in the sample (subject to time-scale and resolution limitations).

Electron Paramagnetic Resonance

Electron paramagnetic resonance studies were undertaken to distinguish between a mixture of spin states and a single ground state. The low temperature EPR spectra of Cp''_2Mn and $Cp^{\ddagger}_2Mn$ were collected, both as microcrystalline solids and as glasses in methylcyclohexane, to serve as high-spin and low-spin standards. The high-spin Cp''_2Mn, compound exhibited a broad, featureless resonance. No hyperfine coupling was resolved and only an averaged g-value of 6.03 is observable at 4 K (Figure 64).

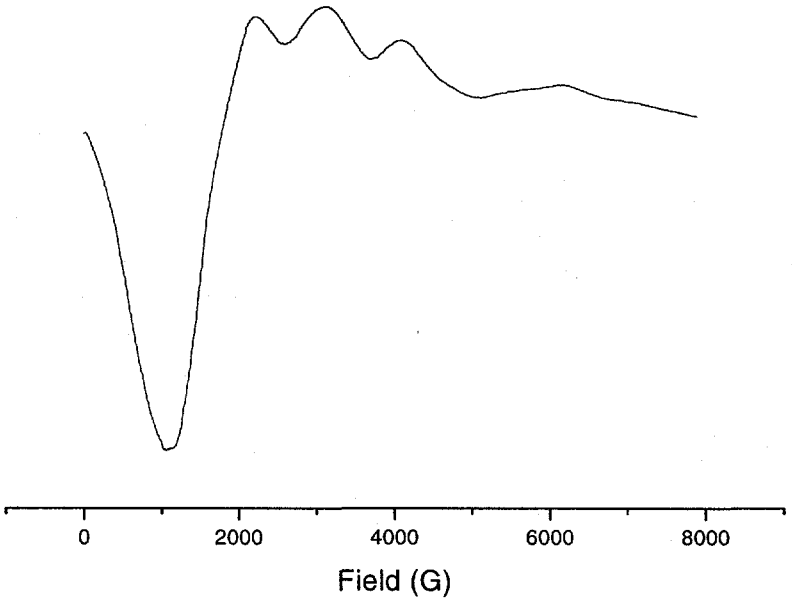

Figure 64: EPR spectrum of Cp''_2Mn in methylcyclohexane, 4 K

In the spectrum of the low-spin, $Cp^{\ddagger}_2Mn$, compound, $g_{\parallel}$ and $g_{\perp}$ are resolvable at 2.57 and 1.90 respectively.

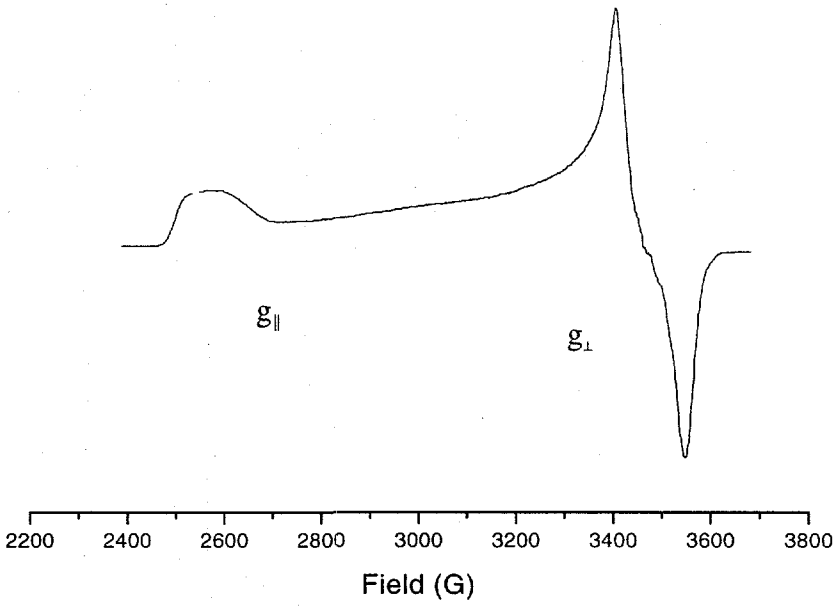

Figure 65: EPR spectrum of $Cp^{\ddagger}_2Mn$ in methylcyclohexane, 4 K

The spectrum of the (t-butyl)(trimethylsilyl)substituted cyclopentadienyl complex, Cp^{tt}_2Mn, contains a superposition of the two standard spectra. A broad resonance at g = 5.95 corresponds to the high-spin fraction, and $g_{\parallel}$ = 2.88 and $g_{\perp}$ = 1.95 indicate the low-spin species is also present. No other resonances, specifically none corresponding to a quartet state, were observed.

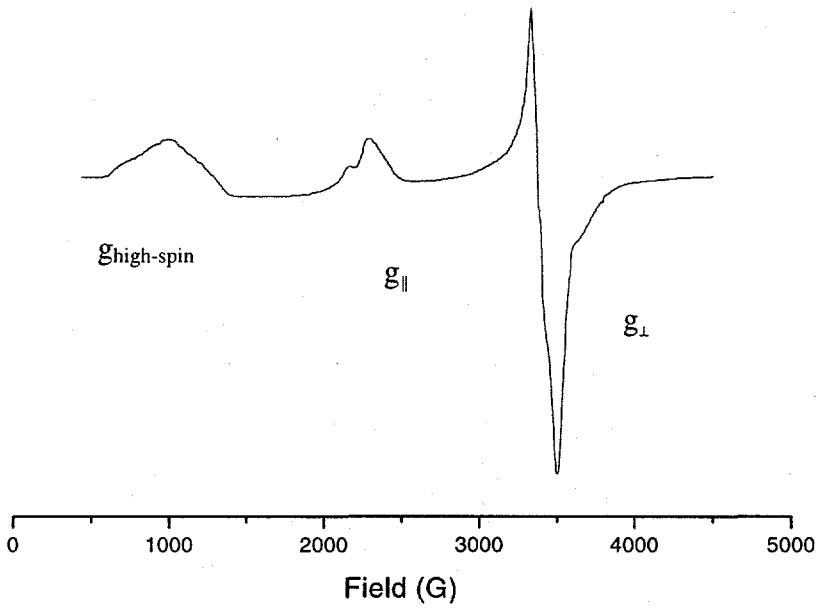

Figure 66:EPR spectrum of Cp^{tt}_2Mn in methylcyclohexane, 4 K

Spin-equilibria

In the intermediate temperature regime, the change in magnetic moment with temperature suggests that the Cp^{tt}_2Mn sample is an equilibrium between the high-spin and low-spin forms.

$$Cp^{tt}_2Mn\ (\text{Low-spin}) \rightleftharpoons Cp^{tt}_2Mn\ (\text{High-spin})$$

$$K = \frac{[Cp^{tt}_2Mn\ (\text{High - spin})]}{[Cp^{tt}_2Mn\ (\text{Low - spin})]}$$

Equation 8

Presumably, the high-spin form has the same magnetic moment as the high-spin species examined earlier, Cp''_2Mn, and the low-spin form has the same moment as $Cp^{\ddagger}_2Mn$ (in the region where the sample obeyed Curie Law). With approximate values for the high-

spin and low-spin moments, the equilibrium constant for the reaction can be calculated and the enthalpy and entropy change for the equilibrium can be determined.

$$K = e^{-\Delta G/RT}$$

$$\ln K = -\Delta G/RT = -\Delta H/RT + \Delta S/R$$

Equation 9

The actual concentrations of the species are not necessary, since a ratio of the partial populations is the same as the ratio of the concentrations.

$$P_{(high\text{-}spin)} = \frac{[Cp^{tt}{}_2Mn\ (High\text{-}spin)]}{[Cp^{tt}{}_2Mn\ (High\text{-}spin)] + [Cp^{tt}{}_2Mn\ (Low\text{-}spin)]}$$

$$P_{(Low\text{-}spin)} + P_{(High\text{-}spin)} = 1$$

$$\mu_{obs}{}^2 = P_{(High\text{-}spin)}\, \mu_{(High\text{-}spin)}{}^2 + P_{(Low\text{-}spin)}\, \mu_{(Low\text{-}spin)}{}^2$$

$$P_{(High\text{-}spin)} = \frac{\mu_{obs}{}^2 - \mu_{(Low\text{-}spin)}{}^2}{\mu_{(High\text{-}spin)}{}^2 - \mu_{(Low\text{-}spin)}{}^2}$$

$$K = \frac{P_{(High\text{-}spin)}}{P_{(Low\text{-}spin)}} = \frac{P_{(High\text{-}spin)}}{1 - P_{(High\text{-}spin)}}$$

Equation 10

The plot of lnK vs. T^{-1} is linear with a slope of $-\Delta H/R$ and an intercept of $\Delta S/R$. The transformation from low-spin $Cp^{tt}{}_2Mn$ to high-spin $Cp^{tt}{}_2Mn$ is endothermic (ΔH = 6.3 kJ/mol (1.26 kcal/mol)) with an entropy increase of 46 J/mol K (11 cal/mol K).

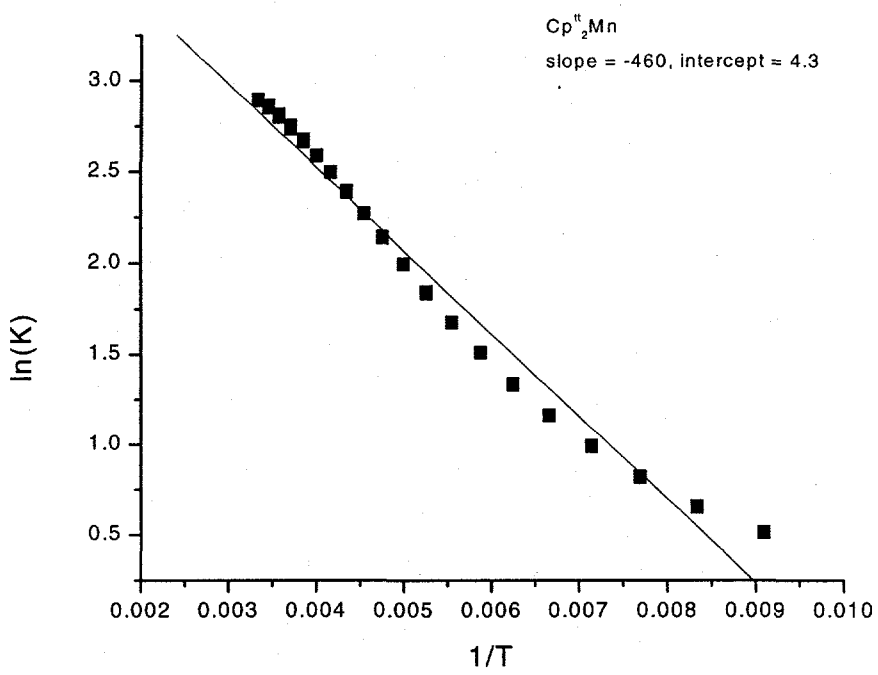

Figure 67: ln(K) vs. T^{-1}, Cp^{tt}_2Mn Low-spin/High-spin equilibrium, from magnetic susceptibility

These values are lower than those obtained by Ammeter and coworkers for related molecules ($[Me_3CC_5H_4]_2Mn$, ΔH = 12.7 kJ/mol, ΔS = 44 J/mol K) [7].

Variable Temperature UV-vis Spectroscopy

During preparation of EPR samples of Cp^{tt}_2Mn, it was observed that cooling the sample in liquid nitrogen caused the orange color to intensify significantly and the color faded as the sample was warmed to room temperature. Based on the solid-state magnetic susceptibility measurements, the equilibrium favors the high-spin species at room temperature and the low-spin contribution increases as the temperature decreases. In free-energy terms, the entropy term dominates at high temperature and favors the high-

spin species. As the temperature decreases, the TΔS term becomes smaller and the enthalpy term dominates the equilibrium.

$$Cp^{tt}{}_2Mn_{(Low\text{-}spin)} \rightleftharpoons Cp^{tt}{}_2Mn_{(High\text{-}spin)}$$

$$\Delta G = \Delta H - T\Delta S$$

The fact that Cp''_2Mn is nearly colorless and $Cp^{\ddagger}{}_2Mn$ is orange allows the spin equilibrium to be probed using UV-visible spectroscopy. The low-spin complex, $Cp^{\ddagger}{}_2Mn$, exhibits a λ_{max} at 430nm corresponding to a strong d-d transition[17]. For the high-spin species, the transition is forbidden by selection rules since it would require a spin-state change ($\Delta S \neq 0$).[26]

The variable temperature UV-vis experiment clearly showed an increase in absorption at 430 nm as the sample was cooled to 170 K (Figure 68).

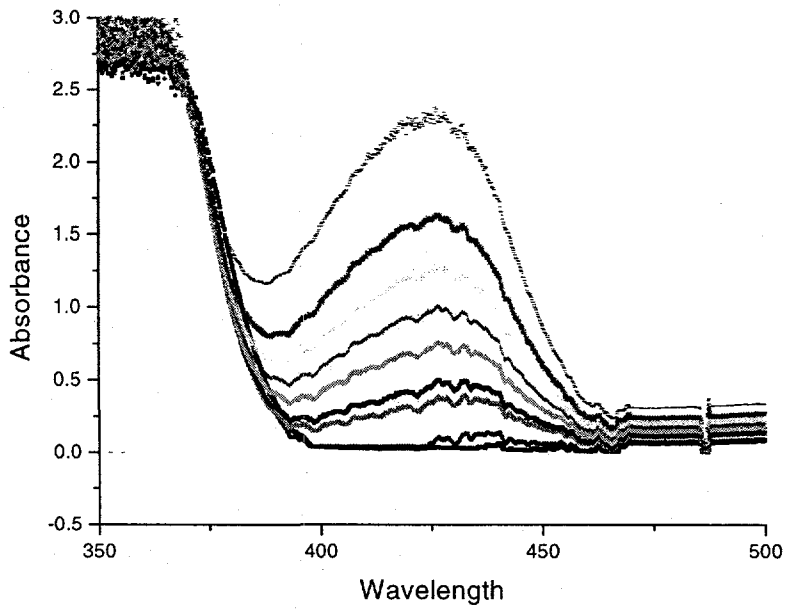

Figure 68: Variable temperature UV-vis spectra, $Cp^{tt}{}_2Mn$

Samples for variable temperature UV-vis spectroscopy were prepared as methylcyclohexane solutions (0.1-1 M). At all accessible temperatures, the low-spin Cp^{tt}_2Mn is in equilibrium with the high-spin species so the concentration of either the high-spin or low-spin species, at any given temperature, is unknown, but the sum of the high-spin and low-spin concentrations is the concentration of the sample. In order to quantify the measured absorbances an independent measure of the extinction coefficient was required. The an extinction coefficient for the high-spin complex, $Cp"_2Mn$, can be used to approximate an extinction coefficient for the high-spin form of Cp^{tt}_2Mn. Both species exhibit a sharp absorbance at 269 nm. The absorbance of $Cp"_2Mn$ is independent of temperature at 269 nm (Figure 69) and the extinction coefficient is 25 L/mol. The constant concentration of the high-spin species agrees with the solid-state magnetic susceptibility data, which indicated that the sample was high-spin at all temperatures (Figure 59).

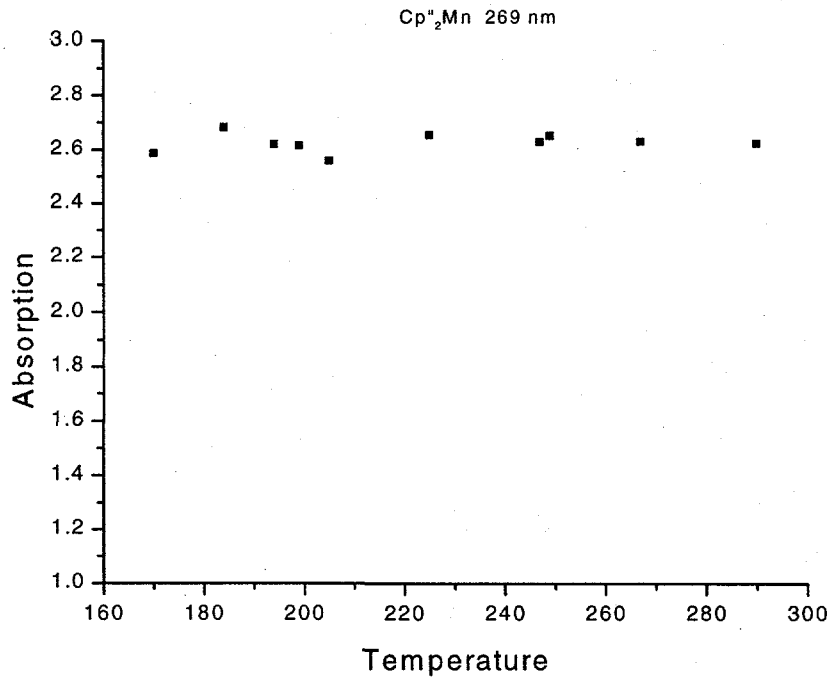

Figure 69: Absorbance vs. temperature, $Cp"_2Mn$

Recall that the data from the solid-state magnetic susceptibility measurements of $Cp^{‡}_2Mn$ indicate a deviation from Curie behavior above 250 K (Figure 61). The data suggest that above 250 K, the equilibrium between low-spin $Cp^{‡}_2Mn$ and high-spin $Cp^{‡}_2Mn$ begins to shift toward the high-spin form. The absorbances at 269 and 430 nm for high- and low-spin $Cp^{‡}_2Mn$, respectively, were temperature dependent, showing, at 430 nm, a significant decrease in absorbance as the temperature increased (Figure 70).

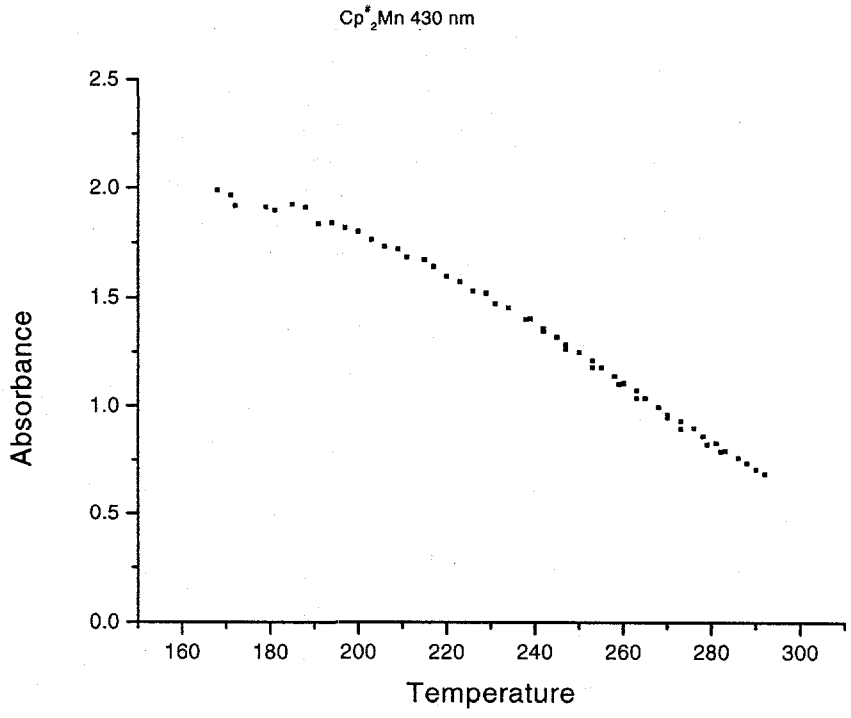

Figure 70: Absorbance vs. T, $Cp^{‡}_2Mn$

A corresponding increase in the UV absorbance at 330 nm demonstrates the increase in population of the high-spin species (

Figure 71).

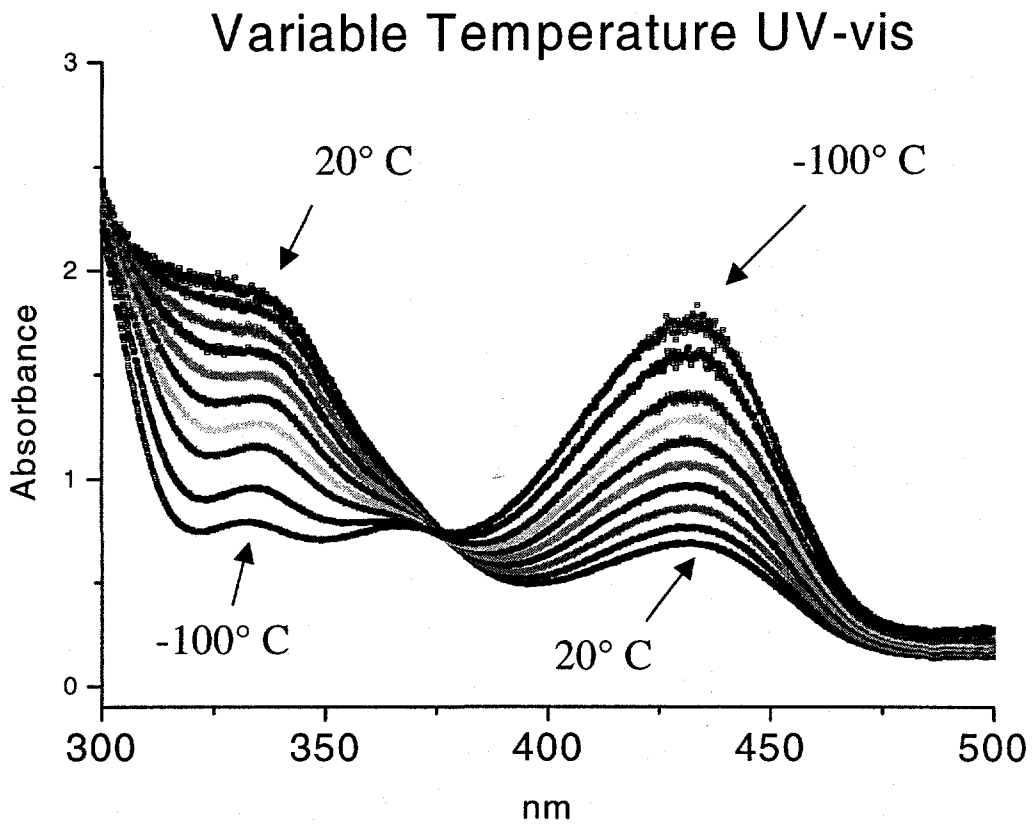

Figure 71: Variable temperature UV-vis spectra, $Cp^{\ddagger}_2Mn$

The enthalpy change for the reaction was determined in a method analogous to that used for the solid-state determination. The value for the extinction coefficient was estimated since, at the lower limit of the experiment, the absorbance of $Cp^{\ddagger}_2Mn$ at 430 nm changes little with temperature and the partial populations were determined from absorbance instead of magnetism (Equation 11).

$$\text{Absorbance} = \varepsilon_{(\text{low-spin})}[Cp^{\ddagger}_2Mn_{(\text{Low-spin})}]$$

Equation 11

$$[Cp^{\ddagger}_2Mn_{(\text{High-spin})}] = [Cp^{\ddagger}_2Mn_{(\text{total})}] - [Cp^{\ddagger}_2Mn_{(\text{Low-spin})}]$$

$$K = e^{-\Delta G/RT}$$

$$\ln K = -\Delta G/RT \qquad = -\Delta H/RT + \Delta S/R$$

The equilibrium between the low-spin and high-spin forms of $Cp^{\ddagger}_2Mn$ is described by the plot of ln(K) vs. 1/T indicating that reaction is endothermic (15.9 kJ/mol (3.8 kcal/mol)) and the high-spin species is entropically favored (59 J/mol K (14 cal/mol K)) (Figure 72).

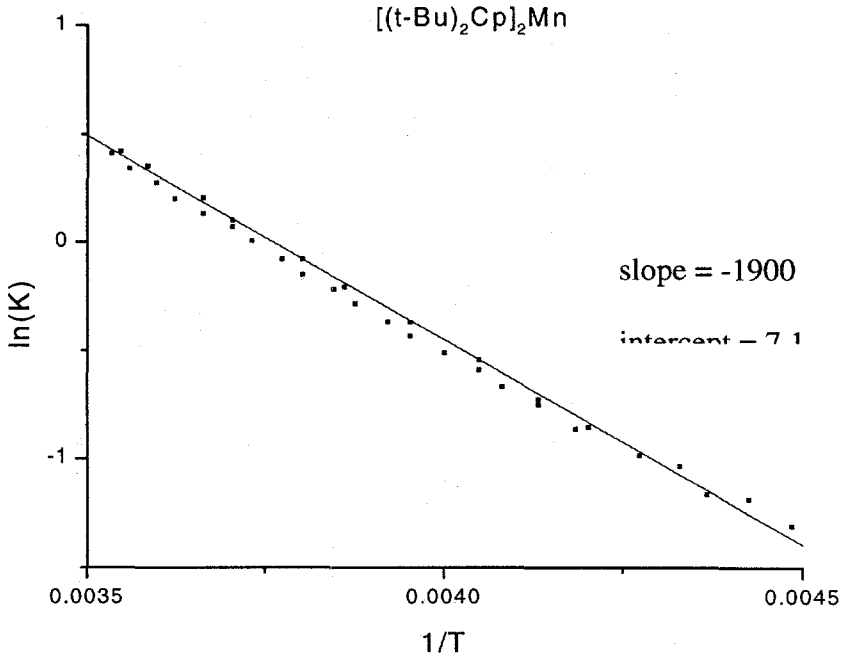

Figure 72: ln(K) vs. T^{-1}, $Cp^{\ddagger}_2Mn$. Low-spin/High-spin equilibrium

$$Cp^{\ddagger}_2Mn_{(Low\text{-}spin)} \rightleftharpoons Cp^{\ddagger}_2Mn_{(high\text{-}spin)}$$

$$\Delta H = 15.9 \text{ kJ/mol} \qquad \Delta S = 59 \text{ J/mol K}$$

The estimate of the extinction coefficient was experimentally corroborated by measuring the extinction for the UV absorption (330 nm) of the high-spin species, Cp''_2Mn. Recall that the solid-state magnetic susceptibility of Cp''_2Mn was independent of temperature and indicated no spin-equilibrium (Figure 59). The solution, variable temperature, UV-visible spectra are also independent of temperature. The extinction coefficient for the absorption at 330 nm was used to independently calculate the relative concentrations of high-spin and low-spin species in Cp^{tt}_2Mn. The concentrations derived from the two extinction coefficients agree.

The plot of absorbance at 430 nm vs. temperature shows that very little of the low-spin species is left at room temperature (Figure 73).

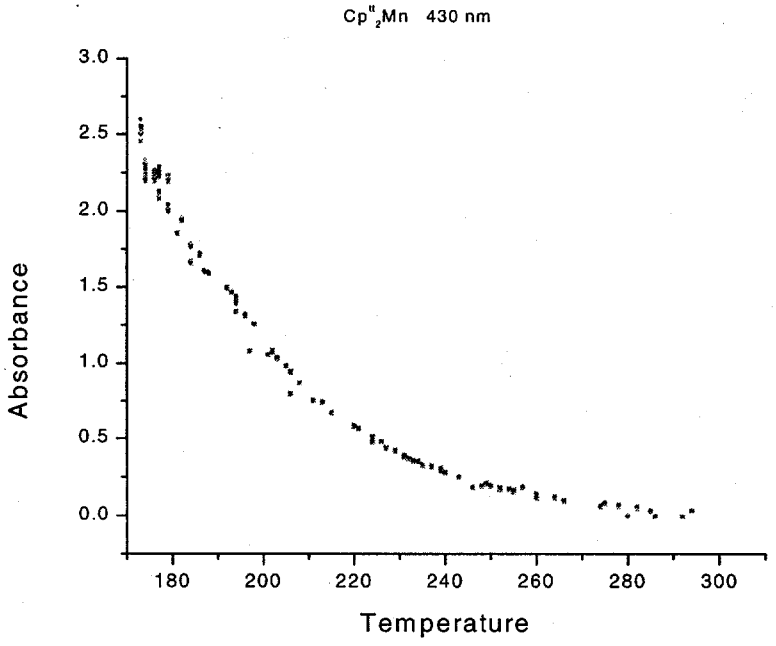

Figure 73: Absorbance vs. temperature, 430 nm, Cp^{tt}_2Mn

The plot of ln(K) vs. 1/T is linear for a simple, two-component equilibrium but the data for Cp^{tt}_2Mn are curved suggesting that another species is involved in the equilibrium expression (Figure 74).

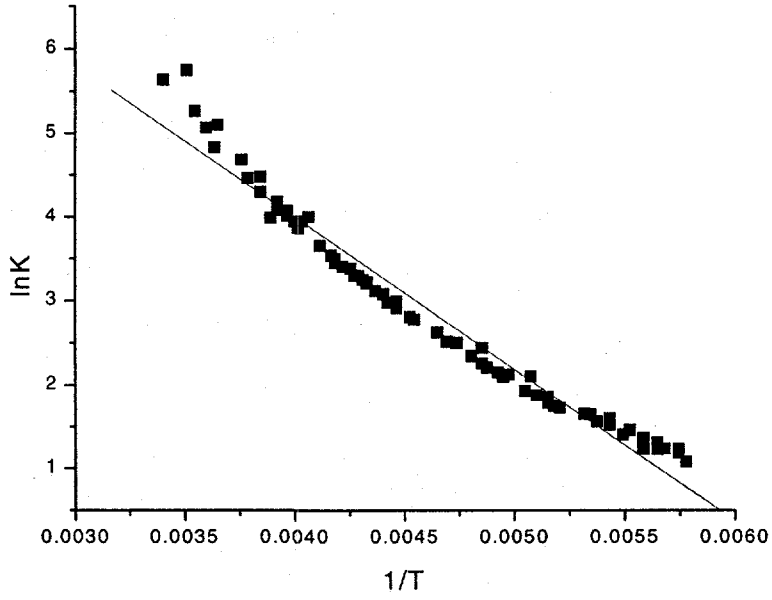

Figure 74: ln(K) vs. T^{-1}, Cp^{tt}_2Mn

A linear approximation of the curve indicates that the enthalpy and entropy changes (14.8 kJ/mol, 90 J/mol K) are consistent with the values obtained for $Cp^{\ddagger}_2Mn$ and the values obtained by Ammeter and coworkers for $(Me_3CC_5H_4)_2Mn$ (Table 27)

	ΔH(soln.)	ΔS(soln)	ΔH(solid)	ΔS(solid)
$Cp^{\ddagger}_2Mn$	15.9 kJ/mol	59 J/mol K	13 kJ/mol	30 J/mol K
Cp^{tt}_2Mn	14.8 kJ/mol	90 J/mol K	6.3 kJ/mol	46 J/mol K
$(Me_3CC_5H_4)_2Mn$[7]	12.7 kJ/mol	44 J/mol K	-	-

Table 27: Enthalpy and entropy changes for spin-equilibria

The (trimethylsilyl)(t-butyl)cyclopentadienyl ligand can form different isomers varying only in the face to which the metal is bound. Depending on which the face coordinated to the metal atom, the cyclopentadienyl group can be right-handed or left-handed (see chapter 3). There are four isomers present in samples of Cp^{tt}_2Mn.

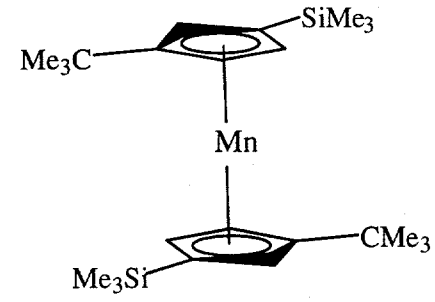

Right/Right

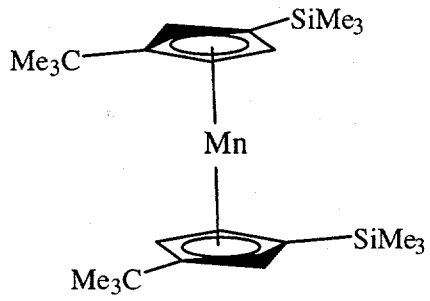

Right/Left

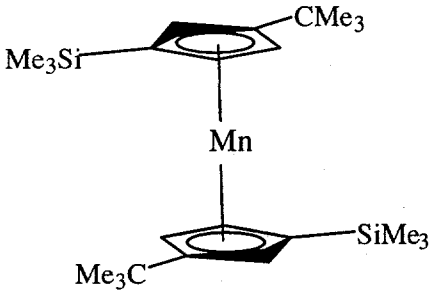

Left/Left

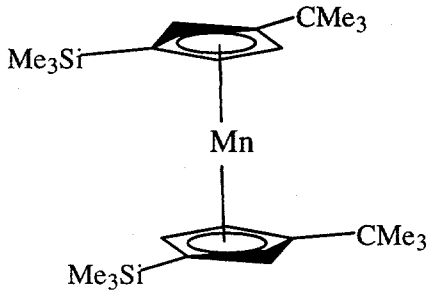

Left/Right

Figure 75: Diastereomers of Cp^{tt}_2Mn

These isomers can be divided into two pairs of enantiomers. The right/right and left/left isomers are enantiomers of each other and are optically active. The left/right and right/left isomers are the same compound, that is, the C_S isomer is *meso* (Figure 76).

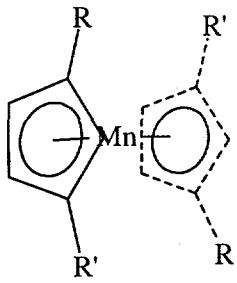

$C_2(rac)$

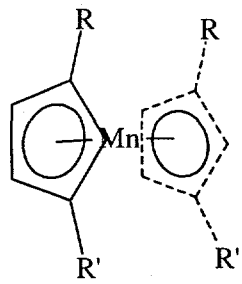

$C_S(meso)$

Figure 76: Diastereomers of Cp^{tt}_2Mn

The two optically active examples are indistinguishable energetically and magnetically but the *meso*-isomer has a different energy surface and, presumably, a slightly different enthalpy change for the low-spin to high-spin reaction.

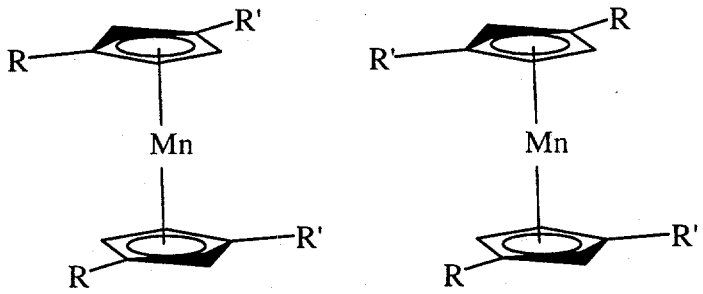

$Cp^{tt}_2Mn_{(High\text{-}spin)}$

$A_{(Low\text{-}Spin)} \rightleftharpoons A_{(High\text{-}spin)}$

ΔH_B ΔH_A

$Cp^{tt}_2Mn_{(Low\text{-}spin)}$

Figure 77: Proposed independent equilibria, Cp^{tt}_2Mn

Although a high spin-d^5 complex mat exhibit different behavior, our experience with cerium and uranium suggests that the barrier for interconversion of species A and B is too large to be a factor in this temperature range. Experiments are underway to determine the barrier for interconversion of other examples of Cp^{tt}_2M species (Cp^{tt}_2Mg, Cp^{tt}_2Fe). In these cases, both isomers are observable by NMR spectroscopy and 2D NMR experiments will illuminate the exchange (see ligand chapter). The manganocene samples are paramagnetic and are not amenable to study by 2D NMR but the data from the corresponding magnesocene and ferrocene samples may add confidence to our assertion that, in the temperature region of our experiment, we have two separate equilibria and not a four-member, compound equilibrium.

$$\begin{array}{ccc} A_{(\text{Low-Spin})} & \rightleftharpoons & A_{(\text{High-spin})} \\ \Updownarrow & & \Updownarrow \\ B_{(\text{Low-spin})} & \rightleftharpoons & B_{(\text{High-spin})} \end{array}$$

If the data from the variable temperature UV-vis experiment are the sum of the data from two independent equilibria, and the two equilibria have different values of ΔH and ΔS, the plot of ln K vs. 1/T will be curved. The curve, in the two, independent equilibria case, is the plot of ($\ln K_A + \ln K_B$) vs. 1/T. Since the λ_{max} values for the low-spin species of A and B are indistinguishable, the partial populations of the two, low-spin species are unknown and the values of K_A and K_B are unknown and it is impossible to determine the slopes of the two lines that make up the curve.

In a related system, a single isomer of Cp^{tt}_3Ce can be crystallized from a mixture of isomers (Chapter 3). This suggests that a single species of Cp^{tt}_2Mn might be isolable. Data from such a sample could be used to determine the thermodynamic parameters for one of the equilibria and thus solve the two equilibria problem.

References

1)Albright, T. A.; Burdett, J. K.; Whangbo, M.-H. *Orbital Interactions in Chemistry*; John Wiley & Sons: New York, 1985.

2)Wilkinson, G.; Cotton, F. A. *Chemistry and Industry*, **1954**, *11*, 307.

3)Riemschneider, R.; Kassahn, H.-G.; Schneider, W. *Z. Naturforsch., B*, **1960**, *15*, 547-551.

4)Heyn, B.; Hipler, B.; Kreisel, G.; Schreer, H.; Walther, D. *Anorganische Synthese-chemie*; Springer-Verlag: Berlin, 1986.

5)Reynolds, L. T.; Wilkinson, G. *J. Inorg. Nucl. Chem*, **1959**, *9*, 86-92.

6)Smart, J. C.; Robbins, J. L. *JACS*, **1978**, *100*, 3936-3937.

7)Ammeter, J. H.; Zoller, L.; Bachmann, J.; Baltzer, P.; Gamp, E.; Bucher, R.; Deiss, E. *Helv. Chim. Acta*, **1981**, *64*, 1063-1082.

8)Sitzmann, H.; Schar, M.; Dormann, E.; Kelemen, M. *Z. Anorg. Allg. Chem.*, **1997**, *623*, 1609-1613.

9)Hebendanz, N.; Köhler, F. H.; Müller, G.; Riede, J. *J. Am. Chem. Soc.*, **1986**, *108*, 3281-3289.

10)Freyberg, D. P.; Robbins, J. L.; Raymond, K. N.; Smart, J. C. *JACS*, **1979**, *101*, 892-897.

11)Fernholt, L.; Haaland, A.; Seip, R.; Robbins, J. L.; Smart, J. C. *J. Organomet. Chem.*, **1980**, *194*, 351-355.

12)Robbins, J. L.; Edelstein, N. M.; Cooper, S. R.; Smart, J. C. *J. Am. Chem. Soc.*, **1979**, *101*, 3853-3857.

13)Cauletti, C.; Green, J. C.; Kelley, M. R.; Powell, P.; Tilborg, J. V.; Robbins, J.; Smart, J. *Journal of Electron Spectroscopy and Related Phenomena*, **1980**, *19*, 327-353.

14)Köhler, F. H.; Hebendanz, N. *Chem. Ber.*, **1983**, *116*, 1261-1263.

15)Bünder, W.; Weiss, E. *Z. Naturforsch*, **1978**, *33b*, 1235-37.

16)Wilkinson, G.; Cotton, F. A.; Birmingham, J. M. *J. Inorg. Nucl. Chem.*, **1956**, *2*, 95-113.

17)Switzer, M. E.; Wang, R.; Rettig, M. f.; Maki, A. H. *J. Am. Chem. Soc.*, **1974**, *96*, 7669-7674.

18)Ammeter, J. H.; Bucher, R.; Oswald, N. *J. Am. Chem. Soc.*, **1974**, *96*, 7833-7835.

19)Evans, D. F. *J. Chem. Soc.*, **1959**, 2003.

20)Rabalais, J. W.; L.O.Werme; Bergmark, T.; Karlsson, L.; Hussain, M.; Siegbahn, K. *J. Chem. Phys.*, **1972**, *57*, 1185-1192.

21)Evans, S.; Green, M. L. H.; Jewitt, B.; King, G. H.; Orchard, A. F. *J. Chem. Soc., Faraday II*, **1974**, *70*, 356-376.

22)Derome, A. E. *Modern NMR Techniques for Chemistry Research*; Pergamon Press: New York, 1987; Vol. 6.

23)Carlin, R. L. *Magnetochemistry*; Springer-Verlag: New York, 1986.

24)Moffitt, W. *J. Am. Chem. Soc.*, **1954**, *76*, 3386-3392.

25)Dunitz, J. D.; Orgel, L. E. *J. Chem. Phys.*, **1955**, *23*, 954-958.

26)Huheey, J. E.; Keiter, E. A.; Keiter, R. L. *Inorganic Chemistry*; Fourth ed.; HarperCollins College Publishers: New York, 1993.

Chapter 5

Cyclopentadienyl Ligands Resistant to Intramolecular Oxidative Addition

Soon after the molecular structure of ferrocene was determined, efforts were directed toward preparation of the analogous, first-row metallocenes. While ferrocene remains an axiomatically inert, d^6-low-spin, compound, other first-row metallocenes represented significant challenges with respect to isolation of pure and characterizable products. Historically, the chemistry of titanocenes has been inseparable from intramolecular oxidative addition reactions and, until recently, no isolable base-free titanocenes were known[1]. The isolobal analogy between titanocene and the R_2C, carbene fragment[2,3] outlines the challenge in isolating stable titanocenes and suggests the types of reactions that have fueled interest in the titanocene moiety [4,5].

Titanocene

"Titanocene" was first prepared from $TiCl_2$ and $Na(C_5H_5)$ by Fischer and Wilkinson in 1956[6]. The green compound sublimes, with some decomposition, at relatively cool temperatures (<100° C) and decomposed without melting at ~130° C.

Reactions were examined in order to describe the chemistry of "titanocene" relative to other first-row metallocenes. Treatment with ferrous chloride failed to produce a detectable amount of ferrocene, indicating that the compound was likely a "sandwich" bonded species analogous to ferrocene, cobaltocene and nickelocene, rather than an "electrostatic" complex with reactivity analogous to manganocene.

Molecular orbital treatments allowed for both singlet and triplet ground-states for titanocene depending on the magnitudes of the stabilization resulting from orbital overlap between the ligands and titanium and the electron pairing energy[7,8]. The compound is diamagnetic both as a solid and in solution (in petroleum ether and in tetrahydrofuran). Wilkinson and Fischer noted that the stabilization of the HOMO on titanocene was not so large that the remaining 3*d* orbitals were inaccessible. The triplet-state was not observed by magnetic susceptibility between 77 and 380 K but a small perturbation resulting from the coordination of a molecule of tetrahydrofuran to titanocene, made both the singlet- and triplet-states observable. The etherate of titanocene is green and diamagnetic but, upon standing for 30 minutes at 25° C, converts quantitatively to a brown, paramagnetic species. Above its melting point, 81° C, the unidentified brown compound turns green and can be recrystallized as the diamagnetic etherate. The compounds received no further attention in the literature but their behavior suggests a small energy barrier between closely related compounds, perhaps in equilibrium with each other.

The titanocene preparation used by Wilkinson and coworkers is difficult to emulate since the composition of "$TiCl_2$" is highly variable. Titanium(II) chloride was prepared from TiH_2 and HCl at 650° C followed by a digestion step to disproportionate the titanium trichloride byproduct[6]. The resulting material analyzed as ~65% $TiCl_2$ and titanocene preparations from this material were unpredictable(info from Birmingham as told by RAA). Other titanocene preparation schemes were investigated.

"Titanocene" was prepared using numerous strategies including reduction of titanocene chlorides, hydrogenation of titanocene alkyls, and thermal decomposition of titanocene hydrides (Figure 78) but questions concerning its characterization ensued[9-11].

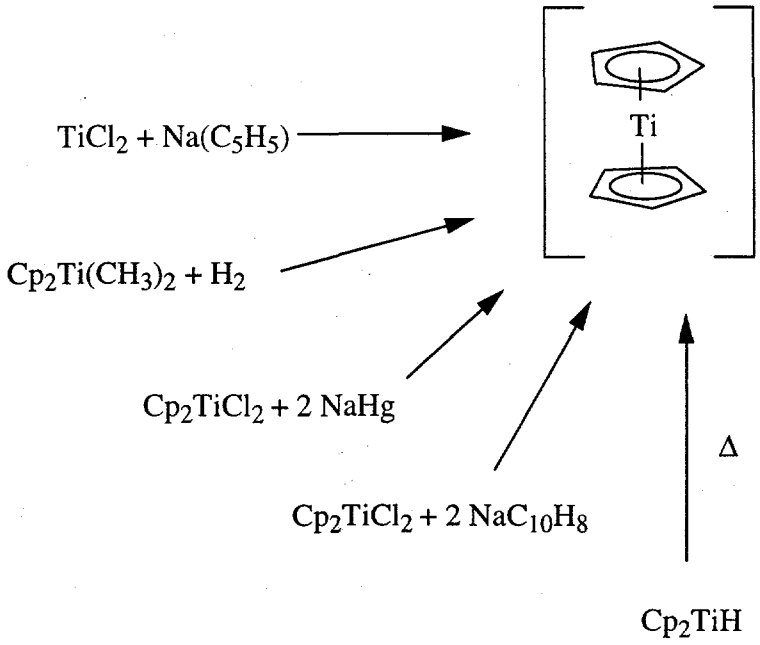

Figure 78: Preparation schemes for titanocene

These preparations yielded a green compound of the empirical formula, $C_{10}H_{10}Ti$ but evidence suggesting that the green compound was not structurally analogous to ferrocene included the solution molecular weight, which indicated that the compound was dimeric[10], and the infrared and NMR spectra which exhibited features inconsistent with $(\eta^5\text{-}C_5H_5)_2Ti$[11]. Brintzinger and Bercaw elucidated the nature of the green, "titanocene" compound by showing that the compound behaved as a metal hydride[12]. No terminal, titanium-hydride stretches were observed in the infrared spectrum but a stretch corresponding to a bridging hydride (1230 cm^{-1}) was detected similar to the one observed for $(Cp_2TiH)_2$ (1450 cm^{-1})[13] (Table 28)*.

---

* Brintzinger and Bercaw estimated terminal Ti-H stretches at ~2000 cm^{-1} but they have been observed between 1489 and 1650 cm^{-1}

	Bridging Ti-H (cm^{-1})	Terminal Ti-H (cm^{-1})
"Cp_2Ti"	1230	
$(Cp_2TiH)_2$	1450	
$Cp_2TiH_2BH_2$	1370	
$(C_5Me_5)_2TiH$[14]		1490
$(PhC_5Me_4)_2TiH$[15]		1505
$Cp^{\ddagger}_2TiH$		1550
$Cp^{\ddagger}_2TiH_2$		1650

Table 28

Based on these studies, Brintzinger and Bercaw proposed that $(\eta^5\text{-}C_5H_5)_2Ti$ was formed but rapidly underwent intramolecular oxidative addition of a C-H bond on a cyclopentadienyl ring to form $(\eta^1\text{-}C_5H_4)(\eta^5\text{-}C_5H_5)TiH$. The bridging hydride stretches in the infrared spectrum and ebulliometric studies[10] both indicate that the complex is a dimer and two structures for the dimer were postulated. The first proposed structure contained two η^1-cyclopentadiene ligands, two η^5-cyclopentadienyl ligands, and a $\mu\text{-}(H)_2$ bridge (Figure 79).

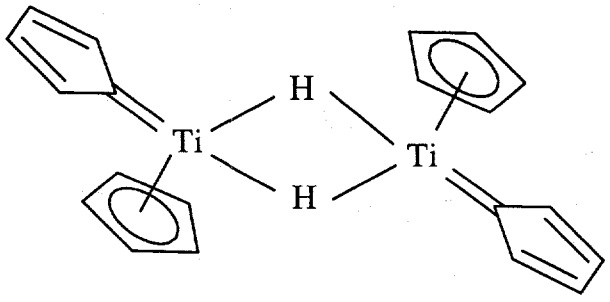

Figure 79

The second structure proposed coupling of the C_5H_4 groups to form a bridging fulvalene ligand (Figure 80).

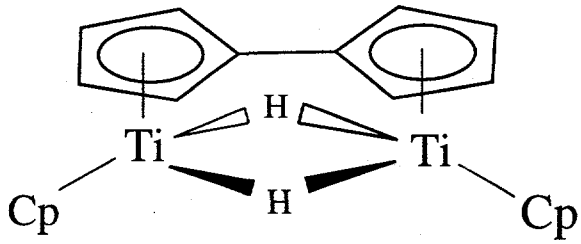

Figure 80

The second structure was supported by experimental evidence including a peak corresponding to $C_{10}H_8^+$ in the mass spectrum, and later by ^{13}C NMR spectroscopy[16] and X-ray crystallography[17,18].

Calderazzo and coworkers observed that "titanocene" reacts with carbon monoxide to form $Cp_2Ti(CO)_2$[19] suggesting that the intramolecular oxidative addition might be reversible (Figure 81).

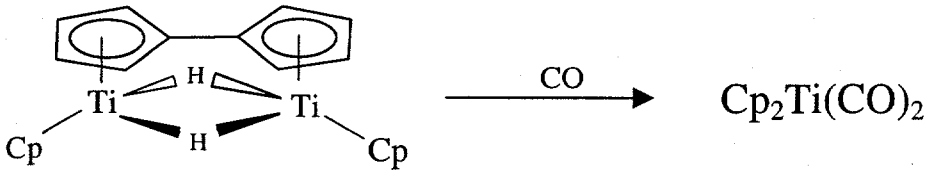

Figure 81

This reaction produced a poor yield of $Cp_2Ti(CO)_2$ and it is possible that the fulvalene-hydride complex cannot undergo reductive elimination to regenerate titanocene but that the monohapto/pentahapto dimer can.

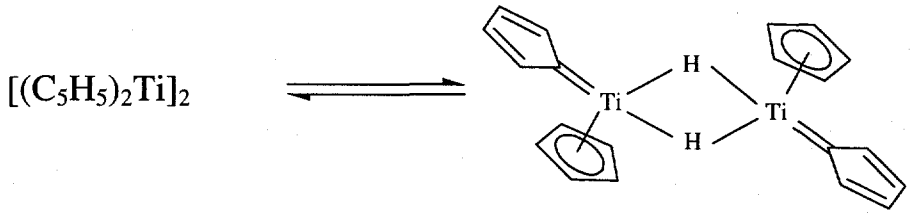

Brintzinger and coworkers demonstrated that deuterium is incorporated into all of the ring positions of titanocene when the metastable, $[Cp_2Ti]_2$ was treated with deuterium and postulated that this was accomplished through reversible oxidative addition of a C-H bond[20]. "Titanocene" could be a mixture of the two isomers and only $[(\eta^1\text{-}C_5H_4)(\eta^5\text{-}C_5H_5)TiH]_2$ will react with carbon monoxide to form $Cp_2Ti(CO)_2$ (Figure 82).

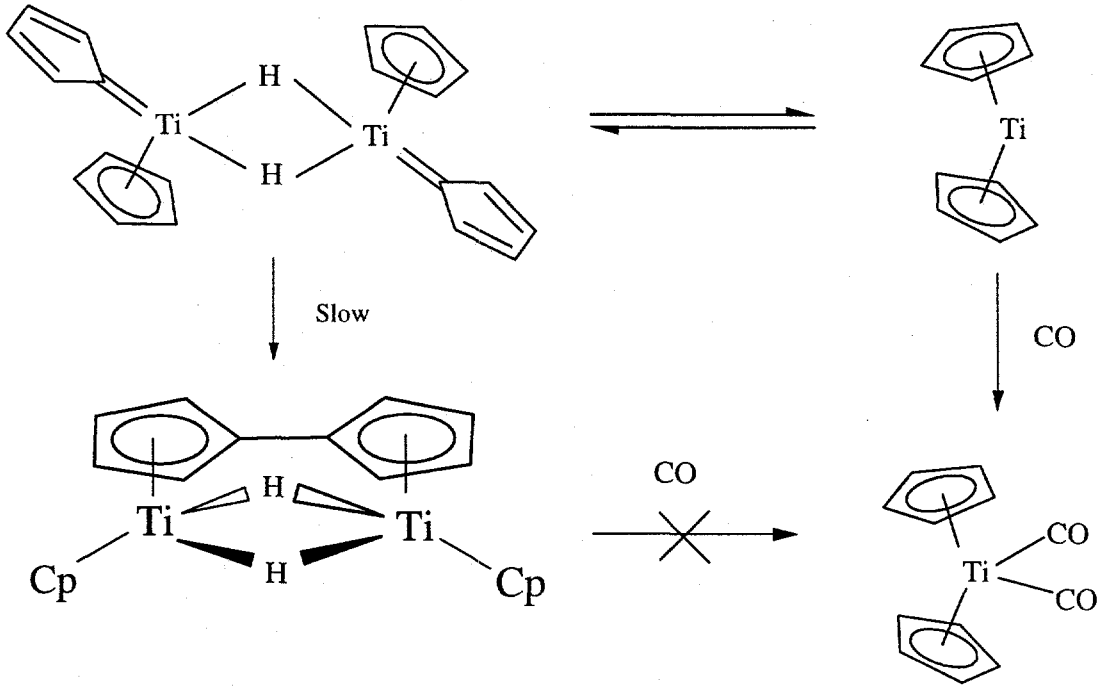

Figure 82: Proposed scheme for Calerazzo observation

Decamethyltitanocene

Brintzinger and coworkers, having identified the intramolecular oxidative addition in "titanocene", prepared the permethylcyclopentadienyl derivative in an attempt to prohibit the "ring-to-metal hydrogen shift" by removing all ring hydrogens[20,21]. Decamethyltitanocene was prepared by spontaneous dehydrogenation of $(Me_5C_5)_2TiH_2$ in pentane solution (Figure 83). Decamethyltitanocene chloride was prepared from sodium

pentamethylcyclopentadienide and $TiCl_3$ in tetrahydrofuran. The monochloride was oxidized to $(Me_5C_5)_2TiCl_2$ with HCl and treated with methyllithium to generate $(Me_5C_5)_2TiMe_2$. The dimethyl compound was treated with hydrogen at 5° C to isolate the thermally unstable, $(Me_5C_5)_2TiH_2$.

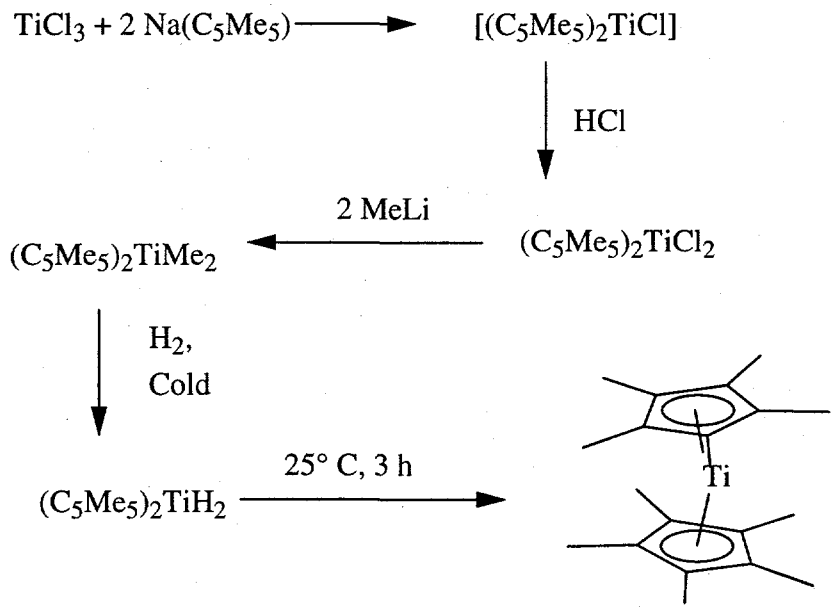

Figure 83: Preparation of decamethyltitanocene

Despite having no ring C-H bonds, decamethyltitanocene also undergoes an intramolecular oxidative addition reaction which is reversible and the oxidative addition product is in equilibrium with the "sandwich" compound[22] (Figure 84).

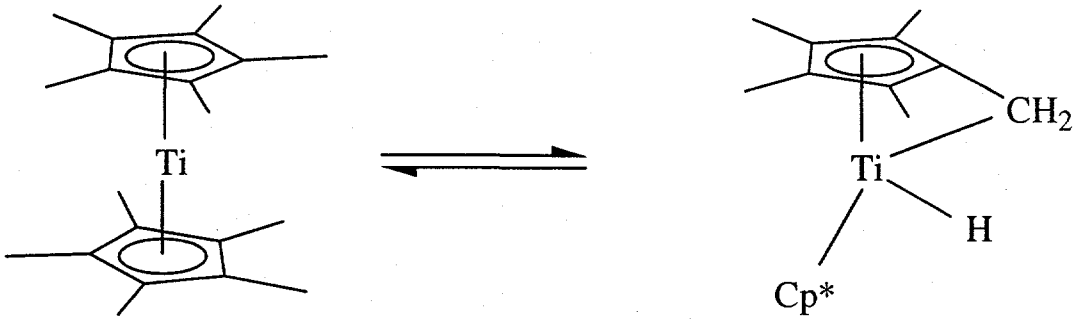

Figure 84: Decamethyltitanocene equilibrium

Tetra-*t*-butyltitanocene

In our hands, the C-H bonds of the di-*t*-butylcyclopentadienyl ligand have not been susceptible to oxidative addition and the ligand seemed a likely candidate for exploration of new titanocene chemistry. The geometry of a *t*-butyl substituent on a cyclopentadienyl ring helps to stabilize the complex with respect to intramolecular oxidative addition. The methyl groups on an η^5-pentamethylcyclopentadienyl ligand coordinated to titanium are ~3.55 Å from the metal center while the proximal methyl group of a *t*-butyl substituent on an η^5-cyclopentadienyl ligand coordinated to titanium is ~3.99 Å from the metal center. Obviously the three remaining C-H bonds on the cyclopentadienyl ring are not geometrically isolated from the titanium orbitals. Presumably, the *t*-butyl substituent inhibits the reorganization, such as a slip from η^5- to η^1- coordination of the cyclopentadienyl group, which facilitates oxidative addition of these bonds.

Several literature preparations exist for $[(Me_3C)_2C_5H_3]_2TiCl$, ($Cp^{‡}_2TiCl$)[23-26]. The earliest preparation specified treatment of $TiCl_4$ with $LiCp^{‡}$ in hexane to form $Cp^{‡}_2TiCl_2$, followed by reduction to $Cp^{‡}_2TiCl$ with potassium in hexane. The bis(di-*t*-butylcyclopentadienyl)titanium(III) chloride can also be prepared from $TiCl_3 \cdot 3THF$[27] and cyclopentadienide salts, eliminating the need for the reduction step (Figure 85).

$$MgCp^{‡}_2 + TiCl_3 \cdot 3THF \xrightarrow[25° C.\ 4\ h]{THF} Cp^{‡}_2TiCl + MgCl_2$$

Figure 85: Preparation of $Cp^{‡}_2TiCl$

The tetrahydrofuran adduct of titanium(III) chloride was prepared by loading $TiCl_3$ into a Soxhlet thimble and extracting exhaustively with tetrahydrofuran.

One of the preparations of "titanocene" involved hydrogenation of the Cp_2TiMe_2. Hydrogenation of alkyl compounds is a potentially clean synthetic route and the tetra-*t*-butyltitanocene methyl compound was prepared. Tetra-*t*-butyltitanocene chloride was treated with methyl lithium in ether to form $Cp^{\ddagger}_2TiMe$. The green compound was crystallized from hexane and can be sublimed at 100° C (10^{-3} torr). When treated with hydrogen, however, the compound converts quantitatively to $Cp^{\ddagger}_2TiH$. The hydride is red and has an infrared absorption at 1550 cm^{-1} corresponding to the Ti-H stretch. The Ti-H stretching energy is higher than those observed for the bridging hydrides $(Cp_2TiH)_2$ and "titanocene", suggesting that $Cp^{\ddagger}_2TiH$ is monomeric with a terminal Ti-H bond, as is $(C_5Me_5)_2TiH$[14].

Hydrogenation of the dimethyl- complex of tetra-*t*-butyltitanocene could not be attempted since $Cp^{\ddagger}_2TiMe_2$ could not be isolated. Tetra-*t*-butyltitanocene chloride, $Cp^{\ddagger}_2TiCl$, was treated with CCl_4 to generate $Cp^{\ddagger}_2TiCl_2$. The dark-red dichloride complex has been prepared by alternate routes. The dichloride was treated with methyllithium in ether and formed green, $Cp^{\ddagger}_2TiMe$ quantitatively. If the reaction mixture is kept cold, no reaction occurs at –78° C ($Cp^{\ddagger}_2TiCl_2$ is sparingly soluble) and upon warming slowly to 0° C, the green monomethyl complex forms before the $Cp^{\ddagger}_2TiCl_2$ is consumed.

Several different reducing agents were used to prepare the parent "titanocene" from Cp_2TiCl_2. Lemenovskii and coworkers used potassium metal in hexane to reduce $Cp^{\ddagger}_2TiCl_2$ to $Cp^{\ddagger}_2TiCl_2$ but did not comment on any further reduction[23]. Tetra-*t*-butyltitanocene chloride was reduced with sodium amalgam in tetrahydrofuran under an argon atmosphere. The starting material and product are both blue but the λ_{max} for the solution shifts. Layered, blue crystals were formed from hexane. The paramagnetic

compound has only a single, broad, ^{1}H NMR resonance (3.2 ppm, $\nu_{1/2}$ = 300 Hz), presumably the *t*-butyl resonance. Diamagnetic species containing the di-*t*-butylcyclopentadienyl ligand have three (observable) resonances, a *t*-butyl resonance (18 H) and two ring-resonances (2H and 1H). Presumably, the ring resonances for the paramagnetic, high-spin $Cp^{\ddagger}_2Ti$ are too broad to be observed. The infrared spectrum shows no distinguishing features (no Ti-H or $Ti(\mu\text{-}H)_2Ti$ stretches, Table 28). The empirical formula by elemental analysis is $C_{26}H_{42}Ti$ and the mass spectrum shows a molecular ion, $Cp^{\ddagger}_2Ti^+$.

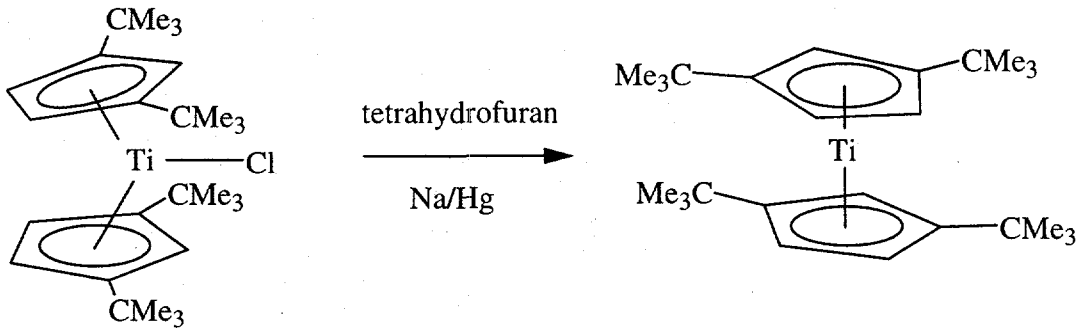

Figure 86.

The preparation of $Cp^{\ddagger}_2Ti$ is not ideal. Leaving the reaction stirring over an amalgam for more than a few hours leads to decomposition as identified by significant amounts of brown solid and by a reduced isolated yield. If the reaction time is kept conservatively short (< 2h), unreacted titanocene chloride co-crystallizes with the product. For these reasons, other reducing agents were investigated in an attempt to prepare the titanocene in high yield and without persistent chloride impurities.

Reduction of $Cp^{\ddagger}_2TiCl$ with potassium graphite in tetrahydrofuran generates tetra-*t*-butyltitanocene but, since the reducing agent will react with the solvent, it is difficult to ensure that the stoichiometry is correct. Potassium metal in hexanes was used

to reduce $Cp^{\ddagger}_2TiCl_2$ to $Cp^{\ddagger}_2TiCl$ but further reduction under these conditions failed to yield the Ti(II) product.

$$Cp^{\ddagger}_2TiCl \longrightarrow Cp^{\ddagger}_2Ti$$

1. Na/Hg / THF
2. KC_8 / THF
or 3. t-BuLi / THF

Figure 87

An *in situ* preparation for Cp^*_2Ti has been used for preparation of ketenimine complexes of decamethyltitanocene[28]. *t*-Butyllithium was added to decamethyltitanocene chloride, presumably forming the transient Cp^*_2Ti-*t*-Bu, followed by reductive elimination to form titanocene. An analogous preparation using $Cp^{\ddagger}_2TiCl$ successfully generated $Cp^{\ddagger}_2Ti$, but the reaction is carried out in tetrahydrofuran and stoichiometry problems similar to those encountered while using potassium graphite arose.

Reduction of $Cp^{\ddagger}_2TiCl$ with a large excess of potassium amalgam in refluxing hexane is the best preparation examined to date. Little decomposition was detected in the reaction mixture and the yield of titanocene is good indicating that the titanocene is stable with respect to the excess potassium amalgam. Using the silver nitrate test, no chloride was detected either in crystals or mother liquors from this preparation.

$$Cp^{\ddagger}_2TiCl + \text{xs K/Hg} \xrightarrow{\Delta} Cp^{\ddagger}_2Ti$$

The crystals grow in a layered habit, which has thwarted attempts to crystallographically characterize the complex but no evidence for intramolecular oxidative addition has been detected and the chemistry observed is consistent with that of a base-free titanocene.

If a solution of $Cp^{\ddagger}_2Ti$ is exposed to a nitrogen atmosphere, the solution develops an intense blue color. Crystals from this preparation appear black with metallic golden flakes. The compound is, in fact, blue, as noted when the crystals are crushed, but the very high extinction coefficient gives the compound a metallic luster.

The compound is paramagnetic and the ^1H NMR spectrum consists of a single, very broad resonance ($\nu_{1/2}$ = 500 Hz) and is of little assistance for describing the compound. Elemental analysis of the compound is consistent with an empirical formula of $C_{26}H_{42}NTi$. The dominant peak in the electron impact mass spectrum is $Cp^{\ddagger}_2Ti^+$ (no intact dimer or nitrogen complex was detected in the mass spectrum). The crystals were not suitable for X-ray diffraction but structural information can be inferred from literature examples[29].

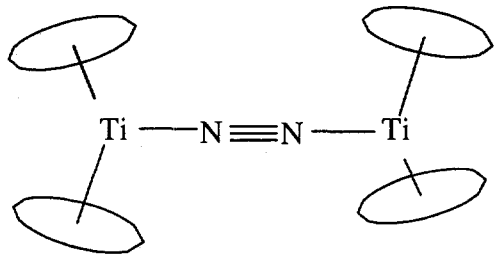

Figure 88

The crystallographically characterized dinitrogen complexes exhibit a linear Ti-N-N-Ti linkage and the N-N bond distances (1.16 – 1.17 Å), although longer than that found in free N_2 (1.10 Å), are shorter than those found in typical N=N double bonds (1.24 Å). It is thought that the Ti b_2 orbitals interact with the π^*-orbitals on N_2, accounting for the linear Ti-N-N-Ti geometry and the slightly reduced N-N bond order[29](and refs therein).

Solid, $Cp^{‡}_2Ti$ also reacts with nitrogen; trace amounts of nitrogen in the argon atmosphere of a glove box are detectable due to the dramatic increase in intensity of the blue color when nitrogen is coordinated to tetra-*t*-butyltitanocene.

$Cp^{‡}_2Ti$ reacts with carbon monoxide to give the dark-red, diamagnetic, $Cp^{‡}_2Ti(CO)_2$ complex. The CO infrared stretching energies are 1960 and 1880 cm^{-1} indicating, as expected, that the cyclopentadienyl groups with two *t*-butyl substituents are more electron-donating than the parent $C_5H_5^-$ [19] but less so than the pentamethylcyclopentadienyl ligand [21] (Table 29).

	ν (CO)
$Cp_2Ti(CO)_2$ [19]	1975, 1897 cm^{-1}
$Cp^{‡}_2Ti(CO)_2$	1960, 1880 cm^{-1}
$(C_5Me_5)_2Ti(CO)_2$ [21]	1930, 1850 cm^{-1}
CO (gas phase)	2143

Table 29: Infrared carbonyl stretches

The diamagnetism of the titanium(II) complex is readily understood using a molecular orbital diagram (Figure 89). The filled σ-donor orbitals of the carbonyl ligands interact with the partially filled titanocene orbitals. The energy separation between what were the $1a_1$ and b_2 orbitals of tetra-*t*-butyltitanocene increases so that it is larger than the electron pairing energy[30].

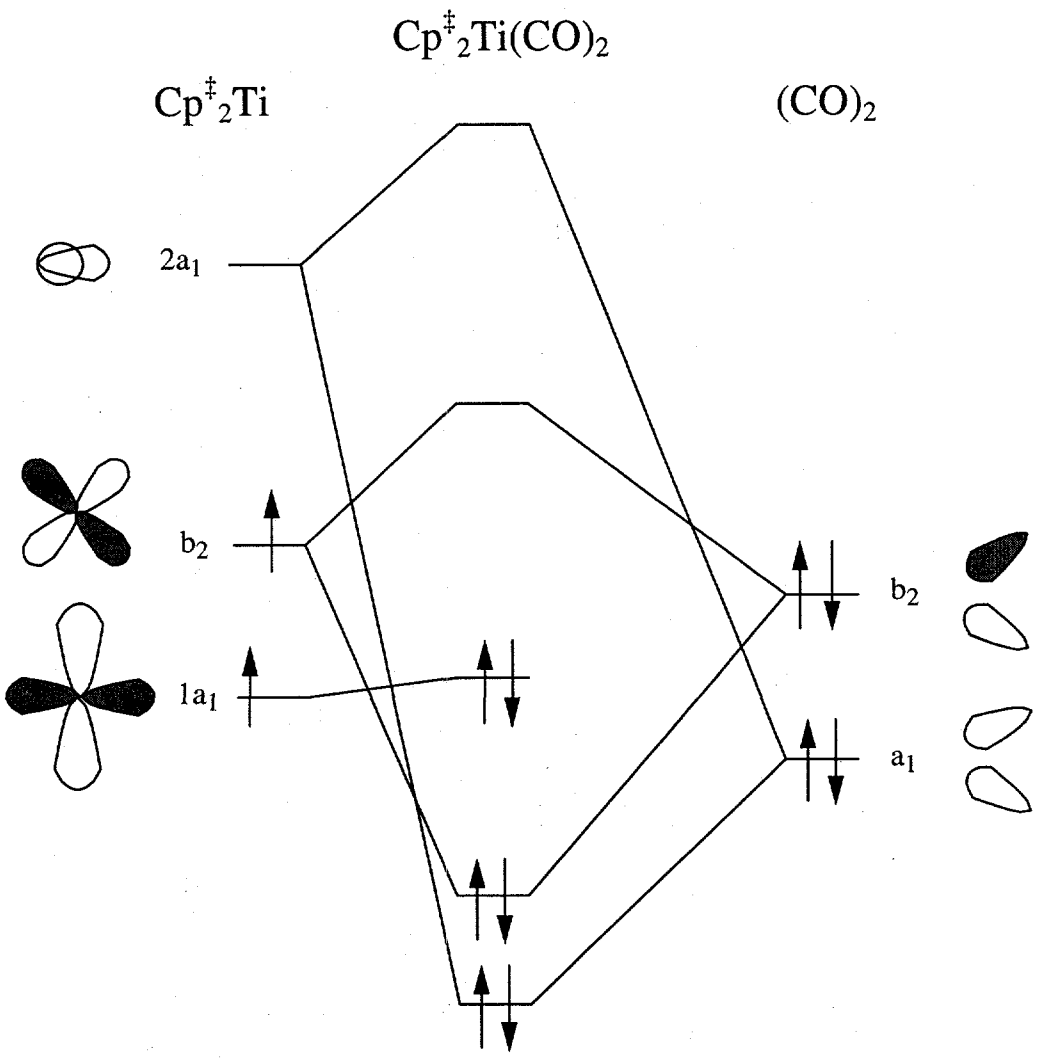

Figure 89; Frontier molecular orbital diagram

The carbonyl complex is stable indefinitely in an argon atmosphere but loses CO slowly in the presence of nitrogen to generate $[Cp^{\ddagger}_2TiN]_2$. Under an atmosphere of CO, the nitrogen complex is converted to the dicarbonyl (Figure 90).

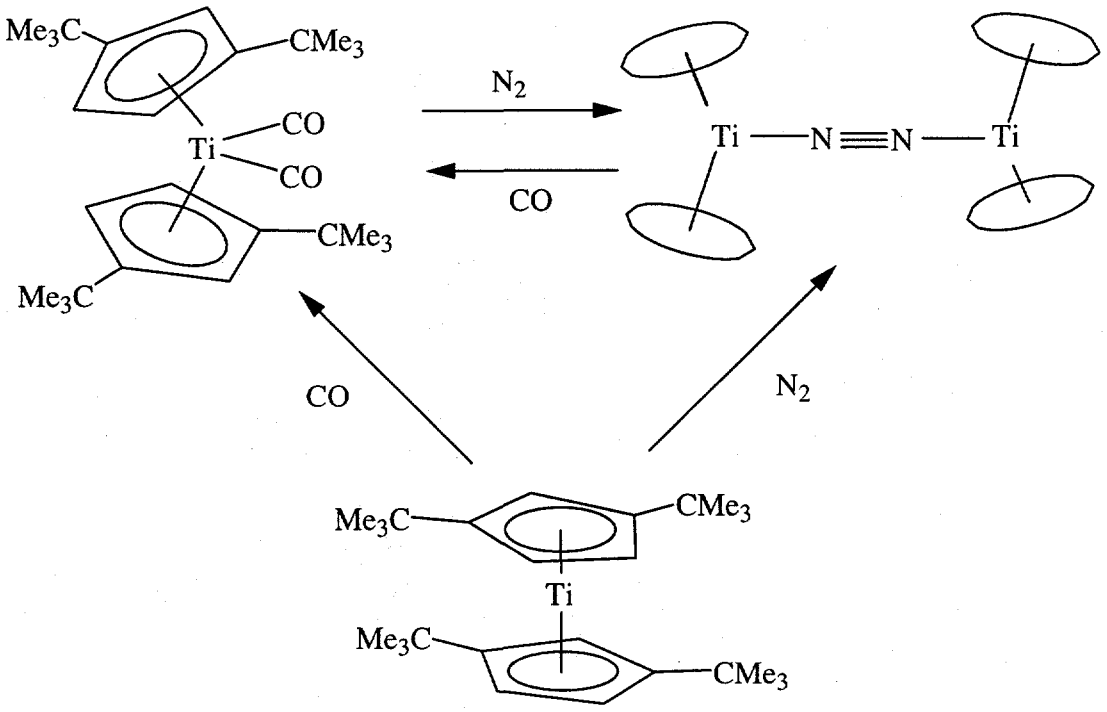

Figure 90

$Cp^{\ddagger}_2Ti$ in hexane was treated with a 1 atm of ethylene, the dark blue solution immediately changed to yellow and light-green, diamagnetic, crystals were isolated. The mass spectrum is dominated by $Cp^{\ddagger}_2Ti^+$ and no mass corresponding to an ethylene complex was detected. The ^1H NMR spectrum exhibits a resonance for coordinated ethylene at 2.93 ppm and the resonance does not shift when the sample is exposed to an atmosphere of ethylene, indicating that the coordinated and free ethylene are not exchanging rapidly on the NMR time scale. The coordinated ethylene resonance in the ^{13}C NMR spectrum appears at 108.9 ppm, shifted upfield slightly from free ethylene (123.2 ppm)(Table 31). The crystals were suitable for X-ray diffraction and the structure was solved.

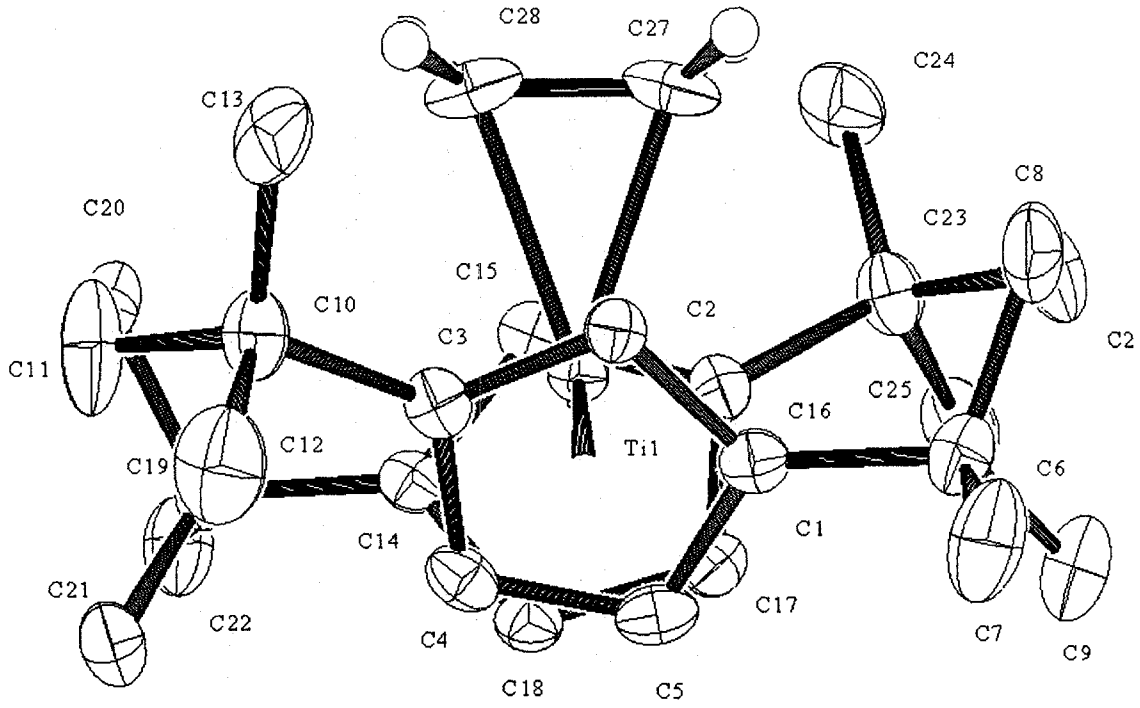

Figure 91: ORTEP diagram of $Cp^{\ddagger}_2Ti(CH_2CH_2)$, 50% thermal ellipsoids

Ti-C1	2.477		Ti-C14	2.466
Ti-C2	2.492		Ti-C15	2.479
Ti-C3	2.451		Ti-C16	2.453
Ti-C4	2.313		Ti-C17	2.326
Ti-C5	2.343		Ti-C18	2.351
Ti-ring centroid	2.094		Ti-ring centroid	2.095
centroid-Ti-centroid	138		angle between Cp planes	51
C27-C28	1.430		Ti-C27, C28	2.157, 2.183

Table 30: Structural data for $Cp^{\ddagger}_2Ti(CH_2CH_2)$, distances in Å, angles in deg.

The C-C bond distance in the ethylene ligand indicates a significant lengthening but the ^{13}C NMR chemical shift indicates that the carbon atoms are essentially sp^2 hybridized (Table 31).

	^{1}H NMR (ppm)	^{13}C NMR (ppm)	M-(C=C) (Å)	C=C distance (Å)	Stalick and Ibers angle
Ethylene[31]	5.25	123.2	-	1.337	0°
$Cp^{‡}_2Ti(CH_2CH_2)$	**2.93**	**108.9**	**2.16, 2.18**	**1.430**	**21°**
$(C_5Me_5)_2Ti(CH_2CH_2)$[32]	2.02	105.1	2.16	1.438	70°
Ethane[33]		5.7	-	1.531	76°

Table 31: ^{13}C NMR chemical shifts and structural data for ethylene complexes

The geometric convention established by Stalick and Ibers[34] can also be used to assess the hybridization of the carbon atom. The angle between the normals of the planes defined by a carbon atom and the two hydrogen atoms bound to it is sensitive to the interaction with the metal center. The ethylene complex of $Cp^{‡}_2Ti$ has a very small "Stalick and Ibers" angle (21°) compared to other compounds with comparable C-C bond lengths[32] (Table 31). Conclusions from these data must be viewed with caution due to the uncertainty of hydrogen positions in X-ray crystallography but the trend indicates that $Cp^{‡}_2Ti(CH_2CH_2)$ is more like a coordinated olefin than an oxidative addition product.

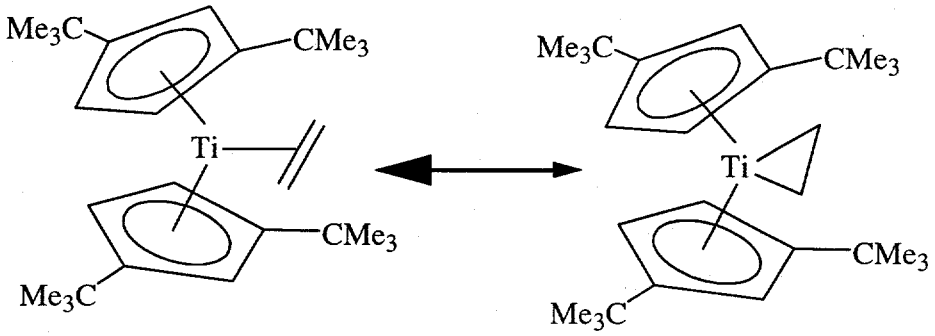

Figure 92

The reactivity of the ethylene coordination compound is nearly identical to that of tetra-*t*-butyltitanocene. The ethylene complex reacts with nitrogen to form $[Cp^{‡}_2TiN]_2$

and with CO to form the dicarbonyl compound (Figure 93). The compound appears to liberate ethylene slowly in the solid state. Light-green crystals of $Cp^{\ddagger}_2Ti(CH_2CH_2)$, stored under vacuum in an ampoule, become a darker green color over a period of months, presumably due to an increased concentration of blue, $Cp^{\ddagger}_2Ti$.

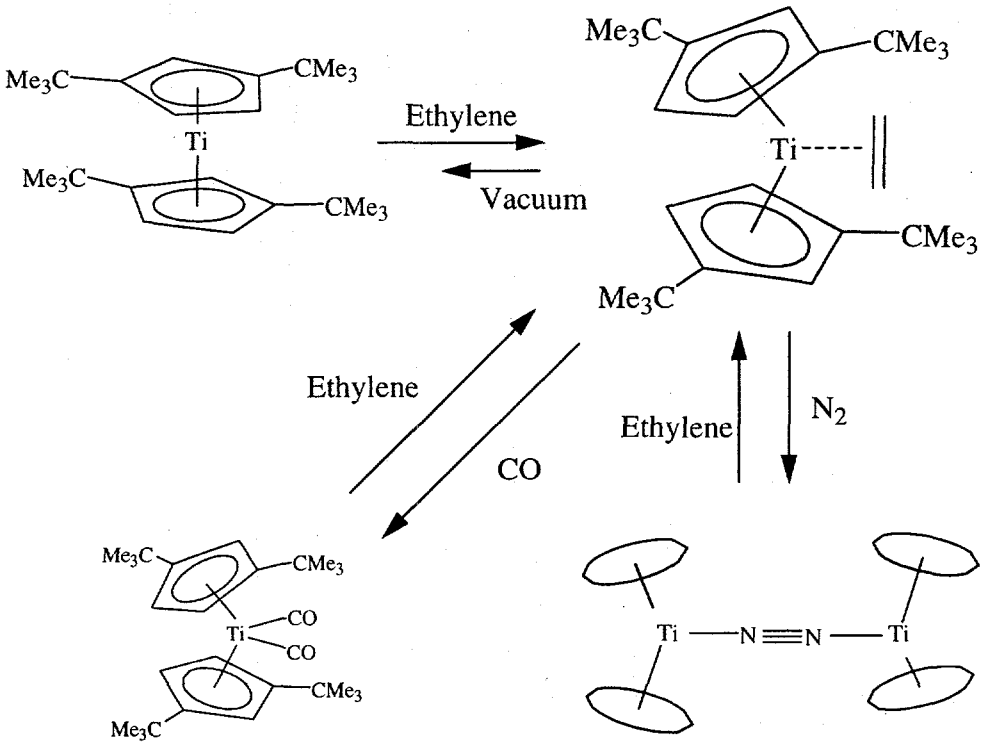

Figure 93

Tetra-*t*-butyltitanocene reacts with diphenylacetylene to yield an orange, diamagnetic, diphenylacetylene complex. The diphenylacetylene complex is more kinetically stable than the other complexes of $Cp^{\ddagger}_2Ti$. No reaction was observed when $Cp^{\ddagger}_2Ti(PhCCPh)$ was treated with nitrogen, or ethylene, either as a solid or in hexane or tetrahydrofuran solution (Figure 94).

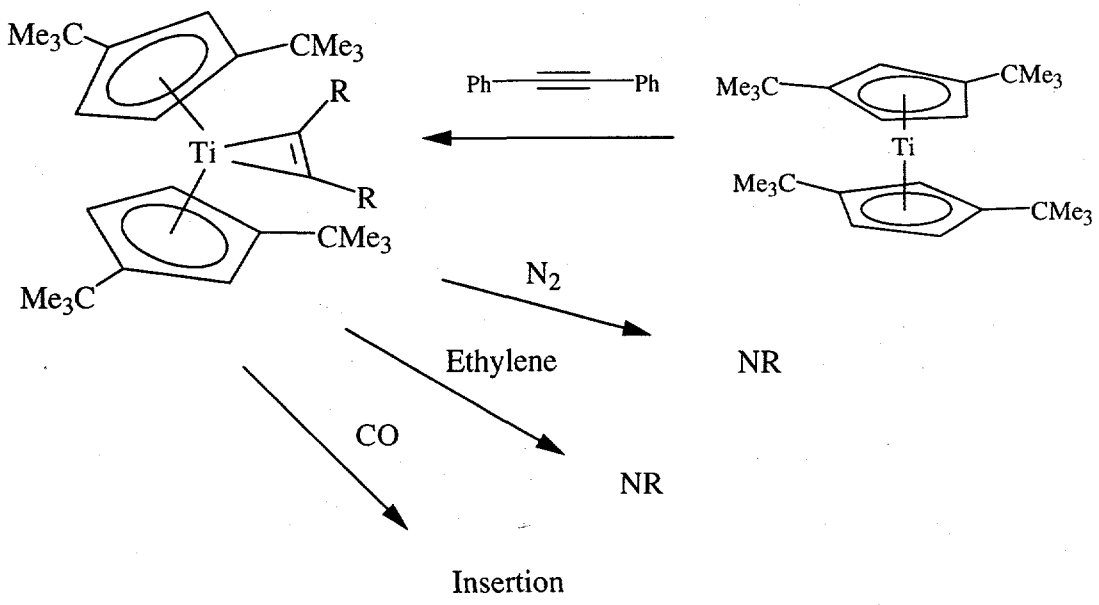

Figure 94

Carbon monoxide reacts with $Cp^{\ddagger}_2Ti(PhCCPh)$ by insertion rather than a simple displacement analogous to the reaction with the ethylene compound (Figure 93). The ^{13}C NMR spectrum of the diphenylacetylene complex indicates that the sp-carbon atoms of diphenylacetylene have chemical shifts characteristic of sp^2-carbon atoms when coordinated to titanocene, suggesting that, in contrast to the ethylene complex, the acetylene complex might be better described as a Ti(IV) metallocyclopropene, the product of an oxidative addition. Similar chemical shifts have been reported for acetylene complexes of other titanocenes (Table 32).

	^{13}C NMR (ppm)	"C≡C" distance (Å)	M-C distance (Å)	C≡C-R angle
$C_6H_5C{\equiv}CC_6H_5$[35]	90.1	1.193	-	178°
$Cp^{\ddagger}_2Ti(PhCCPh)$	**202.7**	**1.29**	**2.07, 2.09**	**136-139°**
$Cp_2Ti(PhCCPh)$[36]	196.5	-	-	-
$(C_5Me_5)_2Ti(PhCCPh)$[5]	200.9	-	-	-
$Cp_2Ti(PhCCSiMe_3)$[37]	219.6, 213.0	1.28-1.29	2.10, 2.12	141-152°
$(C_5Me_5)_2Ti(PhCCSiMe_3)$[37]	224.9, 213.2	1.31	2.09, 2.14	138-141°

Table 32: ^{13}C NMR chemical shifts and structural data for substituted acetylene complexes

The X-ray crystal structure of the compound was solved and the geometry supports the conclusion that the molecule is closer to an oxidative addition product than an acetylene adduct (Figure 95, Table 33).

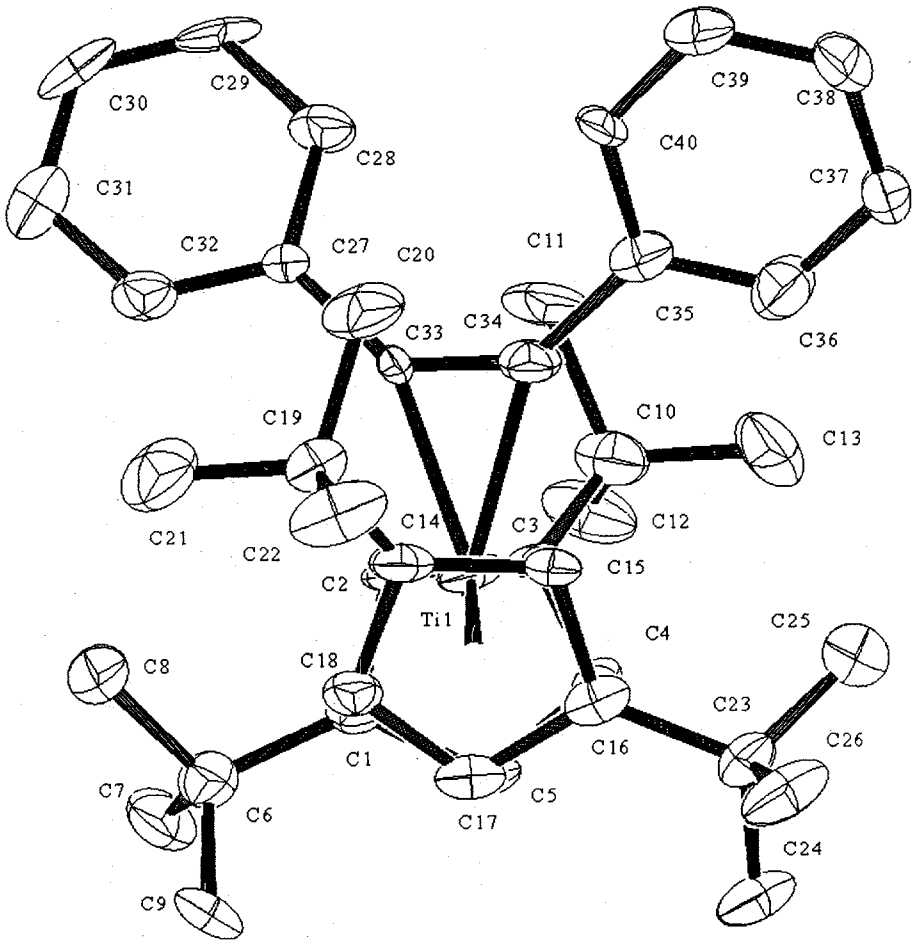

Figure 95: ORTEP diagram of $Cp^{\ddagger}_2Ti(PhCCPh)$, 50% thermal elipsoids

Ti-C1	2.408 Å		Ti-C14	2.505 Å
Ti-C2	2.405 Å		Ti-C15	2.427 Å
Ti-C3	2.507 Å		Ti-C16	2.461 Å
Ti-C4	2.461 Å		Ti-C17	2.440 Å
Ti-C5	2.415 Å		Ti-C18	2.443 Å
Ti-ring centroid	2.110 Å		Ti-ring centroid	2.132 Å
centroid-Ti-centroid	134°		angle between Cp planes	50°
C33-C34	1.29Å		Ti-C33, C34	2.090, 2.073 Å

Table 33: Structural data for $Cp^{\ddagger}_2Ti(PhCCPh)$

The C-C bond distance for the acetylenic carbon atoms and the C-C-R angle are consistent with sp^2-carbon atoms (Table 32).

Tetra-*t*-butyl titanocene reacts, reversibly, with hydrogen to form $Cp^{\ddagger}_2TiH_2$. A blue, hexane solution exposed to one atmosphere of H_2 rapidly changes color to red-brown. Degassing the solution results in regeneration of the blue titanocene solution. If the hydrogen atmosphere is maintained while the solution is cooled, red-brown crystals of $Cp^{\ddagger}_2TiH_2$ can be isolated ($\nu_{Ti-H} = 1640\ cm^{-1}$)*.

$$Cp^{\ddagger}_2Ti + H_2 \rightleftharpoons Cp^{\ddagger}_2TiH_2$$

The hydride positions were located by X-ray crystallography (Figure 96, Table 34) and, within the limits of interpretation for hydride positions by X-ray crystallography, the compound is a Ti(IV) dihydride (H-H distance = 1.96 Å).

---

* The second IR stretch may be too weak to be observed[38]

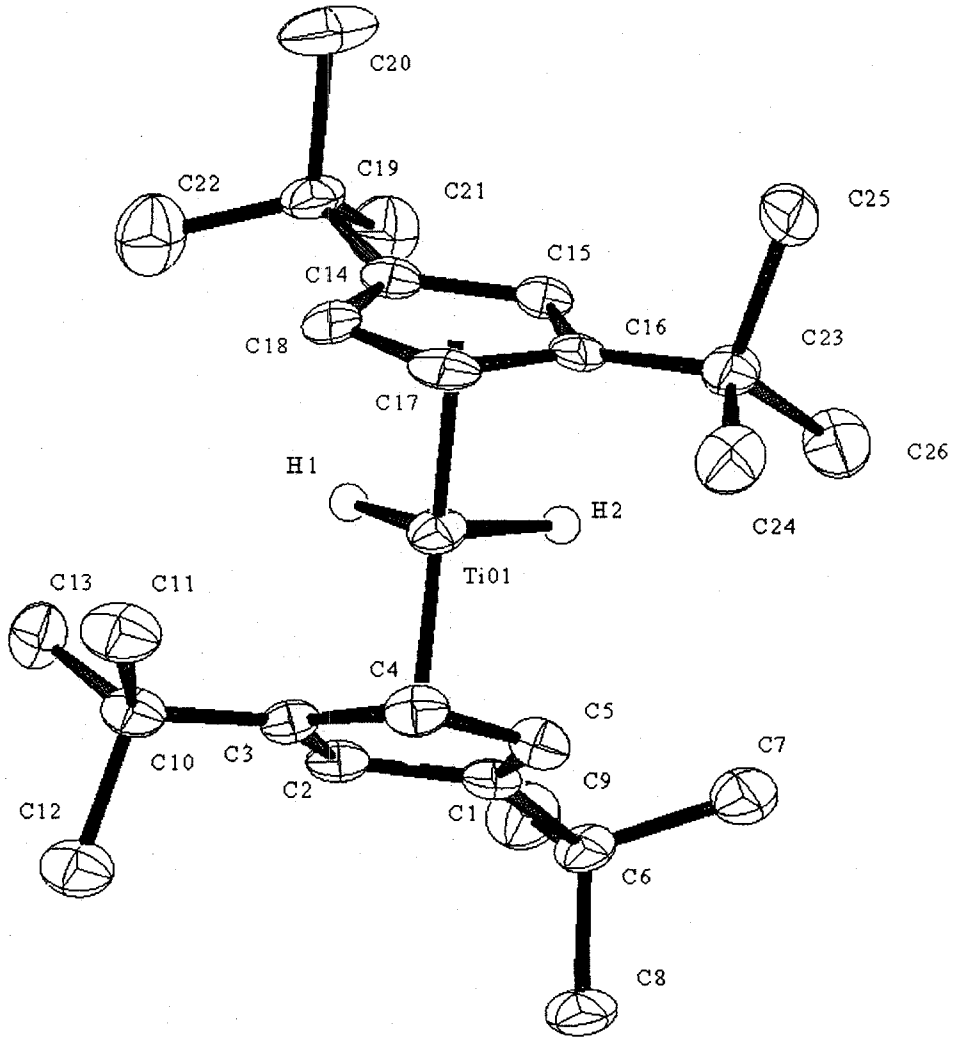

Figure 96

Ti-C1	2.373		Ti-C14	2.376
Ti-C2	2.355		Ti-C15	2.365
Ti-C3	2.392		Ti-C16	2.383
Ti-C4	2.369		Ti-C17	2.371
Ti-C5	2.356		Ti-C18	2.359
Ti-ring centroid	2.034		Ti-ring centroid	2.042
centroid-Ti-centroid	145		angle between Cp planes	35
H1-H2	1.96		Ti-H1, H2	1.51, 1.66

Table 34: Structural data for $Cp^{\ddagger}_2TiH_2$, distances in Å, angles in deg.

Liberation of hydrogen, however, is facile in solution; crystals of the dihydride were dissolved in toluene-d_8 and, at 30° C, the ^{1}H-NMR spectrum represents an averaged spectrum of $Cp^{\ddagger}_2TiH_2$, $Cp^{\ddagger}_2Ti$, and H_2. The single, observed resonance is an average of the *t*-butyl resonances of the two species. Presumably the ring resonances also contribute to a set of averaged ring-resonances, but those, like the ring-resonances in the spectra of $Cp^{\ddagger}_2Ti$, are not observed.

Below -10° C the exchange rate between $Cp^{\ddagger}_2TiH_2$ and $Cp^{\ddagger}_2Ti$ is slow enough that the ^{1}H NMR resonances are no longer averaged. A very broad resonance is observed for the titanocene and four sharp resonances are observed for the titanocene dihydride.

The chemical shift of the coalesced (time-averaged) spectrum is dependant upon the relative concentrations of titanocene and the titanocene dihydride.

$$Cp^{\ddagger}_2TiH_2 \rightleftharpoons Cp^{\ddagger}_2Ti + H_2$$

Increasing the concentration of hydrogen in solution increases the amount of $Cp^{\ddagger}_2TiH_2$ in solution relative to $Cp^{\ddagger}_2Ti$ and the observed, time-averaged chemical shift more closely approximates the chemical shift of the *t*-butyl resonance of pure $Cp^{\ddagger}_2TiH_2$ (Figure 97).

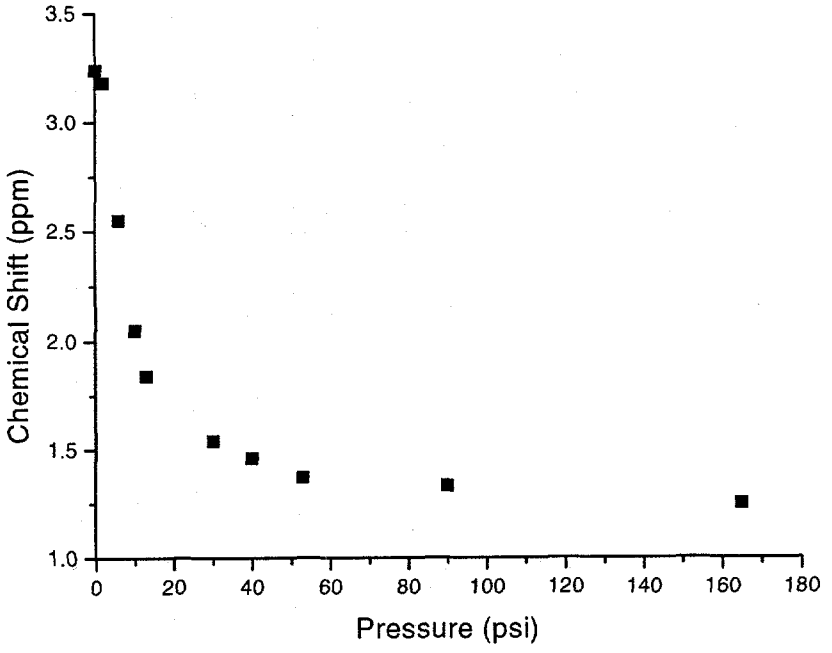

Figure 97: Plot *t*-butyl resonance chemical shift vs. P (H_2)

The plot of pressure vs chemical shift provides information about the enthalpy change for the reaction.

$$Cp^{\ddagger}_2Ti + H_2 \xrightarrow{\Delta H} Cp^{\ddagger}_2TiH_2$$

The activation barrier for this reaction can be determined from the change in chemical shift with temperature. The averaged spectrum can be used to calculate the relative concentrations of the titanocene and the titanocene dihydride. The chemical shift observed in the averaged spectrum is the weighted average of the chemical shifts for pure titanocene and titanocene dihydride.

$$\delta_{obs} = p_{Cp_2TiH_2}\delta_{Cp_2TiH_2} + p_{Cp_2Ti}\delta_{Cp_2Ti}$$

δ_x = chemical shift of species x

p_x = partial population of species x,

$$p_{Cp_2TiH_2} = \frac{N_{Cp_2TiH_2}}{N_{Cp_2TiH_2} + N_{Cp_2Ti}}, \; N_x = \text{moles of species x}$$

$$p_{Cp_2Ti} = 1 - p_{Cp_2TiH_2}$$

$$\delta_{obs} = p_{Cp_2TiH_2}\delta_{Cp_2TiH_2} + (1 - p_{Cp_2TiH_2})\delta_{Cp_2Ti}$$

$$p_{Cp_2TiH_2} = \frac{\delta_{obs} - \delta_{Cp_2Ti}}{\delta_{Cp_2TiH_2} - \delta_{Cp_2Ti}}$$

Equation 12

In order to calculate the partial populations, the chemical shifts of the pure species, $\delta_{Cp_2TiH_2}$ and δ_{Cp_2Ti}, must be determined. The chemical shift of titanocene can be measured from a pure sample but since the dihydride, in solution, is always in equilibrium, no pure sample of $Cp^{\ddagger}_2TiH_2$ can be observed in solution and other methods must be used to determine $\delta_{Cp_2TiH_2}$.

If the chemical shift of the equilibrium mixture is measured as a function of hydrogen pressure, the plot of the averaged chemical shift vs. pressure asymptotically approaches $\delta_{Cp_2TiH_2}$ as the pressure approaches infinity. The value obtained by this method can be verified by directly observing the *t*-butyl resonance of $Cp^{\ddagger}_2TiH_2$ in the low-temperature spectrum of the equilibrium mixture.

The chemical shift of the titanocene can not be determined from a single low temperature spectrum since, for paramagnetic compounds, the chemical shift is

temperature dependant. It would be necessary to extrapolate from the low temperature variable temperature ^{1}H NMR data to determine the room temperature chemical shift.

The partial populations of $Cp^{\ddagger}_2Ti$ and $Cp^{\ddagger}_2TiH_2$ are not sufficient to calculate thermodynamic data for the reaction. The equilibrium depends upon hydrogen concentration.

$$Cp^{\ddagger}_2TiH_2 \rightleftharpoons Cp^{\ddagger}_2Ti + H_2$$

$$K = \frac{[H_2][Cp^{\ddagger}_2Ti]}{[Cp^{\ddagger}_2TiH_2]}$$

To determine the concentration of hydrogen in solution at different pressures the hydrogen resonance in benzene-d_6 was integrated relative to an internal standard. The integrated value must be corrected since 25% of the hydrogen is para-hydrogen and is NMR silent[39]. The concentration of hydrogen in solution varies linearly from 0 to 9 mM with pressure over the range from 0 to 180 psi. The enthalpy and entropy change for the reaction can be calculated from the Van't Hoff plot for the equilibrium. The values are subject to significant errors because the kinetic solubility of hydrogen is poor due to the small surface area of the NMR sample. The concentration vs. pressure data at 25 °C is reliable since the sample can be agitated while attached to the pressure manifold. To evaluate the equilibrium at different temperatures, however, the sample must be agitated at the temperature for which the equilibrium is being evaluated while under pressure from a manifold. An equation of state describing the concentration of hydrogen as a function of temperature and pressure is of limited utility since the system must be at equilibrium and the kinetic solubility of hydrogen is poor under these circumstances. Efforts are underway to develop a reliable technique to quantify the equilibrium.

The facile liberation of hydrogen from $Cp^{\ddagger}_2TiH_2$ suggests that this titanocene system could display intriguing catalytic properties. Future studies will examine the reactivity of this titanocene in the presence of other small molecules. Oxidative addition of a C-H or C-C bond on methane or ethane would have obvious significance. The Oxidative addition of a C-H bond on ethane could be followed by β-hydride elimination to form ethylene and titanocene dihydride, which in turn spontaneously liberates hydrogen (Figure 98).

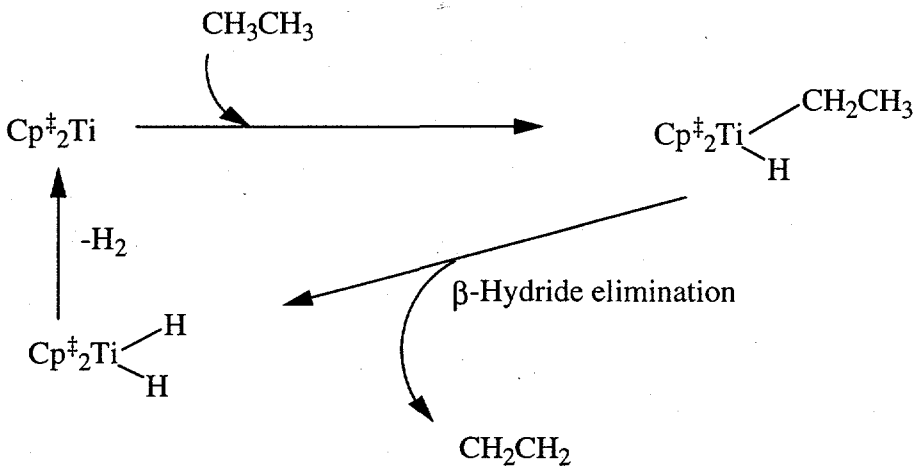

Figure 98: Possibly a dehydrogenation catalyst

The scheme is speculative and the titanocene is quite sensitive to air and water, but catalytic dehydrogenation of ethane is an attractive prospect.

References

1)Hitchcock, P. B.; Kerton, F. M.; Lawless, G. A. *J. Am. Chem. Soc.*, **1998**, *120*, 10264-10265.

2)Vol'pin, M. E.; Dubovitskii, V. A.; Nogina, O. V.; Kursanov, D. N. *Dokl. Akad. Nauk. SSSR*, **1963**, *151*, 1100.

3)Brintzinger, H. H.; Bartell, L. S. *J. Am. Chem. Soc.*, **1970**, *92*, 1105-1107.

4)Pez, G. P.; Armor, J. N. *Adv. Organomet. Chem.*, **1981**, *19*, 1-49.

5)Beckhaus, R. *Metallocenes*; Togni, A., Ed.; Wiley-VCH: New York, 1999; Vol. 1, pp 164.

6)Fischer, A. K.; Wilkinson, G. *J. Inorg. Nucl. Chem.*, **1956**, *2*, 149-152.

7)Moffitt, W. *J. Am. Chem. Soc.*, **1954**, *76*, 3386-3392.

8)Dunitz, J. D.; Orgel, L. E. *J. Chem. Phys.*, **1955**, *23*, 954-958.

9)Watt, G. W.; Baye, L. J. *J. Inorg. Nucl. Chem.*, **1964**, *26*, 2099-2102.

10)Watt, G. W.; Baye, L. J.; Drummond, F. O., Jr. *J. Am. Chem. Soc.*, **1966**, *88*, 1138-1140.

11)Salzmann, J.-J.; Mosimann, P. *Helv. Chim. Acta*, **1967**, *50*, 1831-1836.

12)Brintzinger, H. H.; Bercaw, J. E. *J. Am. Chem. Soc.*, **1970**, *92*, 6182-6185.

13)Bercaw, J. E.; Brintzinger, H. H. *J. Am. Chem. Soc.*, **1969**, *91*, 7301-7306.

14)Lukens, W. W.; Matsunaga, P. T.; Andersen, R. A. *Organometallics*, **1998**, *17*, 5240-5247.

15)de Wolf, J. M.; Meetsma, A.; Teuben, J. H. *Organometallics*, **1995**, *14*, 5466-5468.

16)Davison, A.; Wreford, S. S. *J. Am. Chem. Soc.*, **1974**, *96*, 3017-3018.

17)Guggenberger, L. J.; Tebbe, F. N. *J. Am. Chem. Soc.*, **1976**, *98*, 4137-4143.

18)Troyanov, S. I.; Antropiusová, H.; Mach, K. *J. Organomet. Chem.*, **1992**, *427*, 49-55.

19)Calderazzo, F.; Salzmann, J. J.; Mosimann, P. *Inorg. Chim. Acta.*, **1967**, *1*, 65.

20)Bercaw, J. E.; Marvich, R. H.; Bell, L. G.; Hans, H. B. *J. Am. Chem. Soc.*, **1972**, *94*, 1219-1238.

21)Bercaw, J. E.; Brintzinger, H. H. *J. Am. Chem. Soc.*, **1971**, *93*, 2045-2046.

22)Bercaw, J. E. *J. Am. Chem. Soc.*, **1974**, *96*, 5087-5095.

23)Urazowski, I. F.; Ponomaryov, V. I.; Ellert, O. G.; Nifant'ev, I. E.; Lemenovskii, D. A. *J. Organomet. Chem.*, **1988**, *356*, 181-193.

24)Okuda, J. *J. Organomet. Chem.*, **1990**, *385*, C39-C42.

25)Jibril, I.; Abuorabi, S.; Klaib, S. A.; Imhof, W.; Huttner, G. *J. Organomet. Chem.*, **1992**, *433*, 253-259.

26)King, W. A.; Di Bella, S.; Gulino, A.; Lanza, G.; Fragala, I. L.; Stern, C. L.; Marks, T. J. *J. Am. Chem. Soc.*, **1999**, *121*, 355-366.

27)Manzer, L. E. *Inorg. Synth.*, **1979**, *21*, 135-136.

28)Fandos, R.; Lanfranchi, M.; Otero, A.; Pellinghelli, M. A.; Ruiz, M. J.; Teuben, J. H. *Organometallics*, **1997**, *16*, 5283-5288.

29)Sanner, R. D.; Duggan, D. M.; McKenzie, T. C.; Marsh, R. E.; Bercaw, J. E. *J. Am. Chem. Soc.*, **1976**, *98*, 8358-8365.

30)Albright, T. A.; Burdett, J. K.; Whangbo, M.-H. *Orbital Interactions in Chemistry*; John Wiley & Sons: New York, 1985.

31)Silverstein, R. M.; Bassler, G. C.; Morrill, T. C. *Spectrometric Identification of Organic Compounds*; 4th ed ed.; John Wiley and Sons: New York, 1981.

32)Cohen, S. A.; Auburn, P. R.; Bercaw, J. E. *J. Am. Chem. Soc.*, **1983**, *105*, 1136-1143.

33)Streitwieser, A., Jr.; Heathcock, C. H. *Introduction to Organic Chemistry*; 3rd ed. ed.; Macmillan Publishing Co.: New York, 1985.

34)Stalick, J. K.; Ibers, J. A. *J. Am. Chem. Soc.*, **1970**, *92*, 5333.

35)Espiritu, A. A.; White, J. G. *Z. Kristall.*, **1978**, *147*, 177-186.

36)Shur, V. B.; Burlakov, V. V.; Volpin, M. E. *J. Organomet. Chem.*, **1988**, *347*, 77-83.

37)Burlakov, V. V.; Polyakov, A. V.; Yanovsky, A. I.; Struchkov, Y. T.; Shur, V. B.; Volpin, M. E.; Rosenthal, U.; Gorls, H. *J. Organomet. Chem.*, **1994**, *476*, 197-206.

38)Girling, R. B.; Grebenik, P.; Perutz, R. N. *Inorg. Chem.*, **1986**, *25*, 31-36.

39)Heinekey, D. M.; Voges, M. H.; Barnhart, D. M. *J. Am. Chem. Soc.*, **1996**, *118*, 10792-10802.

Chapter 6

Experimental Details

All air-sensitive compounds were prepared using standard Schlenk techniques. Solvents for reactions and recrystallization were freshly distilled from Na/benzophenone ketyl except for toluene, which was distilled from molten sodium. NMR, EPR, and UV-vis solvents were dried with potassium metal and were distilled and degassed before storage in a greaseless flask inside an argon atmosphere glove-box. Except where indicated, reagents were used as received without purification.

Melting points were measured in glass capillaries under argon and are uncorrected. Infra-red spectra were recorded as Nujol mulls between CsI plates on a Perkin-Elmer 283 spectrometer. Gas chromatography was performed using a Hewlett-Packard 5790A chromatograph with a 25 m column containing crosslinked 5% phenylmethylsilicone support. Unless otherwise indicated, NMR spectra were recorded as solutions in benzene-d_6 at 30 °C on a Jeol FX-90Q 90 MHz NMR spectrometer equipped with a LIBRA pulse generator and a Tecmag computer interface. ^{1}H NMR chemical shifts are reported as δ values relative to tetramethylsilane and are referenced using residual protons in the solvent. High field NMR spectra were recorded on a Brucker DRX 500 MHz spectrometer. EPR spectra were recorded either as powdered samples or as frozen glasses in methylcyclohexane on a Varian E-12 spectrometer equipped with an EIP-548 microwave frequency counter and a Varian E-500 NMR Gaussmeter. Mass spectra were recorded using the electron impact technique at the microanalytical facility at U.C. Berkeley. Elemental analyses were also performed at the U.C. Berkeley microanalytical facility. Single crystal X-ray experiments are described in Appendix B.

The solid-state magnetic susceptibilities were measured using a Superconducting QUantum Interference Device (SQUID) susceptometer. Data were collected from 5 to 300 K at two different field strengths (typically 5 and 20 kG) on either a SHE model 500 SQUID susceptometer or a QD susceptometer.

UV-visible samples were prepared as methylcyclohexane solutions in cells equipped to hold air-sensitive samples. Variable temperature UV-vis spectrometers are commercially available but their low temperature capability is typically very limited and the temperature range of interest for this system extends from 300 to 170 K. A fiber-optic UV-vis spectrometer (Ocean Optics) was adapted for low temperature observation and temperatures of 170 K and lower are accessible with a simple, liquid-nitrogen cooled, cell holder (appendix A). Routine UV-vis spectra were recorded on a Varian Cary 5G spectrophotometer.

When necessary, spectra were digitized using UNSCANIT. Data manipulation and analysis were performed using Microcal Origin and Microsoft Excel.

Ligands and Magnesocenes

Di-*t*-butylcyclopentadiene ($Cp^{‡}H$)

In a modified version of a preparation by Venier and Casserly[1], potassium hydroxide (1 kg, 20 mol) was dissolved in 750 mL of water in a 3-L, 3-necked flask equipped with an overhead stirrer. The KOH solution was allowed to cool to room temperature and Adogen 464 (Aldrich, ~5g), freshly cracked cyclopentadiene (100 mL, 1.21 mol), and t-butyl bromide (Fluka, 300 mL, 2.65 mol), were added. A large excess

t-butylbromide added at this point is wasted; the sequential addition gives a higher yield. The reaction mixture was stirred vigorously for 12 h. An additional 50 mL (0.44 mol) of *t*-BuBr was added and the mixture was stirred for another 24 h, followed by addition of another 50 mL of *t*-BuBr and further stirring. Progress of the reaction was monitored by gas chromatography (GC) and after 4-5 days, only 5% Me_3CCpH, and no C_5H_6 remained in the mixture. The organic layer was separated and washed with 1M HCl (100 mL). The product was dried over anhydrous $Mg(SO_4)$ and distilled at 40 °C (10^{-2} torr). The distilled product was analyzed by GC and was typically >98% pure $Cp^{‡}H$ (150 g, 71% yield).

$Cp^{‡}_2Mg$ $[(Me_3C)_2C_5H_3]_2Mg$

A heptane solution of "dibutylmagnesium" (FMC corporation, Aldrich) (250 mL, 0.90 M, 250 mmol) was added to di-*t*-butylcyclopentadiene (89.4 g, 501 mmol). Upon addition, the mixture began to evolve butanes and warmed slightly. The mixture was heated to reflux for 24 h at which point no further gas evolution was detected (The system was isolated for 15 min at constant temperature and then vented to an oil bubbler to detect gas evolution.). The clear solution was cooled to –20 °C producing large colorless crystals (39 g, 41% yield). Concentrating the mother liquor by one half and cooling produced a second crop of crystals (39 g, 83% overall yield). The compound sublimes at 120 °C at 10^{-3} torr, mp 138-141° C. Anal. Calcd. for $C_{26}H_{42}Mg$: C, 82.41; H, 11.17. Found: C, 82.45; H, 11.18. IR 1635 m, 1545 m, 1295 w, 1250 s, 1230 m, 1200 s, 1160 w, 1085 w, 1050 m, 1025 m, 975 w, 935 m, 805 s, 760 m, 740 s, 695 s, 675 m, 500 s, 410 m, 345 w, 245 w. ^{1}H NMR 1.31 (s, 18H), 5.94 (m, 3H). $^{13}C\{^1H\}$ NMR 133.7

(ring C), 103.0 (ring C), 99.9 (ring C), 32.49 ($\underline{C}Me_3$), 32.56 ($C\underline{Me}_3$). The E.I. mass spectrum showed a molecular ion at m/e = 378 amu. The parent ion isotopic cluster was simulated: (calcd. %, obsvd. %); 378 (100, 100), 379 (42.2, 41.7), 380 (21.8, 21.5), 381 (5.0, 4.9).

Mono-*t*-butylcyclopentadiene $[Me_3CC_5H_5]$

Potassium hydroxide (1 kg, 18 mol) was dissolved in 750 mL of water and the solution was allowed to cool to room temperature. Freshly cracked cyclopentadiene (100 mL, 1.21 mol), Adogen 464 (Aldrich, 5g), and *t*-butyl bromide (200 mL, 1.76 mol) were added and the mixture was stirred vigorously for 12 h. The organic layer was separated, washed with 1 M HCl (100 mL), and dried over anhydrous $Mg(SO)_4$. The product was distilled at 40 °C and ~ 8 torr and was analyzed by gas chromatography (100g, 68% yield). This compound has been prepared using other routes[2-4].

1,1'-Di-*t*-butylmagnesocene $[(Me_3CC_5H_4)_2Mg]$

Mono-*t*-butylcyclopentadiene (100 g, 0.82 mol) was treated with a heptane solution of "dibutylmagnesium" (470 mL, 0.87 M, 0.41 mol). The solution became quite warm and gas evolution was vigorous. The mixture was stirred at room temperature for 12 h. The solution was concentrated to a volume of 250 mL and cooled slowly to –80 °C. Colorless crystals were isolated (69 g, 63 % yield). A second crop of crystals was obtained by concentrating the mother liquor and cooling to –20 °C (15 g, 76% overall yield). The compound has been prepared by an alternate method[5].

(Trimethylsilyl)(*t*-butyl)cyclopentadiene ($Cp^{tt}H$)

1,1'-Di-*t*-butylmagnesocene (74 g, 0.28 mol) was dissolved in tetrahydrofuran (100 mL) and trimethylsilyl chloride (60 g, 0.56 mol) was added dropwise. The reaction is noticeable exothermic and a colorless precipitate formed before the addition was complete. The product was distilled at 40 °C and 10^{-2} torr (110 g, 96% yield).

$Mg(Cp^{tt})_2$

To $Cp^{tt}H$ (110 g, 0.57 mol) was added a solution of "dibutylmagnesium" in heptane (Aldrich) (320 mL, 0.87 M, 0.28 mol). The mixture was heated to reflux and the butane evolution was monitored with an oil bubbler. After 12 h the reaction was complete as determined by isolating the system from the oil bubbler for ten minutes without generation of pressure. The solution was cooled slowly to –80 °C and colorless crystals were obtained (88 g, 76% yield). The mother liquor was concentrated to a volume of 50 mL and cooled to produce a second crop of crystals (6.4 g, 82% overall yield). mp 107-108 °C. IR: 1330w, 1290w, 1250s, 1205w, 1180m, 1170m, 1085, 1055m, 1025w, 945m, 930m, 835s, 825s, 755s, 725w, 690m, 650w, 635m, 510m, 485m, 450m, 450w, 430m, 360w, 340w, 325w, 290w. ^{1}H NMR (500 MHz): 0.30 (18H), 0.31 (18H), 1.30 (18H), 1.31 (18H), 6.16 d,d (2H, 2 Hz, 2 Hz), 6.16 d,d (2H, 2 Hz, 2 Hz), 6.20 d,d (2H, 10 Hz, 2 Hz) 6.21 d,d (2H, 10 Hz, 2 Hz), 6.28 d,d (2H, 10 Hz, 2 Hz), 6.28 d,d (2H, 10 Hz, 2 Hz). Anal. Calcd. for $C_{24}H_{42}MgSi_2$: C, 70.1; H, 10.3. Found: C, 70.0; H, 10.6. The E.I. mass spectrum showed a molecular ion at m/e = 411 amu. The parent ion isotopic cluster was simulated: (calcd. %, obsvd. %); 409 (0, 1), 410 (100, 100), 411 (50, 51), 412 (31, 33), 413 (10, 10), 414 (3, 3).

a-($Cp^{‡}H)_2$ [$Me_2Si(C_5H_3[CMe_3]_2)_2$]

Dibromodimethylsilane was prepared according the literature preparation[6]. Tetra-*t*-butylmagnesocene (10 g, 26 mmol) was dissolved in 50 mL of tetrahydrofuran and cooled to 0 °C. Dibromodimethylsilane (3.4 mL, 26 mmol) was added slowly using a syringe. The reaction mixture was allowed to warm to room temperature and was stirred overnight producing a yellow solution with a colorless precipitate. The solvent was removed under reduced pressure and the solid was extracted with 50 mL of hexane. The extract was concentrated to a volume of 15 mL and cooled to -20 °C. Colorless crystals grew slowly (3 days) (5.4 g, 50 % yield). mp ^{1}H NMR 1.55 (s, 36H), 0.11 (s, 6H), 6.69 (s, 4H), 5.0 (broad s, 2H). Anal. calcd. for $C_{28}H_{46}Si$: C, 81.47; H, 11.72. Found: C, 81.50; H, 11.88.

"a-$Cp^{‡}_2Mg$"

ansa-Bis-*t*-butylcyclopentadiene [a-($Cp^{‡}H)_2$] (8.2 g, 20 mmol) was treated with "dibutylmagnesium" in heptane (26 mL, 0.76 M, 20 mmol). The mixture was heated to a vigorous reflux and stirred for 7 days. The solution was cooled to 20 °C and the solvent was removed under reduced pressure leaving a colorless solid. Attempts to crystallize the product from heptane, hexane, toluene, diethylether were unsuccessful. The ^{1}H NMR spectrum of the unpurified product appears to be relatively clean. The product was used without further characterization. ^{1}H NMR: -0.01 (6H), 1.25 (36H), 6.58 (4 H).

a-$(Cp''H)_2$ $[Me_2Si(C_5H_3[SiMe_3]_2)_2]$

Tetra(trimethylsilyl)magnesocene (Cp''_2Mg) (10 g, 26 mmol) was dissolved in 50 mL of THF and cooled to 0 °C. Dibromodimethylsilane (3.4 mL, 26 mmol) was added slowly using a syringe. The reaction mixture was allowed to warm to room temperature and was stirred overnight producing a yellow solution with a colorless precipitate. The solvent was removed under reduced pressure and the residue was extracted with hexane (50 mL). The solution was filtered and the solvent was removed under reduced pressure. The product was distilled at 140 °C (10^{-5} torr) as a yellow oil.

"a-Cp''_2Mg"

ansa-bis(Trimethylsilyl)cyclopentadiene [a-$(Cp''H)_2$] (7.0 g, 15 mmol) was treated with "dibutylmagnesium" in heptane (19 mL, 0.76 M, 15 mmol). The mixture was heated to a vigorous reflux and stirred for 7 days and the solvent was removed under reduced pressure leaving a colorless solid. Attempts to crystallize the product from heptane, hexane, toluene, diethylether were unsuccessful. ^1H NMR: -0.04 (36H), 0.24 (6H), 6.83 m (4H). The product was used without further characterization.

$(Me_3C)_3C_5H_3$ tri-*t*-butylcyclopentadiene

t-Butylbromide (8.7 g, 64 mmol) cooled to 0 °C and tetra-*t*-butylmagnesocene ($Cp^{\ddagger}_2Mg$) (11 g, 29 mmol) was added in small portions. The reaction mixture turned dark brown and the mixture was stirred for 2 h. The reaction mixture contained a 5:1 ratio of $(Me_3C)_3C_5H_3$ to $Cp^{\ddagger}H$ by gas chromatography. Water was added and the organic

layer was separated, dried over anhydrous $Mg(SO_4)$, and distilled at 110 °C (10^{-5} torr). The straw-colored liquid has been prepared using several other strategies[1,7-9].

$[(Me_3C)_3C_5H_2]_2Mg$ 1,1',2,2',4,4'-hexa-*t*-butylmagnesocene

Tri-*t*-butylcyclopentadiene (12.8 g, 55 mmol) was treated with "dibutylmagnesium" (31 mL, 0.87 M, 27 mmol) and the mixture was heated to a vigorous reflux and stirred for 7 days. The solution was cooled slowly to –20 °C and colorless crystals formed (2.0 g, 32 % yield). ^{1}H NMR: 1.38 (18H), 1.51 (36H), 6.12 (4H). Anal. Calcd. for $C_{34}H_{58}Mg$: C, 83.15; H, 11.90. Found: C, 82.95; H, 12.09.

Cerium

$[Cp^{\ddagger}_2CeCl]_2$

To di-*t*-butylcyclopentadienyl potassium[10] (4.74 g, 21.9 mmol) and anhydrous $CeCl_3$ (2.70 g, 11.0 mmol) was added 200 mL of tetrahydrofuran. The mixture was stirred at reflux for 12 h producing a greenish-yellow solution. The solution was filtered and the solvent was removed under reduced pressure. The resulting yellow solid was dissolved in hot toluene (150 mL). Filtering and cooling the solution to –80 °C produced a yellow precipitate (3.90 g, 67 % yield). mp. 336-337 °C, IR: 1294w, 1250s, 1168m, 1089w, 1025m, 931m, 807s, 757s, 679s, 664m, 611w, 538w, 487w, 453w, 423m, 348m, 268w, 239w. ^{1}H NMR: 40.1 (1H, $\nu_{1/2}$ = 200 Hz), 11.6 (2H, $\nu_{1/2}$ = 150 Hz), -3.89 (18H, $\nu_{1/2}$ = 10 Hz). Anal. Calcd. for $C_{26}H_{42}CeCl$: C, 58.90; H, 7.98. Found: C, 59.06; H, 8.01. The E.I. mass spectrum showed a parent ion at m/e = 1061 amu. The parent ion isotopic

cluster was simulated: (calcd. %, obsvd. %); 1059 (95, 97), 1060 (57, 55), 1061 (100, 100), 1062 (53, 53), 1063 (42, 42), 1064 (17, 17), 1065 (7, 7). This compound has been independently prepared and characterized[11].

$[Cp^{\ddagger}_2CeI]_2$

To a mixture of $CeI_3 \cdot 3THF$[12] (21.7 g, 29.4 mmol) and $Cp^{\ddagger}_2Mg$ (11.1 g, 29.4 mmol) was added 250 mL of toluene. After stirring for 12 h, the solvent was removed under reduced pressure from the transparent orange solution. The orange solid was loaded into a Soxhlet extraction thimble and extracted exhaustively with hexane (72 h). Cooling the extract produced orange crystals. The compound was recrystallized from hot toluene (16 g, 86% yield). mp 265-267 °C. IR 2370 w, 2320 w, 2140 w, 1300 w, 1250 s, 1230 w, 1205 m, 1165 m, 1090 m, 1055 m, 1025 m, 930 m, 8020 s, 8010 s, 770 m, 760 s, 680 m, 660 m, 610 w, 490 w, 430 w, 350 m, 270 m, 250 m. ^{1}H NMR: -1.66 (18H, $\nu_{1/2}$ = 9 Hz), 23 (2H, $\nu_{1/2}$ = 140 Hz), 59 (1H, 180). Anal. Calcd. for $C_{26}H_{42}CeI$: C, 50.24; H, 6.82. Found: C, 49.93; H, 6.71. The E.I. mass spectrum showed a molecular ion at m/e = 621 amu. The parent ion isotopic cluster was simulated: (calcd. %, obsvd. %); 621 (66, 66), 622 (20, 25), 623 (11, 14), 624 (3, 3). This reaction, performed in THF, produces an equilibrium mixture of $Cp^{\ddagger}_2CeI$ and $Cp^{\ddagger}_3Ce$. Using a large excess of $Cp^{\ddagger}_2Mg$ affords isolable amounts of $Cp^{\ddagger}_3Ce$ but a significant amount of $Cp^{\ddagger}_2CeI$ remains.

$[Cp^{\ddagger}_2CeOSO_2CF_3]_2$

Trimethylsilyltrifluoromethane sulfonate (2.22 mL, 11.5 mmol) was added to a suspension of $Cp^{\ddagger}_2CeI$ (7.13 g, 11.5 mmol) in hexane (50 mL). The mixture slowly

changed from and orange suspension to a yellow solution and finally precipitated a bright yellow powder. The solid was isolated by filtration and washed with cold hexane (25mL) yielding 7.0 g (94% yield). mp 261-264 °C. Anal. Calcd. for $C_{27}H_{42}CeF_3O_3S$: C, 50.37; H, 6.58. Found: C, 50.17; H, 6.54. IR 1315 s, 1295 w, 1245 m, 1220 s, 1190 m, 1180 w, 1160 w, 1045 w, 1010 s, 925 w, 815 m, 810 w, 765 w, 755 m, 715 w, 675 w, 655 w, 620 s, 515 m, 425 w, 365 w, 345 w. ^{1}H NMR: -3.78 (18H, $\nu_{1/2}$ = 17 Hz), 16.4 (2H, $\nu_{1/2}$ = 130 Hz), 32.7 (1H, $\nu_{1/2}$ = 125 Hz). The E.I. mass spectrum showed the parent ion M^+ at m/e = 643 amu. The parent ion isotopic cluster was simulated: (calcd. %, obsvd. %); 647 (2, 1), 646 (6, 6), 645 (22, 23), 644 (32, 30), 643 (100, 100).

$Ce(OSO_2CF_3)_3$

Triflic acid (1 M in water) was added in small portions to a slurry of $Ce_2(CO_3)_3 \cdot xH_2O$ (Strem) in water until the solution remained acidic[13]. The solvent was removed under reduced pressure and coordinated water was removed by heating finely ground $Ce(OSO_2CF_3)_3 \cdot xH_2O$ to 200° C under vacuum for at least 48 h. The resulting white powder was examined by infrared spectroscopy to ensure that water and triflic acid were absent.

$Cp^{\ddagger}_3Ce$ $\{[(Me_3C)_2C_5H_3]_3Ce\}$

To a mixture of anhydrous $Ce(OSO_2CF_3)_3$ (7.54 g, 12.8 mmol) and $[(Me_3C)_2C_5H_3]_2Mg$ (7.30 g, 19.3 mmol) was added 150 mL of THF. The reaction mixture was stirred for 24 h, gradually producing a purple solution and a small amount of white precipitate. The solution was filtered and the solvent was removed under reduced

pressure. The residue was extracted with 150 mL of hexane and the resulting purple solution was filtered and cooled to –40 °C, giving royal blue crystals (2.4g, 28% yield). Concentrating and cooling the mother liquor yielded two additional crops of crystals (2.6 g and 1.4 g , 74% yield). The solvent was removed from the mother liquor and additional product was obtained by vacuum sublimation of the residue (200 °C at 10^{-3} torr). mp 214-217 °C. IR: 1305 w, 1255 s, 1240 w, 1205 m, 1160 m, 1090 w, 1055 m, 1025 m, 930 m, 810 s, 740 s, 700 w, 680 w, 665 m, 610 w, 490 w, 430 w, 355 m, 250 m. ^{1}H NMR -4.63 (18H, $\nu_{1/2}$ = 12 Hz), 17.0 (2H, $\nu_{1/2}$ = 45 Hz), 25.8 (1H, $\nu_{1/2}$ = 34 Hz). Anal. Calcd. for $C_{39}H_{63}Ce$: C, 69.70; H, 9.45. Found C, 69.37; H, 9.70. The E.I. mass spectrum showed a molecular ion at m/e= 671. The parent ion isotopic cluster was simulated: (calcd. %, obsvd. %); 671 (100, 100), 672 (44, 41), 673 (22, 23), 674 (7, 7). The compound was also prepared from $Cp^{‡}_2CeOSO_2CF_3$ and one half of an equivalent of $MgCp^{‡}_2$ with a similar isolated yield.

$Cp"_3Ce$ $\{[(Me_3Si)_2C_5H_3]_3Ce\}$

This compound was prepared previously by another method[14]. To a mixture of anhydrous $Ce(OSO_2CF_3)_3$ (2.73 g, 4.65 mmol) and $[(Me_3Si)_2C_5H_3]_2Mg$[15] (3.09 g, 6.98 mmol) was added 100 mL of THF. The reaction mixture was stirred for 24 h, gradually producing a royal blue solution and a small amount of white precipitate. The solution was filtered and the solvent was removed under reduced pressure. The residue was extracted with 150 mL of hexane, filtered, and concentrated to a volume of 80 mL and cooled to –40 °C. Royal blue crystals were formed (1.7 g, 48% yield). Concentrating and cooling the mother liquor produced a second crop of crystals (0.83 g, 71% yield).

The compound sublimes at 200 °C at 10^{-3} torr. m.p. 226-228 °C IR: 1325 w, 1245 s, 1210 w, 1205 w, 1070 s, 920 s, 835 s, 780 m, 755 m, 695 m, 645 m, 625 w, 485 m, 380 m, 360 w, 335 w, 305 m, 280 w, 245 w. Anal. Calcd. for $C_{33}H_{63}Ce$: C, 51.6; H, 8.26. Found: C, 49.3; H, 8.18. ^{1}H NMR -4.47 (18H, $\nu_{1/2}$ = 5 Hz), 17.1 (2H, $\nu_{1/2}$ = 44 Hz), 26.8 (1H, $\nu_{1/2}$ = 28 Hz). The E.I. mass spectrum showed a molecular ion at m/e = 767 amu. The molecular ion isotopic cluster was simulated: m/e (calcd. %, obsvd. %); 767 (100, 100), 768 (67, 69), 769 (54, 48), 770 (25, 24), 771 (11, 10).

Cp^{tt}_3Ce {$[(Me_3Si)(Me_3C)C_5H_3]_3Ce$}

Tetrahydrofuran (50 mL) was added to a mixture of $Ce(OSO_2CF_3)_3$ (1.73 g, 2.95 mmol) and $Mg(Cp^{tt})_2$ (1.82 g, 4.43 mmol). The mixture, which began to turn purple immediately, was heated to 60° C and stirred for 12 h. The resulting solution was dark purple with little or no precipitate. The solvent was removed under reduced pressure and the product was extracted with 50 mL of hexane. The solution was filtered and the filtrate was concentrated to a volume of 5 mL and cooled to -20 °C. Purple crystals (0.90 g, 42% yield) were isolated and the mother liquor was taken to dryness. An additional 1.05 g (91% overall yield) was obtained by vacuum sublimation of the residue (200 °C at 10^{-3} torr).

mp. 174-178 °C. IR: 1305w, 1285w, 1260m, 1250s, 1210w, 1190m, 1180m, 1085s, 1060m, 1030w, 1025w, 980w, 970w, 940m, 920s, 830s, 765s, 755s, 725w, 690w, 680m, 650m, 630m, 595w, 490w, 430m, 370w, 355m, 345w, 315m, 285w, 250w. 500 MHz ^{1}H NMR: -11.81 (9H), -8.80 (18H), -1.78 (18H), -1.42 (9H), 27.6 (2H), 19.6 (2H), 14.1 (2H), 25.6 (1H), 24.9 (1H), 15.2 (1H). Anal. Calcd. for $C_{36}H_{63}CeSi_3$: C, 60.0; H, 8.82.

Found: C, 59.86; H, 9.10. The E.I. mass spectrum showed a molecular ion at m/e = 719 amu. The molecular ion isotopic cluster was simulated: m/e (calcd. %, obsvd. %); 719 (100, 100), 720 (56, 56), 721 (38, 37), 722 (15, 14).

$Cp^{\ddagger}_2CeCp''$

Tetrahydrofuran (50 mL) was added to a mixture of $Cp^{\ddagger}_2CeOTf$ (1.00 g, 1.55 mmol) and Cp''_2Mg (0.34 g, 0.78 mmol). The solution changed to a purple color in less than 15 min and the solution was stirred for 1 h. The solvent was removed under reduced pressure and the residue was extracted with hexane (50 mL). The purple solution was filtered, concentrated to a volume of about 25 mL, and cooled to –80 °C. Purple crystals formed (0.83 g, 76% yield). mp 185-187 ° C. IR (cm^{-1}): 1318w, 1304w, 1245s, 1207m, 1168m, 1075s, 1060w, 1025w, 930w, 922s, 835s, 818m, 809m, 774s, 760m, 745s, 738m, 691w, 678m, 670m, 642m, 618m, 485m, 432w, 387m, 345m, 325w, 295m, 275w, 245m. ^1H NMR –6.55 (36H), -2.30 (18H), 9.50 (2 H, Hz), 21.11 (4H, Hz), 23.86 (2H, Hz), 29.55 (1H, Hz). Anal. Calcd. for $C_{37}H_{63}CeSi_2$: C, 63.11; H, 9.02. Found: C, 62.95; H, 8.87.

$Cp^{\ddagger}_2CeMe$

Diethyl ether (50 mL) was added to $Cp^{\ddagger}_2CeOTf$ (5.0 g, 7.8 mmol) and the mixture was cooled to -78 °C. Using a syringe, a solution of methyllithium in diethylether (8.7 mL, 0.89 M, 7.8 mmol) was added. The mixture was warmed slowly to 0° C and the bright yellow suspension changed to a dark orange solution. The flask was placed in an ice bath and the solvent was removed under reduced pressure. The residue was extracted with

100 mL of hexane, filtered and concentrated to a volume of 30 mL. The solution was cooled and the resulting orange solid (1.4 g, 35%) was collected. mp 250 °C (dec). IR (cm^{-1}): 1300w, 1243s, 1237w, 1200m, 1165m, 1090w, 1058m, 1050m, 1022m, 975w, 929m, 820m, 810m, 802s, 750s, 725m, 677m, 664m, 607w, 427w, 345w, 290w, 278w. ^1H NMR: -4.98 (36H, $\nu_{1/2}$ = 14 Hz), 12.8 (4H, $\nu_{1/2}$ = 60 Hz), 13.7 (2H, $\nu_{1/2}$ = 55 Hz). Anal. Calcd. for $C_{27}H_{45}Ce$: C, 63.6; H, 8.9. Found: C, 63.15; H, 9.26. The parent ion is not observed in the E. I. mass spectrum. $[Cp^{\ddagger}_2Ce]_2Me$ and smaller fragments are observed.

Iron

Cp^{tt}_2Fe

The adduct, $FeBr_2 \cdot 2THF$ (0.88 g, 2.4 mmol) and Cp^{tt}_2Mg (1.00 g, 2.43 mmol) were dissolved in tetrahydrofuran (50 mL). The mixture turned a red-brown color and was stirred for 3 h. The solvent was removed under reduced pressure and the residue was extracted with hexane (50 mL). The solution was filtered and concentrated to a volume of 25 mL and cooled to –20 °C. Red-orange crystals were isolated (0.81 g, 75 % yield). mp 137-139 °C. ^1H NMR (500MHz) 0.307 (18H), 0.314(18H), 1.267 (18H), 1.270(18H), 4.065 d,d (2H, 8 Hz, 2 Hz), 4.067 d,d (2H, 8 Hz, 2 Hz), 4.60 d,d (2H, 2 Hz, 2 Hz), 4.80 d,d (2H, 2 Hz, 2 Hz), 4.187 d,d (2H, 8 Hz, 2 Hz) 4.189 d,d (2H, 8 Hz, 2 Hz)

$Fv^{\ddagger}_2Fe_2$

The adduct, $FeBr_2 \cdot 2THF$ (1.21 g, 3.37 mmol) and $Fv^{\ddagger}_2Mg_2$ (1.27 g, 1.68 mmol) were combined and 50 mL of cold (-78 °C) tetrahydrofuran was added. The reaction mixture slowly turned dark red as the mixture was allowed to warm to room temperature. The mixture was stirred for 8 h and the solvent was removed under reduced pressure. The residue was extracted with hexane (2 X 100 mL) and filtered. The solvent was removed from the combined extracts and the dark red solid was dissolved in toluene (10mL) and cooled slowly to –20 °C. Dark-red crystals formed (0.18 g, 13%). The mother liquor was cooled slowly to –80 °C and large crystals were formed (0.53 g, 51% yield total). mp 285-289 °C. ^{1}H NMR 1.40 (36H), 1.42 (36H), 6.15 d(4H, 3 Hz), 6.36 d(4H, 3 Hz). Anal. Calcd. for $C_{52}H_{80}Fe_2$: C, 76.46; H, 9.87. Found: C, 76.21; H, 9.87. The E.I. mass spectrum showed a molecular ion at m/e = 817 amu. The molecular ion isotopic cluster was simulated: m/e (calcd. %, obsvd. %); 819 (4, 4), 818 (20, 19), 817 (64, 60), 816 (100, 100), 815 (8, 8), 814 (13, 13).

a-$Cp^{\ddagger}_2Fe$

Tetrahydrofuran (200 mL) was added to a mixture of $FeBr_2 \cdot 2THF$ (4.09 g, 11.4 mmol) and "a-$Cp^{\ddagger}_2Mg$" (4.95 g, 11.4 mmol). The solution turned dark reddish-brown immediately and over the next 48 h became dark red. The solvent was removed under reduced pressure and the solid was extracted with hexane (200 mL) and filtered. The dark red filtrate was concentrated to a volume of 10 mL and cooled slowly to -40 °C. Large red crystals formed (1.50 g, 28% yield), mp 140-142 °C. IR (cm^{-1}): ^{1}H NMR 0.67 s

(6 H), 1.30 s (36 H), 4.28 s (2 H), 4.31 s (2H). Anal. Calcd. for $C_{28}H_{46}FeSi$: C, 72.08; H, 9.94. Found: C, 71.79; H, 9.80.

a-Cp"$_2$Fe

Tetrahydrofuran (100 mL) was added to a mixture of $FeBr_2$·2THF (0.72 g, 2.0 mmol) and Mg(anzaCp") (1.0 g , 2.0 mmol). The solution turned dark reddish-violet immediately. After 12 h, the solvent was removed under reduced pressure and the solid was extracted with hexane (100 mL) and filtered. The dark red-violet filtrate was concentrated to a volume of 10 mL and cooled slowly to -40° C. Large red-violet crystals formed (0.19 g, 10% yield). mp. 203-205 °C. IR: 1248s, 1152m, 1137w, 1075m, 990m ,924w, 909w, 832s, 800w, 787w, 753m, 722w, 687w, 665w, 628w, 553w, 486w, 419w, 357m, 280w. ^{1}H NMR 0.47 s (6 H), 0.35 s (36 H), 4.42 m (4 H). Anal. Calcd. for $C_{22}H_{46}FeSi_5$: C, 54.3; H, 8.73; Found: C, 52.8; H, 8.66.

Manganese

MnI_2·2THF

This compound was prepared as reported[16,17]. Manganese(II) carbonate (30 g, 260 mmol) was added, in small portions, to a mixture of hydriodic acid (150 g, 57%, 670 mmol) and water (130mL). After gas evolution ceased, the water was removed under reduced pressure. The residue was redissolved in water and the water was removed again under reduced pressure. The dissolution and evaporation step was repeated two more times. The residue was loaded into a Soxhlet thimble and extracted exhaustively with

tetrahydrofuran. The tetrahydrofuran solution was cooled to –80° C yielding colorless crystals of MnI_2·2THF (yield). The product was used without further characterization.

$Cp^{‡}_2Mn$

Tetrahydrofuran (50 mL) was added to a mixture of $Cp^{‡}_2Mg$ (2.6 g, 6.8 mmol) and MnI_2·2THF (3.1 g, 6.8 mmol). The reaction mixture immediately turned orange and a small amount of colorless precipitate formed. The solvent was removed under reduced pressure and the residue was extracted with hexane (50 mL). The solution was filtered and then cooled to –80° C and dark-orange crystals formed. The crystals were redissolved in hexane and recrystallized (1.9 g, 68 %). mp. 145-46° C. ^{1}H NMR: 14.5 ppm, ($\nu_{1/2}$ =700 Hz). IR (cm^{-1}): 1293s, 1250s, 1230w, 1197s, 1162m, 1083w, 1048w, 1040m, 1020m, 930m, 920m, 910m, 838s, 800s, 737m, 720w, 685m, 655m, 640m, 615w, 604w, 507m, 475br w, 405w, 325w, 300w. Anal. Calcd. for $C_{26}H_{42}Mn$: C, 76.25; H, 10.34. Found: C, 75.91; H, 10.43.

Cp''_2Mn

A solution of Cp''_2Mg (3.9 g, 8.8 mmol) in tetrahydrofuran (75 mL) was added to MnI_2·2THF (4.0 g, 8.8 mmol). A colorless precipitate formed immediately. The reaction mixture was stirred for 30 min and the precipitate was allowed to settle (2 h). The pale yellow/green solution was filtered and the solvent was removed under reduced pressure. The residue was extracted with hexane and filtered. The solvent was removed under reduced pressure, the residue was sublimed (10^{-3} torr, <100° C) and the sublimed product was crystallized from hexane (pale straw-colored crystals 2.4 g, 58%). The mass

spectrum showed no peak corresponding to $Cp"_2Mg$. mp 90-91 °C. IR (cm^{-1}): 1303m, 1245s, 1208m, 1070s, 1048m, 920s, 825br s, 768s, 750s, 690m, 642m, 630s, 470s, 365br m, 275m, 235w. ^1H NMR: 11.1 ppm, ($\nu_{1/2}$ =500 Hz). The E.I. mass spectrum showed a parent ion at m/e = 473 amu. The parent ion isotopic cluster was simulated: (calcd. %, obsvd. %); 473 (100, 100), 474 (45, 46), 475 (23, 23), 476 (7, 6), 477 (2, 2).

Cp^{tt}_2Mn

Tetrahydrofuran (50 mL) was added to a mixture of $Cp^{‡}_2Mg$ (2.6 g, 6.8 mmol) and MnI_2·2THF (3.1 g, 6.8 mmol). The reaction mixture immediately turned orange and a small amount of colorless precipitate formed. The solvent was removed under reduced pressure and the residue was extracted with hexane (50 mL). Solution was filtered and cooled to –80° C and dark-orange crystals formed. The crystals were redissolved in hexane and recrystallized (1.9 g, 68 %). IR (cm^{-1}): 1325m, 1287m, 1250br s, 1200m, 1170br s, 1075s, 1045s, 1020w, 935m, 915s, 825br s, 750br s, 687m, 674m, 628s, 480m, 450w, 423s, 385br s, 333m, 290m. ^1H NMR: 12.5 ppm, ($\nu_{1/2}$ =700Hz)(the Me_3Si and Me_3C resonances are not resolved). Anal. Calcd. for $C_{26}H_{42}Mn$: C, 65.26; H, 9.58. Found: C, 64.88; H, 9.69. The E.I. mass spectrum showed a parent ion at m/e = 473 amu. The parent ion isotopic cluster was simulated: (calcd. %, obsvd. %); 441 (100, 100), 442 (37, 37), 443 (13, 13).

$Fv^{‡}_2Mn_2$

Tetrahydrofuran (50 mL) was added to a mixture of $Cp^{‡}_2Mg$ (2.6 g, 6.8 mmol) and MnI_2·2THF (3.1 g, 6.8 mmol). The reaction mixture immediately turned orange and

a small amount of colorless precipitate formed. The solvent was removed under reduced pressure and the residue was extracted with hexane (50 mL). Solution was filtered and cooled to –80° C and dark-orange crystals formed. The crystals were redissolved in hexane and recrystallized (1.9 g, 68 %). mp > 250 °C. Anal. Calcd. for $C_{52}H_{80}Mn_2$: C, 76.63; H, 9.89. Found: C, 76.56; H, 10.02. The E.I. mass spectrum showed a parent ion at m/e = 814 amu. The parent ion isotopic cluster was simulated: (calcd. %, obsvd. %);814 (100, 100), 815(59,58), 816(17,16), 817(3,3), 818(0.4,0.5), 819(0.1,0.1).

Titanium

$Cp^{\ddagger}_2TiCl$

Tetrahydrofuran (150 mL) was added to a mixture of $TiCl_3$·3THF (13.0 g, 34.9 mmol) and $Cp^{\ddagger}_2Mg$ (13.2g, 34.9 mmol). The solution turned dark blue immediately and the mixturewas stirred for 12 h. The solvent was removed under reduced pressure and the resulting dark-blue solid was extracted with 150 mL of hexane. The solution was filtered and the solid remained blue so a second extraction with 100 mL of hexane was performed. The combined filtrates were concentrated to a volume of 200 mL and cooled to -80° C. Blue needles were isolated (11.6 g, 83% yield). mp 145-46° C. ^{1}H NMR 3.6 ppm ($\nu_{1/2}$ = ~ 600 Hz). IR(cm^{-1}): 3110w, 3090w, 1393m, 1372s, 1364m, 1357s, 1294m, 1253s, 1197m, 1166m, 1059s, 1035w, 1028w, 935w, 928w, 919w, 885w, 878w, 846s, 821w, 808m, 720w, 680w, 655m, 498m, 453m, 400m, 388m, 342w, 325w, 274m. Anal. Calcd. for $C_{26}H_{42}ClTi$: C, 71.31; H, 9.67. Found: C, 71.04; H, 9.57.

$Cp^{‡}_2TiCl_2$

Carbon tetrachloride (5 mL, 50 mmol) was dissolved in tetrahydrofuran (100 mL) and the solution was added to $Cp^{‡}_2TiCl$ (4.48 g, 10.2 mmol) and stirred for 8 h. The dark blue solution gradually changed to dark red and red needles deposited, which were collected (4.32 g, 89 % yield).

A second method; tetrahydrofuran (250 mL) was added to a mixture of $Cp^{‡}_2TiCl$ (7.33g, 16.7 mmol) and $HgCl_2$ (5.00 g, 18.4 mmol). A dark red solution with a colorless precipitate immediately formed. The mixture was stirred for 3 h and the solvent was removed under reduced pressure. The dark red product was sublimed (150° C, 10^{-3} torr) and crystallized from tetrahydrofuran. The compound has been prepared by other methods[18,19]. ^{1}H NMR 1.29(36H), 5.81d (4H, $^3J_{CH}$ = 3Hz), 6.77t (2H, $^3J_{CH}$ = 3Hz).

$Cp^{‡}_2Ti$

Under argon, a potassium amalgam was prepared from 20 mL of mercury and potassium (4.6g, 120 mmol). $Cp^{‡}_2TiCl$ (10.3 g, 23.5 mmol) was dissolved in hexane (200 mL) and the solution was added to the potassium amalgam. The mixture was heated to reflux and stirred for 12 h. The stirring was halted and the mixture was allowed to cool to room temperature. The dark blue solution was filtered and concentrated to a volume of 100 mL. Layered crystals formed (3.85 g, 41 % yield). A second crop of crystals was obtained by concentrating and cooling the solution (2.5 g, 67 % overall yield). mp 148-149 °C. IR (cm^{-1}): 3105w, 3095m, 1489m, 1413m, 1382m, 1369s, 1362s, 1354w, 1318w, 1315w, 1271w, 1253s, 1202m, 1187s, 1098s, 1070m, 1061m, 1029m, 948s, 923s, 904w, 899w, 867s, 835sb, 760s, 728w, 700m, 682w, 673w, 640m, 627m, 591w, 495w,

470w, 440s, 420m, 410s, 377w, 365w, 338w, 304m, 268s. ^{1}H NMR 3.2 ppm ($\nu_{1/2}$= 500 Hz). Anal. Calcd. for $C_{26}H_{42}Ti$: C, 77.59; H, 10.52. Found: C, 77.29; H, 10.52. The E.I. mass spectrum showed a parent ion at m/e = 402 amu. The parent ion isotopic cluster was simulated: (calcd. %, obsvd. %); 405 (3, 3), 404 (13, 17), 403 (36, 45), 402 (100, 100), 401 (13, 17), 400 (11, 14), 399 (0, 2). Pure solutions of the titanocene can be prepared by degassing solutions of the titanocene dihydride.

$[Cp^{\ddagger}_2TiN]_2$

Tetra-*t*-butyltitanocene (1.0 g, 2.5 mmol) was dissolved in hexane (25 mL) and the solution was exposed to 1 atm of nitrogen. The solution was cooled to –78 °C and very dark crystals with metallic gold flakes were formed (0.78 g, 75 % yield). The compound appears homogeneous and blue when crushed in a mortar. mp (N_2 loss) 130-140 °C. IR (cm^{-1}): 1300m, 1255s, 1235w, 1210m, 1200m, 1170s, 1055w, 1050m, 1020m, 950m, 940w, 930m, 855s, 830s, 815m, 785s, 740w, 725w, 670m, 660m, 590w, 500w, 460w, 405w. Anal. Calcd. for $C_{26}H_{42}NTi$: C, 74.98; H, 10.16; N, 3.36. Found: C, 74.88; H, 10.19; N, 3.43. The E.I. mass spectrum is consistent with $Cp^{\ddagger}_2Ti$.

$Cp^{\ddagger}_2Ti(CO)_2$

Tetra-*t*-butyltitanocene (1.0 g, 2.5 mmol) was dissolved in hexane (50 mL) and exposed to 1 atm of carbon monoxide (CO). The solution quickly changed from blue to red. After stirring for 5 min, the solution was concentrated to a volume of 10 mL and cooled to –20 °C. Dark-red crystals formed (0.67 g, 59 % yield). mp 125-127 °C. IR

(cm^{-1}): 1960s, 1880s, 1783m, 1308w, 1258s, 1206m, 1172m, 1055s, 950w, 935w, 922w, 899w, 855w, 830s, 815m, 777s, 766m, 745w, 730w, 705w, 680w, 660w, 565w, 500w, 455w, 400m, 360w, 320w. ^{1}H NMR: 1.17 (36H), 4.83 d (4H, 2Hz), 5.13 t (2H, 2 Hz). Anal. Calcd. for $C_{28}H_{42}O_2Ti$: C, 73.35; H, 9.23. Found: C, 73.32; H, 9.41. The E.I. mass spectrum showed a parent ion at m/e = 458 amu. The parent ion isotopic cluster was simulated: (calcd. %, obsvd. %); 456 (10, 8), 457 (13, 12), 458 (100, 100), 459 (38, 36), 460 (15, 12), 461 (3, 0).

$Cp^{\ddagger}_2Ti(C_2H_4)$

Tetra-*t*-butyltitanocene (5.8 g, 13 mmol) was dissolved in hexane (50 mL) and exposed to 1 atm of ethylene. The solution changed color from blue to yellow in < 5 min. The solution was concentrated to a volume of 25 mL and cooled to –20 °C. Green-yellow needles formed (2.2 g, 36% yield). mp 122-123 °C. IR (cm^{-1}): 1289m, 1249s, 1231m, 1198m, 1180w, 1164m, 1098s, 1055m, 1020m, 944w, 933m, 929m, 918w, 863w, 850s, 817w, 800s, 788s, 725w, 678w, 659s, 610w, 488s, 435m, 384m, 308w. ^{1}H NMR: 1.06 (36H), 2.93 (4H), 4.36 d (4H, $^3J_{CH}$ = 2 Hz), 9.25 t (2H, 2Hz). Anal. Calcd. for $C_{28}H_{46}Ti$: C, 78.11; H, 10.77. Found: C, 77.84; H, 10.87. The E. I. mass spectrum showed M-$(CH_2CH_2)^+$ as the parent ion.

$Cp^{\ddagger}_2Ti(PhCCPh)$

Sublimed diphenylacetylene (0.84 g, 4.7 mmol) and $[(Me_3C)_2C_5H_3]_2Ti$ (1.00 g, 2.34 mmol) were combined in a Schlenk flask and hexane was added (50mL). The

mixture produced a dark-red solution as it dissolved. Red crystals began to nucleate before all of the diphenylacetylene had dissolved. The solution was cooled to -20° C and red-orange crystals were isolated (1.07 g, 75%). mp 169-170° C. IR (cm^{-1}): 1642s, 1587s, 1300w, 1250s, 1195w, 1167m, 1065m, 1022m, 975w, 925w, 886w, 839s, 810w, 802w, 791s, 676w, 670s, 709w, 695s, 680w, 675w, 665w, 658w, 605w, 551w, 435m, 399m, 355m, 328m. ^{1}H NMR 1.12(36H), 5.51d (4H, $^3J_{CH}$ = 3Hz), 7.99t (2H, $^3J_{CH}$ = 3Hz). Anal. Calcd. for $C_{40}H_{52}Ti$: C, 82.73; H, 9.02. Found: C, 82.91; H, 9.14.

$Cp^{\ddagger}_2TiH_2$

Tetra-*t*-butyltitanocene (4.28 g, 10.6 mmol) was dissolved in hexane (50 mL) and exposed to 1 atm of hydrogen. The blue titanocene solution turned dark red. While under the hydrogen atmosphere, the solution was cooled slowly to -80° C. Dark-red crystals were isolated and are stable with respect to hydrogen loss under vacuum. mp 152-154° C. IR (cm^{-1}): 1640br s, 1295w, 1250s, 1231w, 1202m, 1166m, 1050m, 1024w, 925m, 847m, 821m, 806s, 762m, 722w, 683m, 665m, 464m, 398m. ^{1}H NMR (-54 °C) 1.13 (36H), 2.62 (2H), 5.10 d (4H, $^3J_{CH}$ = 3Hz), 8.01 t (2H, $^3J_{CH}$ = 3Hz). Anal. Calcd. for $C_{26}H_{44}Ti$: C, 77.2; H, 10.96. Found: C, 77.28; H, 11.23.

$Cp^{\ddagger}_2TiMe$

Diethylether (50 mL) was added to $Cp^{\ddagger}_2TiCl$ (3.9 g, 8.8 mmol). Methyllithium in diethylether (11 mL, 0.81 M, 8.8 mmol) was added to the blue solution using a syringe. The solution immediately turned green and a colorless solid precipitated. The solvent was removed under reduced pressure and the green solid was extracted with hexane (50

mL). The solution was filtered and concentrated to a volume of 25 mL and cooled to –20 °C. Green crystals formed (1.67 g, 45 % yield). mp 119-121 °C. IR (cm^{-1}): 1297w, 1252s, 1238w, 1200m, 1168m, 1108w, 1062m, 1023m, 939m, 931m, 844s, 820w, 812w, 802m, 791s, 721w, 680w, 658s, 605w, 495w, 442w, 387w, 310w. No resonances were observed in the ^1H NMR spectrum at 30 °C. Anal. Calcd. for $C_{27}H_{45}Ti$: C, 77.7; H, 10.86. Found: C, 77.58; H, 11.13.

Second method; methyllithium (11 mL, 0.80 M in Et_2O, 8.9 mmol) was added dropwise to an ether suspension of $Cp^{‡}_2TiCl_2$ (2.0 g, 4.2 mmol). The dark-red suspension changed to light green with a colorless precipitate. The mixture was stirred for 30 min and the solvent was removed under reduced pressure. The solid was extracted with hexane (100 mL) and the green solution was filtered and concentrated to a volume of 40 mL and cooled to -80° C. Green needles of $Cp^{‡}_2TiMe$ were isolated.

$Cp^{‡}_2TiH$

Hexane (50 mL) was added to $Cp^{‡}_2TiMe$ (0.50 g, 1.2 mmol) and the green solution was exposed to 1 atm of hydrogen. The solution turned a dark-red color over ~ 5 min. The solution was concentrated to a volume of 10 mL and cooled slowly to –80 °C under an argon atmosphere. Brick-red crystals formed (0.40 g, 83% yield) mp 147-149 °C. IR (cm^{-1}): 1375s, 1355s, 1297m, 1250s, 1233w, 1200m, 1165m, 1050m, 1025w, 945w, 935w, 927m, 852w, 837s, 810m, 781w, 772m, 723m, 690m, 659m, 610w, 585w, 500w, 470m, 397m, 320w, 250w.

No resonances were observed in the ^1H NMR spectrum. Anal. Calcd. for $C_{26}H_{43}Ti$: C, 77.39; H, 10.74. Found: C, 77.22; H, 10.92.

References

1)Venier, C. G.; Casserly, E. W. *J. Am. Chem. Soc*, **1990**, *112*, 2808.

2)Knox, G. R.; Pauson, P. L. *J. Chem. Soc.*, **1961**, 4610-4615.

3)Leigh, T. *J. Chem. Soc.*, **1964**, 3294-3302.

4)Riemschneider, R.; Reisch, A.; Horak, H. *Monatsh. Chem.*, **1960**, *91*, 805-811.

5)Burkey, D. J.; Hanusa, T. P. *Comments Inorg. Chem.*, **1995**, *17*, 41-77.

6)Leffler, A. J. *Inorg. Chem.*, **1968**, *7*, 2651-2652.

7)Dehmlow, E. V.; Bollmann, C. *Z. Naturforsch. B*, **1993**, *48*, 457.

8)Herrmann, W. A. ; Herrmann, W. A., Ed.; Georg Thieme Verlag: New York, 1996; Vol. 1, pp 56-57.

9)Donovan, B. T.; Hughes, R. P.; Trujillo, H. A.; Rheingold, A. L. *Organometallics*, **1992**, *11*, 64-69.

10)Lukens, W. W. Ph.D. Dissertation *Trivalent Metallocene Chemistry of Some Uranium, Titanium, and Zirconium Complexes*; U. C. Berkeley: Berkeley, CA, 1995.

11)Lobkovsky, E. B.; Gunko, Y. K.; Bulychev, B. M.; Belsky, V. K.; Soloveichik, G. L.; Antipin, M. Y. *J. Organomet. Chem.*, **1991**, *406*, 343-352.

12)Hazin, P. N.; Huffman, J. C.; Bruno, J. W. *Organometallics*, **1987**, *6*, 23.-27.

13)Forsberg, J. H.; Spaziano, V. T.; Balasubramanian, T. M.; Liu, G. K.; Kinsley, S. A.; Duckworth, C. A.; Poteruca, J. J.; Brown, P. S.; Miller, J. L. *J. Org. Chem*, **1987**, *52*, 1017.

14)Stults, S. Ph. D. Dissertation *Tris(cyclopentadienyl)cerium and -uranium: Relative Basicity, Structure, and Reactions*; U.C. Berkeley: Berkeley, CA, 1988.

15)Duff, A. W.; Hitchcock, P. B.; Lappert, M. F.; Taylor, R. G. *J. Organomet. Chem*, **1985**, *293*, 271-283.

16)Riemschneider, R.; Kassahn, H.-G.; Schneider, W. Z. *Naturforsch., B*, **1960**, *15*, 547-551.

17)Heyn, B.; Hipler, B.; Kreisel, G.; Schreer, H.; Walther, D. *Anorganische Synthese-chemie*; Springer-Verlag: Berlin, 1986.

18)Urazowski, I. F.; Ponomaryov, V. I.; Ellert, O. G.; Nifant'ev, I. E.; Lemenovskii, D. A. *J. Organomet. Chem.*, **1988**, *356*, 181-193.

19)Okuda, J. *J. Organomet. Chem.*, **1990**, *385*, C39-C42.

Appendix A

Variable low-temperature UV-vis spectroscopy

The variable temperature UV-vis spectrometer is an adaptation of an Ocean Optics ST2000 fiber optic UV-vis spectrometer . The cell holder, as obtained from Ocean Optics (CUV-UV), was predrilled for plumbing and the inlet was fitted with a copper coil and a hose barb. The copper coil was arranged so that it could be immersed in liquid nitrogen in a Dewar. During the experiment, nitrogen gas flowed through the coil and then through the base of the cell holder. A thermocouple was attached to the base to monitor the temperature. The sample holder was contained in an acrylic box and the box was fitted with a nitrogen inlet so that the box could be purged with dry nitrogen.

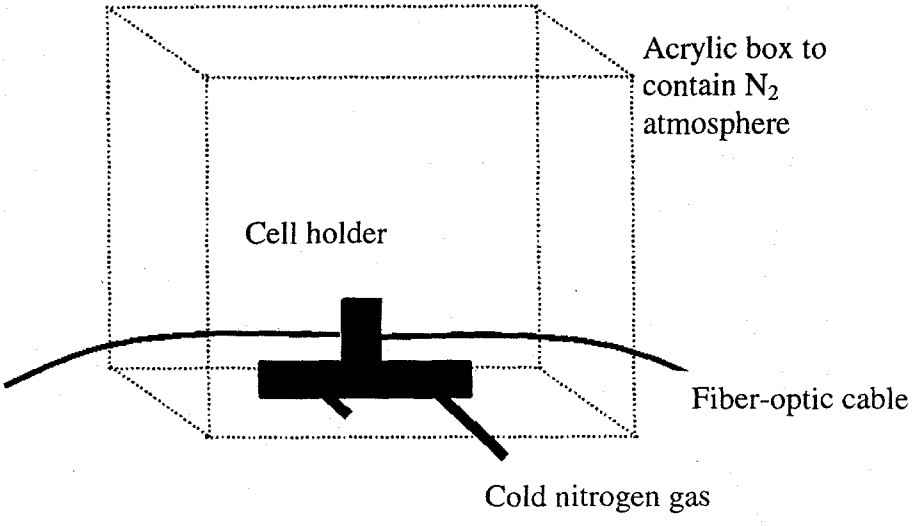

The sample cuvette was fitted with a greaseless Chemglass high vacuum valve. The core of the valve was drilled to accept a small thermocouple which was epoxied in place.

During a typical experiment, the sample was prepared in an inert atmosphere glove box while the acrylic chamber was purged with dry nitrogen. A background spectrum was

collected and saved to minimize the manipulation of the sample during the experiment. The sample was loaded in to the sample holder and the box was purged again. The leads of the thermocouple were connected to a voltmeter (+/- 0.01mV) and the lead connections were immersed in a constant temperature bath (a type K (Chromel-Alumel) thermocouple was used with an ice/water bath).The nitrogen flow through the copper coil was increased and the Dewar was filled with liquid nitrogen. An experiment typically consisted of 20-50 data points between 30 and –110 °C and required 3 h to collect. The thermal mass of the sample holder and sample were sufficient that all temperature changes were slow and there was no need to let the system reach thermal equilibrium before collecting a spectrum. The typical collection time for a spectrum was 3-5 ms.